PHYSICAL REVIEW D VOLUME 49, NUMBER 12 15 JUNE 1994

Nonperturbative QCD: A weak-coupling treatment on the light front

Kenneth G. Wilson, Timothy S. Walhout, Avaroth Harindranath, Wei-Min Zhang,* and Robert J. Perry
Department of Physics, The Ohio State University, Columbus, Ohio 43210-1106

Stanisław D. Głazek
Institute of Theoretical Physics, Warsaw University, ul. Hoża 69, 00-861 Warsaw, Poland
(Received 28 January 1994)

In this work the determination of low-energy bound states in quantum chromodynamics is recast so that it is linked to a weak-coupling problem. This allows one to approach the solution with the same techniques which solve quantum electrodynamics: namely, a combination of weak-coupling diagrams and many-body quantum mechanics. The key to eliminating necessarily nonperturbative effects is the use of a bare Hamiltonian in which quarks and gluons have nonzero constituent masses rather than the zero masses of the current picture. The use of constituent masses cuts off the growth of the running coupling constant and makes it possible that the running coupling never leaves the perturbative domain. For stabilization purposes an artificial potential is added to the Hamiltonian, but with a coefficient that vanishes at the physical value of the coupling constant. The weak-coupling approach potentially reconciles the simplicity of the constituent quark model with the complexities of quantum chromodynamics. The penalty for achieving this perturbative picture is the necessity of formulating the dynamics of QCD in light-front coordinates and of dealing with the complexities of renormalization which such a formulation entails. We describe the renormalization process first using a qualitative phase space cell analysis, and we then set up a precise similarity renormalization scheme with cutoffs on constituent momenta and exhibit calculations to second order. We outline further computations that remain to be carried out. There is an initial nonperturbative but nonrelativistic calculation of the hadronic masses that determines the artificial potential, with binding energies required to be fourth order in the coupling as in QED. Next there is a calculation of the leading radiative corrections to these masses which requires our renormalization program. Then the real struggle of finding the right extensions to perturbation theory to study the strong-coupling behavior of bound states can begin.

PACS number(s): 11.10.Ef, 11.10.Gh, 12.38.Bx

I. INTRODUCTION

The only truly successful approach to bound states in field theory has been quantum electrodynamics (QED), with its combination of nonrelativistic quantum mechanics to handle bound states and perturbation theory to handle relativistic effects. Lattice gauge theory is maturing but has yet to rival QED's comprehensive success. There are four barriers which prohibit an approach to quantum chromodynamics (QCD) that is analogous to QED. The barriers are (1) the unlimited growth of the running coupling constant g in the infrared region, which invalidates perturbation theory, (2) confinement, which requires potentials that diverge at long distances as opposed to the Coulombic potentials of perturbation theory, (3) spontaneous chiral symmetry breaking, which does not occur in perturbation theory, and (4) the nonperturbative structure of the QCD vacuum. Contrasting the gloomy picture of the strong interaction in QCD, however, is that of the constituent quark model (CQM), where only the minimum number of constituents required by the symmetries are used to build each hadron and where Zweig's rule leaves little role for production of extra constituents. Instead, rearrangement of preexisting constituents dominates the physics. Yet the CQM has never been reconciled with QCD—not even qualitatively. Ever since the work of Feynman, though, it has been clear that the best hope of reconciliation is offered by infinite momentum frame (IMF) dynamics.

In this paper, a framework closely related to the IMF will be employed, namely, light-front quantization. The purpose of this paper is to provide arguments that all the barriers to a perturbative starting point for solving QCD can be overcome, at least in principle, when a light-front framework is used. We present the basic formulation for such an approach. Coupled to the choice of coordinates are the introduction of nonzero masses for both quarks and gluons, the use of cutoffs on constituent momenta which eliminate vacuum degrees of freedom, and the addition of an artificial stabilizing and confining potential which vanishes at the relativistic value of the renormalized coupling but nowhere else. One result of these unconventional modifications is a theory with a trivial vacuum. However, the theory has extra terms in the Hamiltonian which are induced by the elimination of vacuum

*Present address: Institute of Physics, Academia Sinica, Taipei 11529, Taiwan, ROC.

degrees of freedom, which account for spontaneous chiral symmetry breaking, yet can be treated perturbatively. It is a theory where a second-order treatment of renormalization effects should closely resemble the phenomenological CQM, while a fourth-order treatment, if all goes well, should begin to replace phenomenology by true results of QCD. We have not carried out these computations but will outline them to show that they are indeed perturbative ones.

Our basic aim, then, is to tailor an approach to QCD which is based on the phenomenologically successful approach of the CQM. Central to our formulation is to start with nonzero masses for both quarks and gluons and to then consider the case of an arbitrary coupling constant g which is small even at the quark-gluon mass scale—a running coupling which is then small everywhere because below this scale it cannot run anymore. This means sacrificing manifest gauge invariance and Lorentz covariance, with these symmetries only being implicitly restored (if at all) when the renormalized coupling is increased to its relativistic value, which we call g_s. The value g_s is a fixed number because it is measured at the hadron mass scale, and by asymptotic freedom arguments such a coupling has a fixed value. For smaller values of g our theory lacks full covariance and is not expected to have the predictive power of QCD, but it allows phenomenology to guide renormalization and is defined to maximize the ease of perturbative computations and extrapolation to g_s.

Some key new ideas in this paper have previously been reported only in unpublished notes [1–5]. Some have been presented in a condensed form in Ref. [6]. These ideas underly two main parts of this paper. The first part is a qualitative power counting analysis of divergences in light-front QCD (LFQCD), which provides a vital basis for the new cutoff scheme and renormalization framework we develop in the second part. More broadly, this paper draws on a range of previous research efforts by the authors and colleagues: The QCD calculations presented in this paper are largely based on the standard gauge-fixed LFQCD Hamiltonian [7], and the specific diagrammatic rules used here are defined with examples in Refs. [8–10] following earlier work [11]. This paper follows recent work on QCD [8–10,12,13] and the similarity renormalization scheme [14,15]; and it is also the outgrowth of a line of research that covers the Tamm-Dancoff approximation [16], light-front QED [17], and light-front renormalization [18]. The relation of this paper to the entire field of light-front field theory will be outlined in Sec. II.

The plan of the paper is as follows. As our formulation is quite different not only from previous approaches to QCD but also to previous studies of light-front dynamics, we start in Sec. II with a general overview and motivation of our approach. We discuss the apparent contradictions between QCD and its precursor, the CQM. Then we outline why a light-front approach can bridge the gap between QCD and the CQM and discuss in turn how each of the equal-time barriers to a weak-coupling treatment of QCD may be overcome. In Secs. III–V, the first major part of the paper, we motivate and discuss the light-front power-counting analysis, describe the canonical LFQCD Hamiltonian, and use a qualitative phase space cell analysis to classify the possible counterterms for ultraviolet and infrared divergences in LFQCD needed for renormalization. Light-front power counting can determine the operator structure of the LFQCD Hamiltonian [2], and we rely on the derivation from the QCD Lagrangian to determine details such as color factors. This canonical LFQCD Hamiltonian will be treated as a Hamiltonian in the many-body space of finite numbers of quark and gluon constituents, a Hamiltonian which with regularization gives finite answers in this many-body space. Three terms in the canonical Hamiltonian *itself* require infrared counterterms because of linear infrared divergences, and we proceed to construct them. We explain the absence of finite parts to many of these counterterms because kinematical longitudinal boost invariance is a scale invariance. Because of this kinematical constraint, only counterterms for logarithmic infrared divergences are allowed to contain finite parts, which as part of the renormalization process must be tuned to reproduce physical results. Counterterms to canonical terms are prime candidates for bringing in phenomena associated with true confinement and with the spontaneously broken vacuum of normal rest frames. We distinguish true confinement in the exact theory from the artificial confinement which we introduce by hand in the weak-coupling starting point.

This leads to the second major part of the paper, where in Secs. VI–X we set up an explicit quantitative scheme for renormalization of the LFQCD Hamiltonian. First, a momentum space cutoff procedure is introduced which regulates the Hamiltonian itself rather than the individual terms of perturbation theory [3]. This cutoff scheme depends on the use of massive constituents and is chosen to ensure that each state has only a finite number of constituents. Both gauge invariance and Lorentz covariance are violated by these cutoffs, and a range of counterterms is needed to enable a finite limit as the cutoffs are removed. Restoration of the violated symmetries can only be established by examining the solution to the theory at the relativistic limit g_s (or good approximations to this solution). This is the price we must pay for achieving the new framework. We proceed to the construction of the effective Hamiltonian. We begin by discussing a novel perturbation theory formalism due to Głazek and Wilson [14,15] designed to transform a cutoff Hamiltonian to band-diagonal form while avoiding small energy denominators that plague other approaches [19]. This is called the "similarity renormalization scheme." The end product of the scheme is a band-diagonal effective Hamiltonian in which dependence on the original cutoffs has been removed to any desired order of perturbation theory. As an example we determine in detail the gluon mass counterterms necessary to remove second-order divergences generated by two-gluon intermediate states. We then proceed to construct order g^2 light-front infrared counterterms, and we identify finite counterterms that may be necessary to compensate for the removal of zero longitudinal momentum modes from the cutoff theory. The next step is to analyze the role of an artificial potential in the model. We use it to maintain the qualitative structure of bound states for small g, except for an overall

scale factor g^4. We argue our theory is closely analogous to a CQM if the band-diagonal Hamiltonian is computed only to order g^2. Our hope is that higher-order computations for the effective Hamiltonian will be invaluable preparation for study of the limit $g \to g_s$.

II. MOTIVATION AND OVERVIEW

A key ingredient in the constituent picture of hadrons, starting with the parton model and then moving to the quark parton model with constituent quarks and gluons, is the infinite momentum frame. The field theoretic realization of the intuitive ideas from the IMF is provided by the light-front dynamics of field theories. Recently there has been renewed interest in LFQCD because of its potential advantages over the normal equal-time formulation, especially due to the triviality of the light-front vacuum in the cutoff theory. However, a basic puzzle has remained — namely, how do confinement, chiral symmetry breaking, and other nonperturbative aspects of QCD emerge from LFQCD?

Since Dirac's formulation of Hamiltonian systems in light-front coordinates [20] and the development of the infinite momentum frame limit of equal-time field theory [21], there has been intermittent progress in this area, initially driven by the recognition of its importance for current algebra [22] and the parton model [23], but later slowed by the many renormalization problems inherent to Hamiltonian field theory. After early progress towards understanding light-front field theory [24], theorists began to consider light-front QCD [7]. No clearly successful approach to nonperturbative QCD emerged, and so some theorists tried to make progress on technically simpler problems such as (1+1)-dimensional field theory [25] and bound states in QED and the Yukawa model in 3+1 dimensions [26]. More recently there has also been much work on the light-front zero-mode problem [27], primarily by theorists who advocate a different approach to the vacuum problem than that developed in this paper— the relationship between most of this work and ours is at present obscure. Unfortunately, the barriers that are discussed in this paper have hindered theorists from attacking nonperturbative QCD in 3+1 dimensions, and so recent work on light-front field theory has not focused on the light-front problem that is of greatest practical interest.

In this paper we establish a new framework for studying QCD in light-front coordinates by building from an unconventional choice of the bare cutoff Hamiltonian. The basic question we try to answer is the following: Can one set up QCD to be renormalized and solved by the same techniques that solve QED, namely, a combination of weak-coupling perturbation theory and many-body quantum mechanics? The changes from the standard approach in QED we introduce are (a) the use of light-front dynamics, (b) the use of nonzero masses for both quarks and gluons, (c) the need to handle relativistic effects which give rise to, for example, asymptotic freedom in QCD, which in turn leads to a fairly strong renormalized coupling constant and hence relativistic binding energies, (d) the presence of artificial stabilizing and confining potentials which vanish at relativistic values of the coupling constant but nowhere else, and (e) the concerns about light-front longitudinal infrared divergences, which cancel perturbatively in QED because of gauge invariance. Our theory is not gauge invariant order by order because we use a nonzero gluon mass. Moreover, we propose that these noncanceling divergences are necessarily the sources of true confining potentials and chiral symmetry breaking in QCD. With the cutoff Hamiltonian we have a trivial vacuum. Furthermore, the free part of the cutoff Hamiltonian exhibits exact chiral symmetry despite the existence of a quark mass. (In the canonical light-front Hamiltonian, chiral symmetry is explicitly broken only by the helicity flip part of the quark-gluon interaction. The free Hamiltonian itself only breaks chiral symmetry if zero mode quarks are included.) We expect light-front infrared divergences to be sources of confinement and chiral symmetry breaking because these are both vacuum effects in QCD, and we show that vacuum effects can enter the light-front theory through light-front longitudinal infrared effects. Because of the unconventional scaling properties of the light-front Hamiltonian, these effects include renormalization counterterms with whole functions to be determined by the renormalization process.

The basic motivation for our approach is physical rather than mathematical. Physically, one's unperturbed or starting Hamiltonian is supposed to model the physics one is after, at least roughly. A Hamiltonian with nonzero (constituent) quark and gluon masses and confining potentials is closer to the physics of strong interactions than a Hamiltonian with zero mass constituents and no confining potentials. Then, in the spirit of QED, we analyze renormalization effects with the confining potential itself treated perturbatively, but only to generate an effective few-body Hamiltonian which can be solved nonperturbatively.

A. Constituent quarks versus QCD

Prior to the establishment of QCD as the underlying theory of strong interactions, there arose the constituent quark model [28] and Feynman's parton model [23]. The CQM provides an intuitive understanding of many low-energy observables. The parton model provides an intuitive understanding of many high-energy phenomena. Then QCD came along, and along with it came the commonly accepted notion that the vacuum of QCD is a very complicated medium. Unfortunately, this is the source of a contradiction between the constituent quark picture and QCD, and 20 years of study of QCD have done little to weaken that contradiction.

The complicated vacuum of QCD plays a crucial role in invalidating any perturbative picture of isolated quarks and gluons. One important function of the vacuum is to produce confining interactions among quarks and gluons at large distances, thus overturning the nonconfining gluon exchange potential of perturbation theory. Another important function of the vacuum is to provide the

spontaneous breaking of chiral symmetry. The equal-time QCD vacuum is an infinite sea of quarks and gluons, and baryons and mesons arise as excitations on this sea. Unfortunately, individual quarks and gluons are lost in this infinite sea.

According to the CQM, however, a meson is a simple quark-antiquark bound state and a baryon is a bound state of three quarks, and Zweig's rule suppresses particle production in favor of rearrangement of constituents. But how can the hadrons be simply a quark-antiquark or a three quark bound state if they are excitations over a complicated vacuum state? One may hope that the effects of quarks and gluons in the vacuum may be treated via weak-coupling perturbation theory. Unfortunately, the coupling of quarks and gluons in the vacuum grows in strength as the average momentum of these constituents decreases as a result of asymptotic freedom. Thus one expects the density of low-momentum constituents in the vacuum to be quite large, thereby invalidating any perturbative treatment of vacuum effects.

The CQM, as we conceive it, requires that both quarks and gluons have sizable masses. For gluons, this violates the gauge invariance of QCD. For quarks, this violates the rule that chiral symmetry is not explicitly broken only for massless quarks.

On the other hand, many high-energy phenomena are most naturally described in the language of the parton model. The constituent picture and the probabilistic interpretation of distribution functions are essential for the validity of the parton model. But it is not at all easy to reconcile the probabilistic picture with the notion of a nontrivial vacuum in the equal-time framework. Thus both the constituent quark model and the parton model are put in peril by QCD with a complicated vacuum structure.

At first glance, the blame for the contradiction rests with the naiveté of the constituent picture. Equal-time QCD seems to clearly indicate that any few-body, perturbative approach to hadron bound states is unfounded. However, in light-front dynamics we argue that the CQM and QCD can be reconciled so that the apparent contradictions disappear.

B. Why the light-front and massive constituents?

A constituent picture of hadrons is certainly very natural in a nonrelativistic context. However, particle creation and destruction need to be a part of any realistic picture of relativistic bound states. Is it possible to build a relativistic constituent picture of hadrons based on nonrelativistic, few-body intuitions?

As pointed out long ago, the most serious obstacles to this goal are overcome by changing to light-front coordinates (the "front-form" in Dirac's original work [20]), or moving to the IMF [21,23,29,30]. In light-front quantization one quantizes on a surface at fixed light-front time, $x^+ = t + z$ (see Fig. 1), and evolves the system using a light-front Hamiltonian P^-, which is the momentum conjugate to x^+. A longitudinal spatial coordinate $x^- = t - z$ arises, with its conjugate longitudinal momentum being P^+.

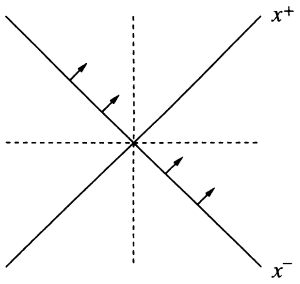

FIG. 1. Light-front coordinate system.

The possibility of building a constituent picture in light-front field theory rests on a simple observation. All physical trajectories lie in or on the forward light cone. This means that all physical trajectories lie in the first quadrant of the light-front coordinate system, so that all longitudinal momenta satisfy the constraint

$$k^+ \geq 0. \tag{2.1}$$

By implementing any cutoff that removes degrees of freedom with identically zero longitudinal momentum, one forces the vacuum to be trivial because it can carry no longitudinal momentum.

For a free massive particle on shell ($k^2 = m^2$), the light-front energy is

$$k^- = \frac{k_\perp^2 + m^2}{k^+}, \tag{2.2}$$

where $k_\perp$ is the transverse momentum. This means that the zero-momentum states we must remove to create a trivial vacuum in theories with positive m^2 have infinite energy unless $k_\perp = 0$ and $m = 0$. This makes it sensible to replace the zero-momentum modes with effective interactions, since this is exactly the strategy used when renormalizing divergences from high-energy degrees of freedom in equal-time field theory. However, such a starting point may be far removed from the canonical field theory.

When field theories simpler than QCD are analyzed in light-front coordinates, it becomes apparent that the assumption of a trivial vacuum can be misleading. If $m^2 < 0$ because of spontaneous or dynamical symmetry breaking, constituents may have exactly zero longitudinal momentum (known as "zero modes") and still have finite energy. In this case the physical vacuum is free to contain an arbitrarily large number of zero longitudinal momentum constituents. The importance of zero modes is most simply illustrated in models with spontaneous symmetry breaking such as the σ model. In the case of the σ model, however, using power-counting arguments and demanding current conservation (see Appendix A) one can easily determine the counterterms needed to preserve the physics, at least on the canonical or tree level, for a theory in which zero modes are removed. We compare and contrast the σ model with and without the zero modes removed. Both are reasonable theories, but the phenomena of the two theories must be described with different languages. The discussion of Appendix A in-

dicates that an alternative way to realize the dynamics of spontaneous symmetry breaking on the light-front is to force the vacuum to be trivial and to include counterterms in the Hamiltonian which are based on power counting and explicitly break chiral symmetry. In Appendix A it is shown that current conservation can be used to fix these counterterms. It has also been shown in Ref. [32] that in some cases one can use the renormalization group and coupling coherence, which is discussed below, to fix such counterterms.

The analysis of QCD is far more complicated than that of the σ model. In QCD, the signal of spontaneous symmetry breaking is still a vanishing pion mass, but the pion is now a composite state. For the weak-coupling starting point, we require all hadrons including the pion to have masses that are close to the sum of their constituent quark masses. One might imagine other limiting procedures, but we require our starting point to be perturbative and the pion cannot be massless initially with this criterion. As the coupling increases, the pion mass must decrease toward zero if spontaneous chiral symmetry breaking is to be recovered as $g \to g_s$. The pion mass should be a continuous function of the coupling, and so it cannot reach zero until the coupling reaches its physical value g_s; it does so only after the inclusion of renormalization effects. In contrast, the σ model illustrates spontaneous symmetry breaking even for arbitrarily small coupling. Thus the complete determination of the terms necessary to counter the elimination of zero modes in QCD will not be simple.

But the major problem in LFQCD is not the question of zero modes. To even address the role of zero modes we need a reliable, practical calculational framework. LFQCD has severe infrared divergences arising from small longitudinal momenta when we eliminate the zero modes [7,12,8–10]. These infrared divergences are separate from and in addition to the infrared problems of equal-time QCD. In equal-time QCD, infrared problems arise due to both zero quark and gluon masses and to the growth of the running coupling constant in the infrared domain. In LFQCD the same infrared problems also exist, but they are divergences associated with small transverse momenta, which are the only momenta that combine directly with masses. The longitudinal infrared divergences are special to LFQCD and for this reason it is normally presumed that they will cancel out if treated properly. An essential part of this supposed cancellation is the maintenance of gauge invariance. To preserve manifest gauge invariance in QCD in perturbation theory one needs massless gluons and carefully chosen regularization schemes. With massless gluons, however, the running coupling constant increases without bound when the energy scale is of the order of hadronic bound state energies. Thus one needs all orders of perturbation theory to compute observables in the hadronic bound state range. But all orders of perturbation theory involve arbitrary numbers of quarks and gluons as intermediate states, thus contradicting the notion that hadrons are mostly a quark-antiquark or three-quark bound state. It is this problem that has caused us to abandon manifest gauge invariance in favor of a weak-coupling picture in which gluons have mass.

Suppose we consider a light-front Hamiltonian whose free part corresponds to that of massive quarks and gluons. What is the justification for taking massive gluons in the free part of the Hamiltonian? As is always the case, the division of the Hamiltonian into a free part and an interaction part is arbitrary; however, it is also true that the convergence of a perturbative expansion depends crucially on how this choice is made. We are free to take advantage of this arbitrariness; we choose the free gluon part of the bare cutoff Hamiltonian to be that of massive gluons. (In QED, in contrast, where electrons and photons appear as free particles in asymptotic scattering states, it would be more difficult to exercise this freedom.) Furthermore, as we show in Sec. XIII, the cutoffs we employ inevitably introduce quadratic mass renormalization for quarks and gluons; thus the bare quark and gluon masses are tunable parameters. Of course, the crucial question is what the renormalized masses used for the bound state computations will be: These might be of the order that phenomenology assigns to constituent quarks and gluons. (In QED, one would tune the bare masses to reproduce physical masses; in QCD, we must tune to fit bound state properties.)

The fact that we are giving the gluon a mass should not create any contradiction with asymptotic freedom when g achieves its relativistic value g_s. The reason is that g_s is a running coupling constant g_Λ at a scale where Λ is of the same magnitude as hadronic masses, $\Lambda \sim \Lambda_{\rm QCD}$. g_Λ is small at extremely large momentum scales, and the running scale is $\Lambda \approx \Lambda_{\rm QCD} e^{c/g_\Lambda^2}$ for small running g_Λ, where c is a positive constant. But changes to amplitudes due to masses can be treated perturbatively at such scales and behave as powers of $\Lambda_{\rm QCD}/\Lambda \approx e^{-c/g_\Lambda^2}$, which vanishes to all orders in a perturbative expansion in powers of g_Λ.

Once we assume the free part to consist of massive gluons, what are the consequences? A gluon mass automatically prevents unbounded growth of the running coupling constant below the gluon mass scale and provides kinematic barriers to unlimited gluon emission. It eliminates any equal-time-type infrared problems. With nonzero quark and gluon masses it is also possible to develop a cutoff procedure for the Hamiltonian such that if the cutoffs are imposed in a specific frame, a large number of states (the upper limit of whose invariant masses are guaranteed to be above a large cutoff) is still available for study even in boosted frames. Another consequence of nonzero gluon mass is that the long-range gluon exchange potential between a pair of quarks is too small in transverse directions, falling off exponentially. Hence an artificial potential must be added to provide a full strength potential to yield realistic bound states for small g.

C. Light-front infrared divergences

Our basic objective is to establish a weak-coupling framework for studying QCD bound states, so that one can smoothly approach the strong-coupling limit and use

bound state phenomenology to guide renormalization. We have argued that the choice of light-front dynamics, massive quarks and gluons, and a particular cutoff scheme eliminates the traditional barriers to a perturbative treatment of QCD. The first step, then, is the construction of a bare Hamiltonian which incorporates confining potentials, massive quarks and gluons, and a trivial vacuum. The cutoffs will violate Lorentz and gauge symmetries, forcing the bare Hamiltonian to contain a larger than normal suite of counterterms to enable a finite limit as the cutoffs are removed.

Now in the equal-time theory, the QCD vacuum is thought to be a complicated medium which presumably provides both confinement and the spontaneous breaking of chiral symmetry. But in the light-front theory with a suitably cutoff Hamiltonian, we have asserted that the vacuum is trivial. So we have to find other sources for confinement and spontaneous chiral symmetry breaking in the cutoff theory. A natural place to look for them is in the divergences associated with light-front infrared singularities.

Explicitly, suppose we regulate infrared divergences (where $k_i^+ \to 0$) by cutting off the longitudinal momentum of each constituent i so that $k_i^+ > \epsilon$, with ϵ a small but finite positive constant. (We will also need to regulate ultraviolet divergences by cutting off large transverse momenta, for example, via $k_\perp^2 < \Lambda^2$, but this is not important for the present discussion.) Because the total longitudinal momentum P^+ of a state is just the sum of the longitudinal momenta of its constituents, $P^+ = \sum_i k_i^+$, it follows immediately that the vacuum of the cutoff theory (for which $P^+ = 0$) contains no constituents; that is, the vacuum is trivial. Moreover, any state with finite P^+ can contain at most P^+/ϵ constituents. Therefore, effects which in an equal-time formulation are due to infinite numbers of constituents, in particular, confinement and chiral symmetry breaking, must have other sources in the cutoff theory on the light front. The obvious candidates are the counterterms which must be introduced in the effective Hamiltonian in order to eliminate the dependence of observables on the infrared cutoff ϵ. Of special interest are counterterms that reflect consequences of zero modes (namely, modes with $k^+ = 0$) in the full theory (see discussions in Secs. IV B and XI).

Now in the canonical Hamiltonian, one particular term of interest is the instantaneous interaction in the longitudinal direction between color charge densities, which provides a potential which is linear in the longitudinal separation between two constituents that have the same transverse positions. In the absence of a gluon mass term, this interaction is precisely canceled by the emission and absorption of longitudinal gluons. The presence of a gluon mass term means that this cancellation becomes incomplete. But what is still lacking is the source of transverse confining interactions.

According to power-counting arguments, the counterterms for longitudinal light-front infrared divergences may contain functions of transverse momenta [2], and there exists the possibility that the *a priori* unknown functions in the finite parts of these counterterms will include confining interactions in the transverse direction. The $g \to g_s$ limit may then be smooth if such confining functions are actually required to restore full covariance to the theory. In the absence of a gluon mass term, the light-front singularities are supposed to cancel among each other in physical amplitudes. This has been verified to order g^2 explicitly in perturbative amplitudes for quarks and gluons rather than physical states, to order g^3 for the quark-gluon vertex [12,10], and to order g^4 in the gluon four-point function [33]. A gluon mass term in the free part of the Hamiltonian, however, spoils this cancellation. What are the consequences?

The light-front infrared singularities give rise to both linear and logarithmic divergences. The linear divergences, however, contain the inverse of the longitudinal cutoff $\frac{1}{\epsilon}$, which violates longitudinal boost invariance, and hence the infinite parts of the counterterms for these divergences also violate longitudinal boost invariance. Thus finite parts for these counterterms are prohibited by longitudinal boost invariance, which is a kinematical symmetry. So we have to analyze logarithmic infrared divergences in order to get candidates for transverse confinement.

There is a specific problem that the complexity of the counterterms creates. In covariant perturbation theory every coupling or mass introduced by renormalization becomes an independent parameter. One might worry that the appearance of whole functions as counterterms could destroy the predictive power of the theory because functions include an infinite number of parameters and may seem to destroy the renormalizability of the theory. We discuss the resolution of this problem at the end of Sec. V.

D. Zero modes and chiral symmetry breaking

How does chiral symmetry breaking arise in the light-front theory with the zero modes removed? The removal of the zero modes has two important consequences for chiral symmetry in LFQCD—namely, the vacuum is trivial, and chiral symmetry is exact for free quarks of any mass. The consequence of a trivial vacuum is that, as with the σ model, the mechanism for effects associated with spontaneous chiral symmetry breaking in the equal time theory will be far different in LFQCD. The consequence of chiral symmetry being exact for massive constituents means that the mechanism for effects associated with explicit chiral symmetry breaking in equal time will also be quite different in LFQCD. We discuss these points further in this subsection but leave most details of the light-front chiral transformation to Appendix B. We just note here for the discussion which follows that the fermion field naturally separates into two-component fields $\psi = \psi_+ + \psi_-$ on the light front, where ψ_+ is dynamical and ψ_- is constrained. The light-front chiral transformation applies freely only to the two-component field ψ_+ [34], because the constraint equations are inconsistent with the chiral transformation rules when explicit breaking is present.

In light-front dynamics chiral symmetry is exact for free quarks of any mass once zero modes have been re-

moved. This is because chiral charge conservation is simply the conservation of light-front helicity, which is a fundamental property of free quarks in light front dynamics in the absence of zero modes (see Appendix B). Despite the conservation of chiral charge, the local chiral current is not conserved. The divergence of the chiral current remains $2im_F\bar{\psi}\gamma_5\psi$. How does one reconcile the conservation of light-front chiral charge with the nonconservation of the axial vector current? From the chiral current divergence equation, the light-front time derivative of the chiral charge is proportional to $\int dx^- d^2x_\perp \bar{\psi}\gamma_5\psi$. When the fields in this integral are expanded in terms of momentum eigenstates, the diagonal terms $b^\dagger b$ and $d^\dagger d$, where b and d are the quark and antiquark annihilation operators, vanish; namely, the matrix elements multiplying them vanish. Moreover, the off-diagonal terms $b^\dagger d^\dagger$ and bd vanish if the zero modes are absent. Thus it is the absence of zero modes which makes it possible for the light-front chiral charge to be conserved irrespective of the nonconservation of the axial vector current for free massive fermions. The light-front time derivative of the chiral charge can avoid vanishing only if "zero-mode quarks and antiquarks" (quarks and antiquarks with exactly zero longitudinal momentum) are permitted to exist. But the cutoffs we use prevent this possibility, and hence chiral symmetry is exact for all free quarks *in the cutoff theory.*

In normal reference frames, the absence of a mass term implies conservation of the axial vector current and hence a conserved axial charge. Given a conserved axial vector current, there are two possibilities: (a) The axial charge annihilates the vacuum, in which case as a consequence of Coleman's theorem ("invariance of the vacuum is the invariance of the world") the symmetry is reflected in the spectrum of the Hamiltonian—that is, we expect degenerate parity doublets in the spectrum; or (b) the axial charge does not annihilate the vacuum, in which case one talks about the spontaneous breaking of chiral symmetry, as a consequence of which massless Nambu-Goldstone bosons should exist. In the real world, the pion, the Goldstone boson, is very light, and the second possibility is thought to be realized. The nonzero mass of the pion is thought to arise from the *explicit* symmetry-breaking terms in the Lagrangian, namely, the small current quark masses.

On the light-front, in the absence of interactions, massive quarks in the cutoff theory do not violate the chiral symmetry of the light-front Hamiltonian thanks to the cutoffs. Now consider interactions in the gauge theory. There remains one explicit chiral-breaking term in the canonical Hamiltonian (see Sec. IV):

$$gm_F \int dx^- d^2x_\perp \psi_+^\dagger \sigma_\perp \cdot \left(A_\perp \frac{1}{\partial^+}\psi_+ - \frac{1}{\partial^+}(A_\perp \psi_+) \right). \tag{2.3}$$

This term, which involves gluon emission and absorption, is linear in the quark mass and couples the transverse gluon field $A_\perp$ to the Dirac matrix $\gamma_\perp$ (actually, the Pauli matrix $\sigma_\perp$ in the two-component notation above), which causes a helicity flip. In the free quark Hamiltonian, $\gamma_\perp$ does not appear, and the quark mass appears only squared. Now the bare cutoff Hamiltonian has canonical terms and counterterms. The chiral charge still annihilates the vacuum state, which is just a kinematical property of the cutoff theory, despite the fact that the chiral charge no longer commutes with even the canonical cutoff Hamiltonian. Thus the vacuum annihilation property of the chiral charge in the cutoff theory has nothing to do with the symmetry of the Hamiltonian and does not appear to have any dynamical consequences. The concept of spontaneous symmetry breaking seems to have lost its relevance in the cutoff theory.

But the pion should emerge as an almost massless particle. How does this become possible on the light-front without zero modes? We may take a hint from the σ model with the zero modes removed, as discussed in Appendix A. In that model terms which explicitly violate the symmetry must be added to the Hamiltonian to yield a conserved chiral current, and at the same time the pion must be held massless. In QCD, the elimination of these modes directly results in effective interactions. The effective interactions (the counterterms in the cutoff theory) can explicitly violate chiral symmetry, yet still *persist* in the limit of zero quark mass. Since spontaneous breaking of chiral symmetry in normal frames is a vacuum effect, we look for interaction terms that are sensitive to zero mode quarks and antiquarks. There is a term in the canonical Hamiltonian of the form

$$g^2 \int dx^- d^2x_\perp \psi_+^\dagger \sigma_\perp \cdot A_\perp \frac{1}{i\partial^+}(\sigma_\perp \cdot A_\perp \psi_+), \tag{2.4}$$

which contains an instantaneous fermion. Some of the interactions which correspond to this term are shown diagrammatically in Fig. 2. These interactions by themselves do not violate chiral symmetry. However, since they are sensitive to fermion zero modes, the counterterms for these interactions need not be restricted by chiral symmetry considerations. The only requirement we can impose is that they obey light-front power counting criteria.

We show later that there are explicit chiral-symmetry-breaking terms which satisfy the power counting restriction. We add such terms to our Hamiltonian. As a result of renormalization, in addition to the emergence of noncanonical explicit symmetry violating terms, the canonical symmetry violating term of Eq. (2.3) is also renormalized. Because of the effects of explicit chiral-symmetry-breaking terms on this renormalization, the coefficient m_F of this symmetry-violating term in the cutoff Hamiltonian need not be zero, even when the full relativistic theory has only spontaneous breaking of chi-

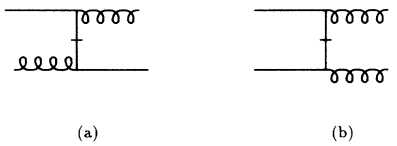

FIG. 2. Examples of instantaneous interactions sensitive to fermion zero modes.

ral symmetry. In fact, in the limit in which chiral symmetry is broken only spontaneously, the same constituent mass scale may appear in both the kinetic energy and the symmetry-breaking interactions. This allows the quark constituent mass to set the scale for most hadron masses, and yet enables chiral-symmetry-breaking interactions to be sufficiently strong to make the pion massless. Thus light-front power-counting criteria and renormalization allow us to introduce effective interactions which explicitly break chiral symmetry and yet may still ensure a massless pion in the relativistic limit $g \to g_s$.

E. Artificial potential

The task of solving the light-front Hamiltonian at the relativistic value of g is far too difficult to attempt at the present time. Instead the goal of this paper is to define a plausible sequence of simpler computations that can build a knowledge base which enables studies of the full light-front Hamiltonian to be fruitful at some future date.

A crucial step in simplifying the computation is the introduction of an artificial potential in the Hamiltonian.

A primary rule for the artificial potential is that it should vanish at the relativistic limit. For example, the artificial potential might have an overall factor $(1-g^2/g_s^2)$ to ensure its vanishing at $g = g_s$. This rule leaves total flexibility in the choice of the artificial potential since no relativistic physics is affected by it.

The first role we propose for the artificial potential is that it ensure that the bound state structure of the theory at very small g is similar to the actual structure seen in nature. However, we also want the weak-coupling behavior of the theory to be similar to QED in weak coupling. This will ensure that methods of computation already developed for QED will be applicable. To ensure these connections we propose to structure the artificial potential so that bound state energies all scale as g^4 for small g, just as QED bound state energies scale as e^4. We then demand a reasonable match to experiment when the scale factor g^4 is set to g_s^4, even when higher-order corrections (of order g^6, g^8, etc.) are neglected.

The second role of the artificial potential is to remove unfortunate consequences of the nonzero gluon mass from the gluon exchange potential. Because of the nonzero mass, the gluon exchange potential falls off too rapidly in the transverse direction, while being too strong in the longitudinal direction. In the longitudinal direction there is an instantaneous linear potential of order g^2 which normally would be completely canceled by the one-gluon exchange, but because of the nonzero mass, the cancellation is incomplete. Without the artificial potential there are even instabilities that prevent the existence of stable bound states at weak coupling. More details on these instabilities are given in Sec. X B.

The third role we assign to the artificial potential is to give the weak-coupling theory a structure close to the CQM so that past experience with the quark model can be used to determine the precise form of this potential and to fit it to experimental data. To ensure this we will define an initial calculation which involves QCD complications only in a very minimal form.

The final role of the artificial potential is to incorporate a linear potential in both the longitudinal and transverse directions to ensure quark confinement for any g. This is important for phenomenology. It is also needed for studying the roles of a linear potential and where it might originate, especially in the relativistic limit where the artificial potential vanishes.

Only broad principles will be laid down here for the artificial potential. Its construction in detail will require a collaboration between specialists in the CQM and in QCD perturbation theory.

The basic need is to incorporate the qualitative phenomenology of QCD bound states into the artificial potential. This qualitative phenomenology comes from three sources: kinetic energy, Coulomb-like potentials, and linear potentials. We propose that all three terms should be present in the weak-coupling Hamiltonian and all should have the same overall scaling behavior with g in bound state computations, namely, g^4. The kinetic and Coulomb-like terms can be constructed directly from the canonical Hamiltonian combined with a one-gluon-exchange term, the latter obtained for the case of zero gluon mass. The Coulomb term, if represented in position space, has the usual form g^2/r, except that the definition of r we propose is

$$r = \sqrt{\frac{(p^+\delta x^-)^2}{m_c^2} + \delta x_\perp^2} \tag{2.5}$$

and there actually are two terms which are added:

$$\mathcal{V}_C = g^2 \frac{1}{2}\left[\frac{m_c}{p^+ r} + \frac{m_c'}{p'^+ r'}\right], \tag{2.6}$$

where δx^- is the light-front longitudinal separation of two constituents, $\delta x_\perp$ the transverse separation, m_c the constituent mass, and p^+ the constituent longitudinal momentum. The prime refers to the second of the two constituents. The p^+/m_c in the definition of r ensures that the dimensions match. The positive or negative SU(3) charges must also be inserted. See Appendix C for details.

A few comments regarding the form of the Coulomb potential are in order here. Our nonrelativistic limit is $g \to 0$ and not the $m_c \to \infty$ limit studied earlier in Ref. [35]. In this limit p^+ is held fixed while δx^- scales as $\frac{1}{g^2}$. In light-front coordinates, the factor p^+ is necessary for dimensions as already stated and in the nonrelativistic limit p^+ is proportional to the center of mass momentum of the bound state independent of the relative coordinate δx^-. Relativistically, r will need a careful definition to avoid possible disastrous behavior when $p_1^+ \ll p_3^+$ or vice versa; this problem has not been studied. Also in the relativistic case, p^+ does not commute with δx^-, and so $p^+\delta x^-$ must be symmetrized to preserve Hermiticity.

Finally, we need a linear potential term—terms proportional to r and r'. In Coulomb bound states, both are of order $1/g^2$. Hence to achieve an energy of order g^4, the linear potential must have a coefficient of order g^6. Thus the linear potential term, in position space,

would be proportional to $g^6 r$. To be precise, and get dimensions straight, its form is

$$\mathcal{V}_L = g^6 \beta \Big[\frac{m_c^3 r}{p^+} + \frac{m_c'^3 r'}{p'^+} \Big], \tag{2.7}$$

with β a numerical constant.

The linear potential needs to exist between all possible pairs of constituents: qq, $q\bar{q}$, $\bar{q}\bar{q}$, qg, $\bar{q}g$, and gg, where q, $\bar{q}$, and g stand for quark, antiquark, and gluon, respectively. The linear potential must always be positive (confining) rather than negative (destabilizing). We show in Sec. X B that it cannot involve products of SU(3) charges as the Coulomb term does. The Coulomb term could be given a Yukawa structure rather than the pure g^2/r term. All of the potential has to be Fourier transformed to momentum space and then restricted to the allowed range of both longitudinal and transverse momenta after all cutoffs have been imposed.

The artificial potential must also contain counterterms that remove the unwanted components of the one-gluon-exchange and instantaneous-gluon terms. Thus in addition to the order g^6 linear potential, linear in both the longitudinal and transverse directions, there is a subtraction to remove the order g^2 linear potential in the longitudinal direction. The potential removed is the potential that remains after the incomplete cancellation of the instantaneous potential in the canonical Hamiltonian by one-gluon-exchange terms.

To ensure that the artificial potential vanishes at g_s without destroying its weak-coupling features, the subtraction term has to be treated with care. We suggest the subtracted linear potential be multiplied by $(1 - g^6/g_s^6)$ so that the subtraction begins to be negated only in order g^8, which is smaller for small g than the artificial g^6 linear potential that needs to be dominant. All other terms in the artificial potential can be multiplied by $(1 - g^2/g_s^2)$ instead.

To ensure that the Coulomb term shows Coulomb behavior, at least roughly, at typical bound state sizes, it is important that the mass used in any Yukawa-type modification of the Coulomb term scale as g^2 rather than being a constant mass.

Finally, the linear potential should be invariant to the full $SU(6)_W$ flavor-spin symmetry of light-front quarks and antiquarks discussed by Lipkin and Meshkov [36], leaving all $SU(6)_W$ violations to come from quark masses in the kinetic energy, Coulomb terms, and the more complex renormalization subtractions. This means that the quark mass scale appearing in the linear potential will be the same for up and down quarks.

The artificial potential would be added to the cutoff canonical Hamiltonian. Then a complete set of counterterms would have to be added to ensure that the theory has a limit as the cutoffs are removed.

The artificial potential is designed to allow confined few-body states to emerge from a field theory. The constraints that dictate its design are severe, and the type of potential we have discussed is the simplest we have found that meets these constraints and does not require large cancellations that thwart a constituent picture. However, this potential has serious flaws. Probably its worst flaw is that it confines everything including color singlets to a single region of space. Any confining interaction that is purely attractive between all particles does not produce scattering states. QCD must manage to produce strong attractive forces between color charges as they separate, without producing such strong forces between color singlets. In lattice gauge theory this is arranged through gauge invariance, which forces links to exist between color charges but not between color singlets. In a field theory calculation without manifest gauge invariance, there is no such obvious mechanism to turn strong forces on and off by hand. Higher-order calculations will hopefully provide clues to how QCD produces the important phenomenological effects of our artificial potential, without producing the unwanted side effects.

III. LIGHT-FRONT POWER COUNTING: CANONICAL STRUCTURE

To construct the bare cutoff LFQCD Hamiltonian with counterterms we will try to follow the procedure adopted in standard canonical covariant theory as much as possible. In the canonical theory, when we begin the analysis the bare cutoff Lagrangian is unknown since the counterterms are unknown prior to the analysis. One can perform perturbative calculations and determine the counterterms order by order in perturbation theory. If one starts with the canonical terms, which include all the possible terms in accordance with covariance and power counting, and if one maintains manifest covariance and gauge invariance at all stages of the calculation, one finds that the counterterms are also of the same form as the canonical terms. Thus in the standard procedure the only unknown parameters are just constants, namely, masses and coupling constants.

Because we are interested in the cutoff light-front Hamiltonian, we cannot use covariance as a guide. Instead we have to consider power counting based on the limited kinematical symmetries of the light front. As discussed in Sec. III C, one consequence of the use of light-front coordinates is that counterterms may contain entire functions of momenta, which is of course a radical difference from renormalization in an equal-time formulation. Before discussing renormalization, however, we establish in this section the power-counting rules for determining the possible structure of operators in the canonical Hamiltonian.

A. Light-front power counting

Light-front power counting is in terms of the longitudinal coordinate x^- and the transverse coordinate $x_\perp$. Why are the two coordinates treated differently? The main objective of the power counting analysis is to deduce the most general structure of divergences that arise from increasing powers of the interaction Hamiltonian in perturbation theory. But power counting based on the kinematical symmetries of the light front is different from power counting based on the kinematical symmetries in equal-time coordinates. This is immediately transparent

from the light-front dispersion relation for free particles, $k^- = \frac{k_\perp^2+m^2}{k^+}$. Because the energy factors into separate k^+ and $k_\perp$ dependences, the subtractions are not constants. For example, when $k_\perp$ gets very large the energy diverges no matter what k^+ is. Thus, in general, we get a divergent constant *multiplied by a function of* k^+. In position space this translates into divergences at small $x_\perp$ being nonlocal in x^- and spread out over the light front. A similar result follows for the case when k^+ gets very small. This situation is to be contrasted with the equal-time case. Recall the relationship between energy and momentum in equal-time theory, $E = \sqrt{\mathbf{k}^2 + m^2}$. In this equal-time form, if $k_\perp \to \infty$ while k_z is fixed, the k_z dependence becomes negligible and arbitrary functions of k_z cannot arise.

When we analyze the canonical light-front Hamiltonian, we confirm that indeed it does scale differently under x^- and $x_\perp$ scaling (strictly speaking, a unique transverse scaling behavior holds only in the absence of masses). To determine the scaling properties of the canonical Hamiltonian it is useful to recall the canonical equal-x^+ commutation relations obeyed by the field variables in the two-component formulation [31,9]. For the two-component gluon field variables $A_a^i, i = 1, 2$, we have

$$\left[A_a^i(x), A_b^j(y)\right]_{x^+=y^+} = -\frac{i}{4}\epsilon(x^- - y^-)\delta^2(x_\perp - y_\perp)\delta_{ij}\delta_{ab}. \tag{3.1}$$

For the two-component quark field variables $\xi(x)$ [the nonvanishing upper components of $\psi_+(x)$] we have

$$\left\{\xi_i(x), \xi_j^\dagger(y)\right\}_{x^+=y^+} = \delta^3(x-y)\delta_{ij}. \tag{3.2}$$

Consider the scaling of the longitudinal coordinate

$$x^- \to x'^- = sx^-. \tag{3.3}$$

From the canonical commutation relations (3.1) and (3.2), under this scale transformation $A^i(x^-) \to U_l^\dagger(s)A^i(x^-)U_l(s) = A^i(sx^-)$ and $\xi(x^-) \to U_l^\dagger(s)\xi(x^-)U_l(s) = s^{\frac{1}{2}}\xi(sx^-)$. $U_l(s)$ is the unitary longitudinal scaling operator. Next consider the scaling of the transverse coordinates

$$x_\perp \to x'_\perp = tx_\perp. \tag{3.4}$$

From (3.1) and (3.2), $A^i(x_\perp) \to U_t^\dagger(t)A^i(x_\perp)U_t(t) = t\,A^i(tx_\perp)$ and $\xi(x_\perp) \to U_t^\dagger(t)\xi(x_\perp)U_t(t) = t\,\xi(tx_\perp)$. Here $U_t(t)$ is the unitary transverse scaling operator. Hence, the power assignments for the field variables are

$$\begin{aligned} A_\perp &: \frac{1}{x_\perp}; \\ \xi &: \frac{1}{\sqrt{x^-}}\frac{1}{x_\perp}. \end{aligned} \tag{3.5}$$

We also need the power assignments for the derivatives

$$\begin{aligned} \partial_\perp &: \frac{1}{x_\perp}; \\ \partial^+ &: \frac{1}{x^-}; \end{aligned} \tag{3.6}$$

and the inverse longitudinal derivative

$$\frac{1}{\partial^+} \quad : \quad x^-. \tag{3.7}$$

It can be verified that under longitudinal scaling, the canonical Hamiltonian density is invariant, $\mathcal{H} \to \mathcal{H}' = \mathcal{H}$ (see Sec. IV), and the Hamiltonian

$$H \to H' = \int dx'^- d^2x_\perp \mathcal{H}' = sH. \tag{3.8}$$

So the Hamiltonian $H = P^-$ scales just like x^-, irrespective of whether there are masses present or not. Similarly, for the interaction Hamiltonian density in the absence of the helicity flip interaction, under transverse scaling $\mathcal{H} \to \mathcal{H}' = \frac{1}{t^4}\mathcal{H}$ and thus

$$H \to H' = \frac{1}{t^2}H. \tag{3.9}$$

So in the absence of masses, the Hamiltonian scales inversely as $x_\perp^2$.

The Hamiltonian we will consider also includes mass terms. Under scale transformations masses scale as constants. The Hamiltonian density for the mass term in the free part, for example, scales as $\mathcal{H} \to \mathcal{H}' = \frac{1}{t^2}\mathcal{H}$. Thus the Hamiltonian does not have a unique scaling behavior when masses are present. For dimensional analysis we assign

$$m \quad : \quad \frac{1}{x_\perp}. \tag{3.10}$$

In the presence of masses, we assign

$$\begin{aligned} \mathcal{H} &: \frac{1}{x_\perp^4}; \\ H &: \frac{x^-}{x_\perp^2}. \end{aligned} \tag{3.11}$$

These assignments have meaning only in dimensional analysis.

B. Structure of the canonical Hamiltonian from power counting

We assume that the canonical LFQCD Hamiltonian density is a polynomial in the six components m, $A_\perp$, ξ, ∂^+, $\partial_\perp$, and $\frac{1}{\partial^+}$. Then the most general structure we can build for the canonical Hamiltonian density, which has dimension $\frac{1}{(x_\perp)^4}$, is

$$(\xi\xi^\dagger)^p(A_\perp, \partial_\perp, m)^{4-2p}(\partial^+)^{-p}. \tag{3.12}$$

Here the expression $(A_\perp, \partial_\perp, m)^{4-2p}$ stands for monomials of order $4-2p$ in any combination of the three variables $A_\perp, \partial_\perp, m$. The resulting structure is

$$\begin{aligned} p=0: &\quad A_\perp^4, A_\perp^3\partial_\perp, A_\perp^2\partial_\perp^2, m^2A_\perp^2; \\ p=1: &\quad \frac{1}{\partial^+}(\xi\xi^\dagger)(A_\perp^2, A_\perp\partial_\perp, \partial_\perp^2, mA_\perp, m\partial_\perp, m^2); \\ p=2: &\quad \left(\frac{1}{\partial^+}\right)^2(\xi\xi^\dagger)^2. \end{aligned} \tag{3.13}$$

We need not specify the action of $\partial_\perp$ since we assume that the inverse of $\partial_\perp$ does not occur in the canonical Hamiltonian. But we need to specify the action of the integration operator $\frac{1}{\partial^+}$, which occurs only because of the constraint equations that eliminate the dependent variables ψ_- and A^-. From ψ_- elimination we get the structure

$$\frac{1}{\partial^+}\{(\xi,\xi^\dagger)(\partial_\perp, A_\perp, m)\}, \tag{3.14}$$

and from A^- elimination we get the structures

$$\frac{1}{\partial^+}\{\partial_\perp A_\perp\}, \left(\frac{1}{\partial^+}\right)^2\{\xi\xi^\dagger, A_\perp\partial^+ A_\perp\}. \tag{3.15}$$

We will require that inverse powers of ∂^+ only appear in these specific combinations in the canonical Hamiltonian. Subject to this constraint, we can include both positive and negative powers of ∂^+.

Specifying the precise way in which $\frac{1}{\partial^+}$ acts, we can enumerate those terms which obey our canonical rules:

$$\begin{aligned}
p=0:\quad & (A_\perp)^4, (A_\perp)^3\partial_\perp, (A_\perp)^2(\partial_\perp)^2, m^2(A_\perp)^2,\\
& (A_\perp\partial^+A_\perp)\frac{1}{\partial^+}(\partial_\perp A_\perp), (A_\perp\partial^+A_\perp)\left(\frac{1}{\partial^+}\right)^2(A_\perp\partial^+A_\perp);\\
p=1:\quad & (\xi\xi^\dagger)\left(\frac{1}{\partial^+}\right)^2(A_\perp\partial^+A_\perp), (\xi\xi^\dagger)\frac{1}{\partial^+}(\partial_\perp A_\perp);\\
& (m,\partial_\perp, A_\perp)\xi^\dagger\frac{1}{\partial^+}\{(m,\partial_\perp,A_\perp)\xi\};\\
p=2:\quad & (\xi\xi^\dagger)\left(\frac{1}{\partial^+}\right)^2(\xi\xi^\dagger).
\end{aligned} \tag{3.16}$$

Comparison with the Hamiltonian derived by the standard canonical procedure (see Sec. IV) reveals that the free terms $m^2A_\perp^2$ and $m\xi^\dagger\partial_\perp\frac{1}{\partial^+}\xi$ are absent. The absence of the first term is because of the presumed gauge invariance. A term such as the latter does appear in the free part when ψ_- is eliminated, but it is canceled by a similar term. When the smoke clears, no $\gamma_\perp$ matrices appear in the free part of the canonical Hamiltonian. Note that our list excludes terms that are equivalent through an integration by parts. This integration by parts is justified because we assume cutoffs are present (see the discussion in Sec. V).

IV. LIGHT-FRONT QCD HAMILTONIAN: CANONICAL TERMS

In the previous section we motivated the structure of allowed terms in the canonical Hamiltonian based on power counting. In this section we use the standard canonical procedure to determine the explicit form of the Hamiltonian, including color factors. This gives a Hamiltonian with terms which obey the canonical rules established in Sec. III. These canonical rules allow us to extend our Hamiltonian to include a gluon mass term, and as we demonstrate in Sec. VIII, our cutoffs will demand such a mass term to appear through renormalization even if we did not include it in the starting Hamiltonian. We choose to extend the definition of the canonical cutoff LFQCD Hamiltonian to include a massive gluon from the outset. Of course, this is just the starting point, for renormalization will eventually force us to add to our Hamiltonian counterterms which do not obey the canonical rules.

A. Canonical Hamiltonian

In this section we follow Ref. [8], to which the reader is referred for further details. The QCD Lagrangian is

$$\mathcal{L} = -\frac{1}{2}\mathrm{Tr}(F^{\mu\nu}F_{\mu\nu}) + \bar\psi(i\gamma_\mu D^\mu - m_F)\psi, \tag{4.1}$$

where $F^{\mu\nu} = \partial^\mu A^\nu - \partial^\nu A^\mu - ig[A^\mu, A^\nu]$ are the gluon field strength tensors and $A^\mu = \sum_a A_a^\mu T^a$ are the 3×3 gluon field matrices, with T^a the Gell-Mann SU(3) matrices: $[T^a, T^b] = if^{abc}T^c$ and $\mathrm{Tr}(T^aT^b) = \frac{1}{2}\delta_{ab}$. The field variable ψ describes quarks with three colors and N_f flavors, and $D^\mu = \partial^\mu - igA^\mu$ are the covariant derivatives, while m_F is a $N_f\times N_f$ diagonal quark mass matrix.

In light-front coordinates with the light-front gauge $A_a^+ = A_a^0 + A_a^3 = 0$, the Lagrangian can be *rewritten* as

$$\mathcal{L} = \frac{1}{2}F_a^{+i}(\partial^- A_a^i) + i\psi_+^\dagger(\partial^-\psi_+) - \mathcal{H} - \left\{A_a^-\mathcal{C}_a + \frac{1}{2}(\psi_-^\dagger\mathcal{C} + \mathcal{C}^\dagger\psi_-)\right\}, \tag{4.2}$$

where

$$\begin{aligned}
\mathcal{H} = {} & \frac{1}{2}\{E_a^{-2} + B_a^{-2}\} + \{\psi_+^\dagger[\alpha_\perp\cdot(i\partial_\perp + gA_\perp) + \beta m_F]\psi_-\}\\
& + \left\{\frac{1}{2}\partial^+(E_a^-A_a^-) - \partial^i(E_a^iA_a^-)\right\}
\end{aligned} \tag{4.3}$$

is the Hamiltonian density and

$$\mathcal{C}_a = \frac{1}{2}\partial^+ E_a^- - (\partial^i E_a^i + g f^{abc} A_b^i E_c^i) + g\psi_+^\dagger T^a \psi_+, \quad (4.4)$$

$$\mathcal{C} = i\partial^+ \psi_- - (i\alpha_\perp \cdot \partial_\perp + g\alpha_\perp \cdot A_\perp + \beta m_F)\psi_+. \quad (4.5)$$

Here, $E_a^- = -\frac{1}{2}\partial^+ A_a^-$, $E_a^i = -\frac{1}{2}\partial^+ A_a^i$ and $B_a^- = F_a^{12}$ are components of the light-front color electric field and the longitudinal component of the light-front color magnetic field, and ψ_+ and ψ_- are the light-front up and down components of the quark field: $\psi = \psi_+ + \psi_-$, $\psi_\pm = \Lambda_\pm \psi = \frac{1}{2}\gamma^0\gamma^\pm\psi$, where $\Lambda_+ + \Lambda_- = I$, ${\Lambda_\pm}^2 = \Lambda_\pm$, and $\Lambda_+\Lambda_- = 0$.

In (Abelian or non-Abelian) gauge theory, only two components, the transverse components, of the vector gauge potentials are physically independent degrees of freedom. From the equations of motion, it becomes clear that the independent dynamical degrees of freedom in LFQCD are the transverse gauge fields A_a^i and the up-component quark field ψ_+. The Lagrangian equations of motion lead to $\mathcal{C}_a = 0$ and $\mathcal{C} = 0$, which imply that the longitudinal gauge fields A_a^- and the down-component quark field ψ_- are Lagrange multipliers. Furthermore, in light-front coordinates the four-component fermion field can be reduced to a two-component field. The two-component quark field can be explicitly formulated in a light-front representation of the γ matrices defined by [37]

$$\gamma^+ = \begin{bmatrix} 0 & 0 \\ 2i & 0 \end{bmatrix}, \quad \gamma^- = \begin{bmatrix} 0 & -2i \\ 0 & 0 \end{bmatrix},$$

$$\gamma^i = \begin{bmatrix} -i\sigma^i & 0 \\ 0 & i\sigma^i \end{bmatrix}, \quad \gamma^5 = \begin{bmatrix} \sigma^3 & 0 \\ 0 & -\sigma^3 \end{bmatrix}. \quad (4.6)$$

Then the projection operators $\Lambda_\pm$ become

$$\Lambda_+ = \begin{bmatrix} 1 & 0 \\ 0 & 0 \end{bmatrix}, \quad \Lambda_- = \begin{bmatrix} 0 & 0 \\ 0 & 1 \end{bmatrix} \quad (4.7)$$

and

$$\psi_+ = \begin{bmatrix} \xi \\ 0 \end{bmatrix}, \quad \psi_- = \begin{bmatrix} 0 \\ \left(\frac{1}{i\partial^+}\right)[\sigma^i(i\partial^i + gA^i) + im_F]\xi \end{bmatrix}. \quad (4.8)$$

Hereafter, we shall simply let ξ represent the (two-component) light-front quark field. The canonical LFQCD Hamiltonian becomes

$$\begin{aligned} H = \int dx^- d^2x_\perp \Bigg\{ & \frac{1}{2}(\partial^i A_a^j)^2 + g f^{abc} A_a^i A_b^j \partial^i A_c^j + \frac{g^2}{4} f^{abc} f^{ade} A_b^i A_c^j A_d^i A_e^j \\ & + \left[\xi^\dagger \{\sigma_\perp \cdot (i\partial_\perp + gA_\perp) - im_F\} \left(\frac{1}{i\partial^+}\right) \{\sigma_\perp \cdot (i\partial_\perp + gA_\perp) + im_F\}\xi \right] \\ & + g\partial^i A_a^i \left(\frac{1}{\partial^+}\right)(f^{abc} A_b^j \partial^+ A_c^j + 2\xi^\dagger T^a \xi) \\ & + \frac{g^2}{2}\left(\frac{1}{\partial^+}\right)(f^{abc} A_b^i \partial^+ A_c^i + 2\xi^\dagger T^a \xi)\left(\frac{1}{\partial^+}\right)(f^{ade} A_d^j \partial^+ A_e^j + 2\xi^\dagger T^a \xi) \Bigg\}. \end{aligned} \quad (4.9)$$

If zero modes are retained, there are additional surface terms [8].

B. Counterterms to canonical terms

Light-front infrared singularities arise when one eliminates the unphysical degrees of freedom by solving the constraint equations, which are the source of the operator $1/\partial^+$ in (4.9). This operator produces tree level, light-front infrared divergences in the instantaneous four-fermion, two-fermion–two-gluon, and four-gluon interactions. These divergences require counterterms, which we now construct.

1. Instantaneous gluon exchange

First, we consider the instantaneous four-fermion term shown in Fig. 3

$$H_{qqqq} = -2g^2 \int dx^- d^2x^\perp \left\{ (\xi^\dagger T^a \xi)\left(\frac{1}{\partial^+}\right)^2 (\xi^\dagger T^a \xi) \right\}. \quad (4.10)$$

In terms of the quark color current $j_q^{+a} = 2\xi^\dagger T^a \xi$ and its partial Fourier transform

$$j_q^{+a}(x^-, x_\perp) = \frac{1}{2(2\pi)} \int_{-\infty}^{\infty} dp^+ \tilde{j}_q^{+a}(p^+, x_\perp) e^{\frac{i}{2}p^+ x^-}, \quad (4.11)$$

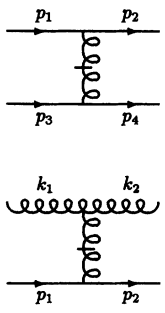

FIG. 3. Instantaneous four-fermion and two-fermion–two-gluon interactions.

we have

$$H_{qqqq} = \frac{g^2}{8\pi}\int d^2x^\perp \int_{-\infty}^{\infty} \frac{dp^+}{(p^+)^2}\tilde{j}_q^{+a}(p^+,x_\perp) \times \tilde{j}_q^{+a}(-p^+,x_\perp). \tag{4.12}$$

Thus we see explicitly that H_{qqqq} has potential divergences.

In the cutoff Hamiltonian $|p^+|$ is restricted to be above ϵ. That is,

$$\int_{-\infty}^{+\infty} dp^+ \to \int_{-\infty}^{-\epsilon} dp^+ + \int_{\epsilon}^{\infty} dp^+. \tag{4.13}$$

To find the divergent part we can do a Taylor expansion of the integrand:

$$\int \frac{dp^+}{(p^+)^2}F(p^+,x^\perp) = \int \frac{dp^+}{(p^+)^2}\left[F(0,x^\perp) + \frac{\partial F}{\partial p^+}\Big|_{p^+=0} p^+ + \cdots\right]. \tag{4.14}$$

The linearly divergent term is

$$\frac{g^2}{8\pi}\frac{2}{\epsilon}\int d^2x_\perp \tilde{j}_q^{+a}(0,x_\perp)\tilde{j}_q^{+a}(0,x_\perp). \tag{4.15}$$

The logarithmically divergent term vanishes because of the symmetric cutoff. Let us suppose we had used separate cutoffs ϵ_+ and ϵ_- for small positive and negative p^+, respectively. Then the potentially logarithmically divergent term is

$$\frac{ig^2}{8\pi}\ln\left(\frac{\epsilon_+}{\epsilon_-}\right)\int d^2x_\perp \int dx^- \int dy^- j_q^{+a}(x^-,x_\perp)(x^- - y^-)j_q^{+a}(y^-,x_\perp), \tag{4.16}$$

which is finite if we choose $\epsilon_+ = \mu\epsilon_-$, with μ some number. This particular operator vanishes because of symmetry under $x^- \to y^-$ exchange, but it forces us to reconsider our original neglect of zero modes in the solution of the constraint equations.

We are finding a potentially divergent sensitivity of the Hamiltonian to modes with small longitudinal momentum, and we regard this as a signal that finite zero-mode effects may arise. The potential divergence arises from the constraint equations and reflects contributions from A^- close to zero longitudinal momentum. It is extremely naive to suppose that the canonical constraint equation for A^- reproduces the nonperturbative effects of a zero mode in any simple manner. We discuss the divergences that arise from the exchange of small longitudinal momentum gluons with physical polarization below, but even here we can think of the counterterms produced by the constraint equation as arising from the exchange of small longitudinal momentum gluons with unphysical polarization. Once one realizes that an exchange is involved and that the divergence is independent of transverse coordinates, it becomes clear that even the assumption that these counterterms will be local in the transverse direction is naive. We therefore allow terms in the Hamiltonian of the form

$$\frac{ig^2}{8\pi}\int d^2x_\perp dx^- \int dy^- d^2y_\perp j_q^{+a}(x^-,x_\perp)(x^- - y^-)\mathcal{O}_G(x_\perp - y_\perp)j_q^{+a}(y^-,y_\perp). \tag{4.17}$$

$\mathcal{O}_G$ is a function of the transverse variables and is restricted by dimensional analysis, kinematical boost invariance, translational invariance, and invariance under rotations about the longitudinal axis. $\mathcal{O}_G$ must be odd under $x_\perp \to y_\perp$ to keep (4.17) from vanishing, and this is not possible here because gluon exchange gives only an even number of polarization vectors ϵ_λ^i with which to contract the transverse indices. Thus there is indeed no finite counterterm associated with logarithmic divergences in H_{qqqq}, and our discussion serves only to illustrate one way candidate vacuum interactions can be identified.

As discussed previously, the requirement of boost invariance means that there can be no finite part associated with the counterterm for the linear divergence (4.15), whose form breaks longitudinal boost invariance. Thus the counterterm for the canonical instantaneous four-fermion interaction is

$$H_{qqqq}^{\rm ct} = -\frac{g^2}{8\pi}\frac{2}{\epsilon}\int d^2x_\perp \int dx^- j_q^{+a}(x^-,x_\perp)\int dy^- j_q^{+a}(y^-,x_\perp). \tag{4.18}$$

In a similar way, the Hamiltonian counterterms for the instantaneous two-fermion–two-gluon and the instantaneous four-gluon interactions are found to be

$$H_{qqgg}^{\rm ct} = -\frac{g^2}{4\pi}\frac{2}{\epsilon}\int d^2x_\perp \int dx^- j_q^{+a}(x^-,x_\perp)\int dy^- j_g^{+a}(y^-,x_\perp) \tag{4.19}$$

and

$$H^{\rm ct}_{gggg} = -\frac{g^2}{8\pi}\frac{2}{\epsilon}\int d^2x_\perp \int dx^- j^{+a}_g(x^-,x_\perp)\int dy^- j^{+a}_g(y^-,x_\perp), \tag{4.20}$$

where the gluon color current is $j^{+a}_g = f^{abc}A^i_b\partial^+A^i_c$. These three counterterms precisely remove the tree level light-front infrared divergences.

2. *Instantaneous fermion exchange*

There are several terms in the canonical Hamiltonian which contain a single inverse derivative $\frac{1}{\partial^+}$. With one exception, all these terms can be rewritten so that $\frac{1}{\partial^+}$ acts on a single field operator. Such terms do not give rise to divergences since the zero modes are removed from single operators. The exception is the two-quark–two-gluon interaction involving an instantaneous fermion exchange H_{qqgg1}. Here $\frac{1}{\partial^+}$ acts on a product of field operators and hence can give rise to a logarithmic divergence (see also Sec. V).

Denoting $\sigma_\perp\cdot A_\perp(x^-,x_\perp)\xi(x^-,x_\perp)$ by $f(x^-,x_\perp)$, we have

$$H_{qqgg1} = g^2\int dx^- d^2x_\perp f^\dagger(x^-,x_\perp)\frac{1}{i\partial^+}f(x^-,x_\perp). \tag{4.21}$$

Introducing the partial Fourier transform as before,

$$\tilde f(p^+,x_\perp) = \int_{-\infty}^{\infty} dx^- e^{\frac{i}{2}p^+x^-}f(x^-,x_\perp), \tag{4.22}$$

we find

$$H_{qqgg1} = \frac{g^2}{4\pi}\int d^2x_\perp\int_{-\infty}^{\infty}\frac{dp^+}{p^+}\tilde f^\dagger(p^+,x_\perp)\tilde f(-p^+,x_\perp). \tag{4.23}$$

A potential logarithmic divergence disappears if we use a symmetric cutoff.

Once again, though, we must be careful with this logarithmic divergence. While there is no divergent dependence on the symmetric longitudinal infrared cutoff ϵ since the divergence due to small p^+ is canceled by the divergence due to small $-p^+$, we still have to worry about nonvanishing contributions from states with exactly $p^+=0$ — that is, from the exchange of zero-mode fermions. Once an infrared cutoff is employed, we have eliminated the possibility of computing this contribution, and so we should include in the Hamiltonian terms which can counter the effects of this exclusion. Such counterterms have the form

$$H^{\rm ct}_{qqgg1} = g^2\int dx^- d^2x_\perp\int dy^- d^2y_\perp f^\dagger(x^-,x_\perp)\mathcal{O}_F(x_\perp-y_\perp)f(y^-,y_\perp), \tag{4.24}$$

where dimensional analysis reveals that $\mathcal{O}_F$ scales as 1. Since this term comes from zero-mode fermion exchange, $\mathcal{O}_F$ is a function of transverse variables and the Pauli matrices $\sigma_\perp$. Since this term arises from vacuum effects, it is not restricted to have a polynomial dependence on transverse variables and the renormalized constituent mass. Thus a term such as $\mathcal{O}_F\sim m_F^{-1}\sigma_\perp\cdot\partial_\perp$ is allowed and should be included in the Hamiltonian. Such a term explicitly violates chiral symmetry and need not be small in the relativistic limit.

This is then the first point at which an arbitrary function enters the Hamiltonian. At the simplest level, the function $\mathcal{O}_F(x_\perp,y_\perp)$ must be determined phenomenologically by fitting bound state properties. It is an open question whether theoretical techniques such as coupling coherence will determine it *a priori*, whether the requirement of relativistic invariance will determine it completely *a posteriori*, or whether phenomenology will still be necessary when renormalization is done at higher orders.

C. Canonical Hamiltonian: free plus interaction terms

Now we add explicitly the gluon mass term to the LFQCD canonical Hamiltonian together with the counterterms for instantaneous interactions. The Hamiltonian is written as a free term plus interactions

$$H = \int dx^- d^2x_\perp(\mathcal{H}_0+\mathcal{H}_{\rm int}), \tag{4.25}$$

with

$$\mathcal{H}_0 = \frac{1}{2}(\partial^iA^j_a)(\partial^iA^j_a)+\frac{1}{2}m_G^2A^j_aA^j_a+\xi^\dagger\left(\frac{-\partial_\perp^2+m_F^2}{i\partial^+}\right)\xi,$$
$$\mathcal{H}_{\rm int} = \mathcal{V}_A+\mathcal{H}_{qqg}+\mathcal{H}_{ggg}+\mathcal{H}_{qqgg}+\mathcal{H}_{qqqq}+\mathcal{H}_{gggg}. \tag{4.26}$$

Here $\mathcal{V}_A$ is the artificial potential, and

$$\mathcal{H}_{qqg}= g\xi^\dagger\left\{-2\left(\frac{1}{\partial^+}\right)(\partial_\perp\cdot A_\perp)+\ \sigma_\perp\cdot A_\perp\left(\frac{1}{\partial^+}\right)(\sigma_\perp\cdot\partial_\perp+m_F)+\left(\frac{1}{\partial^+}\right)(\sigma_\perp\cdot\partial_\perp-m_F)\sigma_\perp\cdot A_\perp\right\}\xi, \tag{4.27}$$

$$\mathcal{H}_{ggg}= gf^{abc}\left\{\partial^i A_a^j A_b^i A_c^j+(\partial^i A_a^i)\left(\frac{1}{\partial^+}\right)(A_b^j\partial^+ A_c^j)\right\}, \tag{4.28}$$

$$\begin{aligned}\mathcal{H}_{qqgg}&= g^2\left\{\xi^\dagger\sigma_\perp\cdot A_\perp\left(\frac{1}{i\partial^+}\right)\sigma_\perp\cdot A_\perp\xi\right\}-\ 2g^2\left\{(f^{abc}A_b^i\partial^+A_c^i)\left(\frac{1}{\partial^+}\right)^2(\xi^\dagger T^a\xi)\right\}+H^{\rm ct}_{qqgg1}+H^{\rm ct}_{qqgg2}\\&=\mathcal{H}_{qqgg1}+\mathcal{H}_{qqgg2},\end{aligned} \tag{4.29}$$

$$\mathcal{H}_{qqqq}= -2g^2\left\{(\xi^\dagger T^a\xi)\left(\frac{1}{\partial^+}\right)^2(\xi^\dagger T^a\xi)\right\}+H^{\rm ct}_{qqqq}, \tag{4.30}$$

$$\begin{aligned}\mathcal{H}_{gggg}&= \frac{g^2}{4}f^{abc}f^{ade}\left\{A_b^iA_c^jA_d^iA_e^j-2(A_b^i\partial^+A_c^i)\left(\frac{1}{\partial^+}\right)^2(A_d^j\partial^+A_e^j)\right\}+H^{\rm ct}_{gggg}\\&=\mathcal{H}_{gggg1}+\mathcal{H}_{gggg2}.\end{aligned} \tag{4.31}$$

In a careful analysis all of these couplings must be allowed to renormalize separately and the quark masses in $\mathcal{H}_0$ and $\mathcal{H}_{qqg}$ are not the same. For simplicity we use one coupling and one mass in our examples. It can be seen that all canonical terms are predicted from the light-front power counting (3.16). The artificial potential has the form described in Sec. II E. The Coulomb part will involve the quark and gluon color currents j_q^{+a} and j_g^{+a} defined above, and the linear part will involve the color singlet currents $j_q^+=2\xi^\dagger\xi$ and $j_g^+=A_a^i\partial^+A_a^i$.

As we have emphasized before, the division of the bare Hamiltonian into a free part and an interaction part is arbitrary. We have chosen the free part to be that of massive quarks and gluons since self-mass corrections are needed in any case. Note that these terms are allowed by the power-counting criteria. Our computations will involve two stages. The first stage is the computation of the effective Hamiltonian, which is to be performed perturbatively. The artificial potential will be considered as part of $\mathcal{H}_I$ for this stage. The second stage is the determination of bound states, and as discussed before we will want to include the (nonrelativistic) Coulomb and linear parts of $\mathcal{V}_A$ as part of the unperturbed Hamiltonian for this stage.

V. POWER COUNTING: PHASE SPACE CELL ANALYSIS AND THE STRUCTURE OF DIVERGENCES

A. Phase space cell division and field operators

Here we perform the power-counting analysis of ultraviolet divergences and infrared divergences arising from the products of interaction Hamiltonians. To facilitate this analysis, we first introduce a phase space cell representation of field variables in terms of wave packet functions [38,39]. A realization of these wave packet functions is given by wavelets. The present considerations are only qualitative in nature, and hence we do not need their many interesting mathematical properties [40]; however, they may be needed by anyone attempting the nonperturbative diagonalization of the renormalized Hamiltonian.

The motivation for a phase space cell analysis and an example of phase space cell division is provided in Appendix D in the context of the more familiar case of equal-time Hamiltonians. Here we discuss the division of phase space cells in the light-front case. For the "plus" momenta we choose

$$p^+_{\rm max}>p_1^+>p_2^+>p_3^+>\cdots>p^+_{\rm min} \tag{5.1}$$

with $p^+_{i+1}=\frac{1}{2}p_i^+$. For the transverse momenta we choose $p_{\perp 0}=0$, $p_{\perp 1}=m$, and then a sequence $p_{\perp j}=2^{j-1}\times m$ until the cutoff $p_{\perp\max}$ is reached. Note that we always use a logarithmic scale for momenta.

For a momentum space cell with centroids p_i^+ and $p_{\perp j}$ which is an annulus in the transverse momentum, position space is divided into a linear grid of cells all with width $\delta x^-=\frac{1}{p_i^+}$ and $\delta x_\perp=\frac{1}{p_{\perp j}}$. These cells are labeled with position indices l^- and $l_\perp=(l^x,l^y)$. A phase space cell is denoted by the indices $ijl=(i,j,l^-,l^x,l^y)$. A wave packet function that belongs to the complete, orthonormal basis set is denoted in position space by $\phi_{ijl}(x)$, and its Fourier transform is denoted by $\tilde\phi_{ijl}(p)$. The x-space widths of these functions are δx_i^- and $\delta x_{\perp j}$ and they are assumed to vanish outside of the cell. Normalization implies that ϕ_{ijl} is of order $\frac{1}{\sqrt{\delta x_i^-}}\frac{1}{\delta x_{\perp j}}$, while $\tilde\phi_{ijl}(p)$ is of order $\sqrt{\delta x_i^-}\,\delta x_{\perp j}$.

Next we consider field operators. For the quark field operator, we have

$$\xi(x)=\sum_s\chi_s\int\frac{dk^+d^2k_\perp}{2(2\pi)^3}[b_{k,s}e^{-ik\cdot x}+d^\dagger_{k,s}e^{ik\cdot x}], \tag{5.2}$$

with

$$\{b_{k,s},b^\dagger_{k',s'}\}=\{d_{k,s},d^\dagger_{k',s'}\}=2(2\pi)^3\delta(k^+-k'^+)\delta^2(k_\perp-k'_\perp)\delta_{ss'}. \tag{5.3}$$

Thus

$$b\,,\,d\;\sim\;\sqrt{x^-}x_\perp. \tag{5.4}$$

We wish to carry out the analysis in such a way that the creation and destruction operators are of order unity. To achieve this goal, we introduce phase space cell operators

$$b_{k,s}\chi_s=\sum_{lij}\tilde{\phi}_{ijl}(k)b_{ijls} \tag{5.5}$$

and

$$d^\dagger_{k,s}\chi_s=\sum_{ijl}\tilde{\phi}^*_{ijl}(k)d^\dagger_{ijls}, \tag{5.6}$$

where

$$b_{ijls}\,,\,d_{ijls}\;\sim\;1\;\text{and}\;\phi_{ijl}(k)\;\sim\;\sqrt{x_i^-}\,x_{\perp j}\,. \tag{5.7}$$

Thus

$$\xi_s(x)=\sum_{ijl}[b_{ijls}\phi_{ijl}(x)+d^\dagger_{ijls}\phi^\dagger_{ijl}(x)\,]. \tag{5.8}$$

It follows that the order of magnitude of ijlth mode's contribution to the operator ξ is $\frac{1}{\sqrt{\delta x_i^-}}\frac{1}{\delta x_{\perp j}}$.

Next consider the transverse gluon field operator. We write

$$A_\perp(x)=\sum_\lambda\int\frac{dk^+d^2k_\perp}{2\sqrt{k^+}(2\pi)^3}\,[\epsilon_{\perp\lambda}a_{k,\lambda}e^{-ik\cdot x}+\epsilon^*_{\perp\lambda}a^\dagger_{k,\lambda}e^{ik\cdot x}\,], \tag{5.9}$$

with

$$\left[a_{k,\lambda},a^\dagger_{k',\lambda'}\right]=2(2\pi)^3\delta(k^+-k'^+)\delta^2(k_\perp-k'_\perp)\delta_{\lambda\lambda'}. \tag{5.10}$$

The operators a_k and $a^\dagger_k$ are again unsuitable for our purposes. We define

$$a_{k,\lambda}=\sum_{ijl}\tilde{\phi}_{ijl}(k)a_{ijl\lambda}, \tag{5.11}$$

where $\tilde{\phi}_{ijl}(k)\sim\sqrt{\delta x_i^-}\,\delta x_{\perp j}$. Now,

$$A_\perp(x)=\sum_{ijl\lambda}\int\frac{dk^+d^2k_\perp}{2\sqrt{k^+}(2\pi)^3}\,[\epsilon_{\perp\lambda}\tilde{\phi}_{ijl}(k)a_{ijl\lambda}e^{-ik\cdot x}+\epsilon^*_{\perp\lambda}\tilde{\phi}^*_{ijl}(k)a^\dagger_{ijl\lambda}e^{ik\cdot x}\,]. \tag{5.12}$$

The order of magnitude of ijlth mode's contribution to $A_\perp(x)$ is $\frac{1}{\delta x_{\perp j}}$.

Because of the cutoffs we impose, the wave packet functions $\phi_{ijl}(x)$ do not have zero modes; that is, $\int dx\phi_{ijl}(x)=0$.

We must also specify the order of magnitude of $\partial_\perp$, ∂^+, and $(\partial^+)^{-1}$ when acting on a specified subset of wavelets in an operator product. For qualitative purposes each gradient needs to be applied only to the most rapidly changing wavelet in the subset, so that $\partial_\perp$ is of order $(\delta x_\perp)^{-1}$, where $\delta x_\perp$ is the smallest width in the subset. A similar result holds for ∂^+. The effect of the inverse operator $(\partial^+)^{-1}$, which involves an integration, is also determined by the smallest width δx^- in the product. Qualitatively, it amounts to multiplication of the subset by the width δx^-; for the other, broader widths act as constants over this width. However, there is a special case we must note.

To see this, consider the action of $(\partial^+)^{-1}$ on a product of field operators. Now the wave packet functions associated with destruction operators have positive k^+ only, and the wave packet functions associated with creation operators have negative k^+ only. If the product contains only creation operators or only destruction operators, then the operation of $(\partial^+)^{-1}$ qualitatively amounts to multiplication by the smaller width among the product in accordance with the rule above. But if the product contains at least one creation and one destruction operator, then wavelets with Fourier modes of positive k^+ and wavelets with Fourier modes of negative k^+ will both occur in the product. When they have the same mean value of k^+, the product acquires a zero mode and then $(\partial^+)^{-1}$ no longer produces a localized function but rather one which covers the whole space. Thus the action of a single $(\frac{1}{\partial^+})$ can lead to a logarithmic infrared divergence and the action of $(\frac{1}{\partial^+})^2$ can lead to both linear and logarithmic infrared divergences already in the canonical terms. We have discussed these divergences and the counterterms which remove them in Sec. IV B.

B. Ultraviolet divergences and counterterms

Consider ultraviolet divergences arising from the products of interaction Hamiltonians. Each term in the interaction Hamiltonian involves an integral over the product of three or four field operators. Each field operator is expanded in terms of wave packet functions. First, we consider the ultraviolet divergences arising from a product of two interaction Hamiltonians. We shall consider

the special case of just two wave packet sectors, one being fixed and the other being arbitrarily large. This corresponds to a single divergent loop integral in the familiar language. The fixed wave packet width corresponds to the fixed external momenta in the loop diagram, and the varying wave packet width corresponds to the diverging loop momenta.

We denote the widths of the fixed and varying wave packet sectors by $(\delta x^-, \delta x_\perp)$ and $(\delta y^-, \delta y_\perp)$, respectively. The energy of the varying wave packet sector scales as $\frac{\delta y^-}{\delta y_\perp^2}$. The energy diverges as $\delta y_\perp \to 0$, corresponding to the traditional type of short-distance ultraviolet divergence, which we consider in this section. The divergences as $\delta y^- \to \infty$ are light-front infrared divergences, which we consider in the next section. Consider ultraviolet divergences which occur when $\delta y_\perp \ll \delta x_\perp$. We set $\delta x^- = \delta y^-$. The interaction Hamiltonian contains only cubic and quartic terms in the field operators $\xi^\dagger$, ξ, and A^i. We now observe that, as a consequence of momentum conservation at the vertices, to produce an ultraviolet divergence *at least two of the three or four operators have to refer to a y sector.* We also note that a transverse gradient will yield $\frac{1}{\delta y_\perp}$ unless it applies to a product of x sectors only.

Now consider the terms in the interaction Hamiltonian. If all operators refer to y sectors, each term scales as $\frac{\delta y^-}{\delta y_\perp^2}$ except for the mass term (the helicity-flip interaction), which scales as $\frac{\delta y^-}{\delta y_\perp}$. But if some operators refer to x sectors, there will be additional factors of $\frac{\delta y_\perp}{\delta x_\perp}$. For each field operator $(\xi^\dagger, \xi, A_\perp)$ belonging to an x sector and for each derivative $\partial_\perp$ acting on only x sectors, there is a factor of $\frac{\delta y_\perp}{\delta x_\perp}$. This gives the contribution from a single sector with width $\delta y^-, \delta y_\perp$ as $\delta y_\perp$ gets small. But many wavelets with different $\delta y_\perp$ can contribute, namely, all wavelets with different centers that overlap a given x-wavelet (see Fig. 13). Since the transverse space has dimension 2, the number of independent wavelets of linear size $\delta y_\perp$ that overlap with the wavelet of size $\delta x_\perp$ is of order $(\delta x_\perp/\delta y_\perp)^2$.

Next consider the second-order perturbation theory formula

$$H_I \frac{1}{D_E} H_I, \tag{5.13}$$

where D_E denotes the energy denominator. For qualitative purposes, we can replace the energy denominator by the energy of the y sector, namely, $\frac{\delta y^-}{\delta y_\perp^2}$. Thus the contribution in second order of a given term to the effective Hamiltonian resulting from wave packet functions of a given width $\delta y_\perp$ scales as

$$\left(\frac{\delta y^-}{\delta y_\perp^2}\right)\left(\frac{\delta y_\perp^2}{\delta y^-}\right)\left(\frac{\delta y^-}{\delta y_\perp^2}\right)\left(\frac{\delta x_\perp}{\delta y_\perp}\right)^2\left(\frac{\delta y_\perp}{\delta x_\perp}\right)^n, \tag{5.14}$$

where n counts the number of $\xi^\dagger$, ξ, $A_\perp$, and $\partial_\perp$ factors that refer to x sectors. If n is greater than 4, there is no divergence, while for n less than or equal to 4 a divergence arises. When n is equal to 4, the contribution from the sector of a given size $\delta y_\perp$ is a constant. Now we have to sum over all scale sizes $\delta y_\perp$. The scale sizes $\delta y_\perp$ allowed are inverse powers of 2 all the way down to a minimum size $\frac{1}{\Lambda}$. A sum over all scale sizes down to $\frac{1}{\Lambda}$ yields a term of order $(\ln\Lambda\ /\ln 2)$, which gives a logarithmic divergence as $\Lambda \to \infty$.

Thus the power-counting rule for ultraviolet counterterms is the same (in $\delta x_\perp$) as for the canonical Hamiltonian, namely, that there can be at most four operators scaling as $\delta x_\perp^{-1}$. Even though we did the analysis for two H_I's, it holds for any number of H_I's, where the first H_I creates one or more y-type constituents, intermediate H_I's maintain at least one y-type constituent, and the last H_I destroys all the remaining y-type constituents. (We are ignoring contributions "disconnected in y" — that is, products which contain an H_I with only x-sector constituents. These diagrams have already acquired counterterms.) Each energy denominator may be replaced by the energy of the y sector, $\frac{\delta y^-}{\delta y_\perp^2}$, since each intermediate state contains at least one y-type constituent by assumption. If there are m factors H_I, there are $m-1$ factors $\frac{\delta y^2_\perp}{\delta y^-}$. Each H_I scales like $\frac{\delta y^-}{\delta y_\perp^2}$ times powers of $(\delta y_\perp/\delta x_\perp)$. An overall factor $(\delta x_\perp/\delta y_\perp)^2$ counts the number of y-type wave packet functions that overlap with a single x-type wave packet function. Thus the final rule for the scaling versus $\delta x_\perp$ and $\delta y_\perp$ is identical for m H_I's as for 2 H_I's — namely, divergences occur for products in the effective Hamiltonian of x operators up to fourth order in $\xi^\dagger$, ξ, $A_\perp$, and $\partial_\perp$.

C. Infrared divergence and counterterms

Light-front infrared divergences are large-energy divergences as can be seen from the light-front dispersion relation $p^- = \frac{p_\perp^2+m^2}{p^+}$, which blows up as $p^+ \to 0$. We have already discussed the counterterms for light-front infrared divergences that arise in the instantaneous interactions in the Hamiltonian. In this section we discuss the infrared divergences which arise in products of the interaction Hamiltonian.

As in the analysis of ultraviolet divergences we will separate out the divergences caused by a specific y-type wave packet function from the operator structure associated with an x-type wavelet. Let us discuss the differences from the analysis of ultraviolet divergences. First of all, the y-wavelet energy scale $\frac{\delta y^-}{y_\perp^2}$ is blowing up because δy^- is approaching ∞. Thus it will be assumed that $\delta y^- \gg \delta x^-$, while to avoid confusion with ultraviolet problems we assume $\delta y_\perp$ is of order $\delta x_\perp$. In contrast with ultraviolet case, light-front infrared divergences are caused by a single y-type wavelet with a width δy^-. The reason for this is that only one y-type wavelet overlaps with a given x-type wavelet, since δy^- is much wider than δx^-. In this case momentum conservation at the vertices implies that to produce a light-front infrared divergence *at least two operators in H_I have to be x type.* Each term in H_I scales as $\frac{\delta y^-}{\delta y_\perp^2}$ times a factor: (a) $(\frac{\delta y^-}{\delta x^-})^{\frac{1}{2}}$ for each ξ or $\xi^\dagger$ referring to an x type, (b) $(\frac{\delta y^-}{\delta x^-})$ for every ∂^+ acting on an x-type operator and a reciprocal factor

$(\frac{\delta x^-}{\delta y^-})$ for every $(\partial^+)^{-1}$ operator when applied to a product including at least one x-type operator, and (c) $(\frac{\delta x^-}{\delta y^-})$ arising from the range of integration in each H_I involving an x-type operator. As in the case of ultraviolet divergences, in the effective Hamiltonian a term with no factor $(\frac{\delta x^-}{\delta y^-})$ diverges logarithmically due to a sum over different widths δy^-. However, exceptions to the above rules occur for terms in the canonical Hamiltonian involving $(\frac{1}{\partial^+})$ or $(\frac{1}{\partial^+})^2$ operators, which we will note below.

Let us now catalogue the factors associated with the scaling behavior of various terms in the interaction Hamiltonian. If we ignore ∂^+ or $\frac{1}{\partial^+}$ factors, then the rules are simple: An x-type ξ produces a factor $(\frac{\partial y^-}{\partial x^-})^{1/2}$, an x-type $A_\perp$ produces no factor, and the presence of any x-type operator in H_I produces $(\frac{\delta x^-}{\delta y^-})$ as result of the change of integration width. Thus, ignoring ∂^+ and $\frac{1}{\partial^+}$ factors, we can compute the impact of any product of x-type operators on the scaling behavior of H_I :

$$\begin{aligned}
\xi\xi &: \text{no factor;}\\
A_\perp\xi &: (\delta x^-/\delta y^-)^{\frac{1}{2}};\\
A_\perp\xi\xi &: \text{no factor;}\\
A_\perp A_\perp &: (\delta x^-/\delta y^-);\\
A_\perp A_\perp\xi &: (\delta x^-/\delta y^-)^{\frac{1}{2}};\\
A_\perp A_\perp\xi\xi &: \text{no factor;}\\
\xi\xi\xi &: (\delta y^-/\delta x^-)^{\frac{1}{2}};\\
\xi\xi\xi\xi &: (\delta y^-/\delta x^-).
\end{aligned} \tag{5.15}$$

Next we classify again the possible x-type operators in H_I by the degree of divergence in H_I that results when the effects of ∂^+ and $\frac{1}{\partial^+}$ factors are included. Here it is assumed that ∂^+ or $(1/\partial^+)$ is applied to a product that contains at least one x-type operator. It is useful to recall the structure of terms in the canonical Hamiltonian (see Sec. IV), which we consider one by one in the following.

When all the operators in the Hamiltonian refer to the y sector, the Hamiltonian scales as δy^-. We have to determine the scale factor that arises as a result of replacing two or more y-type operators by x-type operators. Let us first consider some specific examples. In the following we denote the operators that belong to the x type by a subscript (x) and those belonging to the y type by a subscript (y), respectively. Now consider the term in the Hamiltonian $\int dz^- d^2z_\perp \xi^\dagger A_\perp \frac{1}{\partial^+}\xi$. Here we write the integration variable as z in order to distinguish dz from the widths δx and δy.

(1) For the case $\int dz^- d^2z_\perp (A_\perp)_{(y)}\xi^\dagger_{(x)}\frac{1}{\partial^+}\xi_{(x)}$, from our rules we get $\delta y^- \times (\frac{\delta y^-}{\delta x^-})$ (for two ξ's)$\times$ $(\frac{\delta x^-}{\delta y^-})$ (for $\frac{1}{\partial^+}$) $\times$ $(\frac{\delta x^-}{\delta y^-})$ (arising from the range of integration). Thus the scaling behavior is like δx^- which we write as $\delta y^- \times (\frac{\delta x^-}{\delta y^-})$. Hence the scale factor is $(\frac{\delta x^-}{\delta y^-})$.

(2) For the case $\int dz^- d^2z_\perp (A_\perp\xi^\dagger)_{(x)}\frac{1}{\partial^+}\xi_{(y)}$ we get from our rules $\delta y^- \times (\frac{\delta y^-}{\delta x^-})^{\frac{1}{2}}$ (for $\xi^\dagger$) $\times$ $(\frac{\delta x^-}{\delta y^-})$ (arising from the range of integration). Thus the scaling behavior is like $(\delta x^-\,\delta y^-)^{\frac{1}{2}}$ which we write as $\delta y^- \times (\frac{\delta x^-}{\delta y^-})^{\frac{1}{2}}$. Hence the scale factor is $(\frac{\delta x^-}{\delta y^-})^{\frac{1}{2}}$.

Now there may be exceptions to these rules when $(\partial^+)^{-1}$ or $(\partial^+)^{-2}$ acts on a product of operators, for then it would pick out a zero mode as described above. However, we have eliminated this possibility by imposing a longitudinal cutoff ϵ on such terms and then adding a counterterm to remove the ϵ dependence. Because of this, integration by parts is allowed and can be used to determine the order of magnitude of $(\partial^+)^{-1}$ or $(\partial^+)^{-2}$. The exception to the usual rule occurs, then, when there are not x-sector wavelets on each side of the inverse gradient, for integration by parts allows us to rewrite the product so that the inverse operator acts entirely on y-type wavelets. Then it picks out a y-sector width and so does not produce the factor $(\delta x^-/\delta y^-)$ or $(\delta x^-/\delta y^-)^2$ expected from the above rules. Thus, for example, consider the term $\int dz^- d^2z_\perp (\xi^\dagger A_\perp)_{(y)}\frac{1}{\partial^+}(\xi A_\perp)_{(x)}$. With the zero mode eliminated, we are free to interchange the operation of $\frac{1}{\partial^+}$ to get $\int dz^- d^2z_\perp \frac{1}{\partial^+}\left[(\xi^\dagger A_\perp)_{(y)}\right](A_\perp\xi)_{(x)}$. Thus the scaling is $\delta y^- \times (\frac{\delta y^-}{\delta x^-})^{\frac{1}{2}}$ (from ξ) $\times$ $(\frac{\delta x^-}{\delta y^-})$ (arising from the range of integration). Hence the scaling behavior is $(\delta x^-\,\delta y^-)^{\frac{1}{2}}$, which we write as $\delta y^- \times (\frac{\delta x^-}{\delta y^-})^{\frac{1}{2}}$, and so the scale factor is $(\frac{\delta x^-}{\delta y^-})^{\frac{1}{2}}$.

In the following we determine the scale factor for various terms in the interaction Hamiltonian when two or more operators in them are replaced by x-type operators, the remaining operators being of y type. Each $\frac{1}{\partial^+}$ may apply to y operators too; e.g, $\frac{1}{\partial^+}\xi$ might mean $\frac{1}{\partial^+}(A_\perp\xi)$ with $A_\perp$ of y type. The scale factor is unchanged by any such embedded y operators.

Products of ξ and ξ:

$$\begin{aligned}
\xi\xi &: \text{no factor;}\\
(\partial^+)^{-2}(\xi\xi) &: \text{no factor (exception applies);}\\
\xi(\partial^+)^{-1}\xi &: (\delta x^-/\delta y^-);\\
\xi(\partial^+)^{-2}\xi &: (\delta x^-/\delta y^-)^2.
\end{aligned} \tag{5.16}$$

Products of $A_\perp$ and ξ:

$$\begin{aligned}
A_\perp\xi &: (\delta x^-/\delta y^-)^{\frac{1}{2}};\\
(\partial^+)^{-1}(A_\perp\xi) &: (\delta x^-/\delta y^-)^{\frac{1}{2}} \text{ (exception applies);}\\
\xi(\partial^+)^{-2}(\partial^+A_\perp) &: (\delta x^-/\delta y^-)^{\frac{3}{2}};\\
(\partial^+A_\perp)(\partial^+)^{-2}\xi &: (\delta x^-/\delta y^-)^{\frac{3}{2}};\\
\xi(\partial^+)^{-2}A_\perp &: (\delta x^-/\delta y^-)^{\frac{5}{2}};\\
A_\perp(\partial^+)^{-2}\xi &: (\delta x^-/\delta y^-)^{\frac{5}{2}};\\
\xi(\partial^+)^{-1}A_\perp &: (\delta x^-/\delta y^-)^{\frac{3}{2}}.
\end{aligned} \tag{5.17}$$

Products of ξ, ξ, and $A_\perp$:

$$\begin{aligned}
\xi^2(\partial^+)^{-2}A_\perp &: (\delta x^-/\delta y^-)^2;\\
\xi^2(\partial^+)^{-2}\partial^+A_\perp &: (\delta x^-/\delta y^-);\\
A_\perp(\partial^+)^{-2}\xi^2 &: (\delta x^-/\delta y^-)^2;\\
(\partial^+A_\perp)(\partial^+)^{-2}\xi^2 &: (\delta x^-/\delta y^-);\\
\xi^2(\partial^+)^{-1}A_\perp &: (\delta x^-/\delta y^-);\\
\xi(\partial^+)^{-1}A_\perp\xi &: (\delta x^-/\delta y^-);\\
\xi A_\perp(\partial^+)^{-1}\xi &: (\delta x^-/\delta y^-).
\end{aligned} \tag{5.18}$$

Products of $A_\perp$ and $A_\perp$:

$$\begin{aligned} A_\perp A_\perp &: (\delta x^-/\delta y^-); \\ A_\perp(\partial^+)^{-2}A_\perp &: (\delta x^-/\delta y^-)^3; \\ A_\perp(\partial^+)^{-2}\partial^+ A_\perp &: (\delta x^-/\delta y^-)^2; \\ (\partial^+ A_\perp)(\partial^+)^{-2}\partial^+ A_\perp &: (\delta x^-/\delta y^-); \\ (\partial^+)^{-2}(A_\perp \partial^+ A_\perp) &: \\ &\text{no factor (exception applies),} \\ A_\perp \partial^+ A_\perp &: \text{no factor;} \\ A_\perp \frac{1}{\partial^+} A_\perp &: (\delta x^-/\delta y^-)^2. \end{aligned} \tag{5.19}$$

Products of ξ, $A_\perp$, and $A_\perp$:

$$\begin{aligned} \xi(\partial^+)^{-2}A_\perp\partial^+A_\perp &: (\delta x^-/\delta y^-)^{\frac{3}{2}}; \\ A_\perp\xi(\partial^+)^{-1}A_\perp &: (\delta x^-/\delta y^-)^{\frac{3}{2}}; \\ A_\perp(\partial^+)^{-1}\xi A_\perp &: (\delta x^-/\delta y^-)^{\frac{3}{2}}. \end{aligned} \tag{5.20}$$

Products of ξ, ξ, and ξ:

$$\begin{aligned} \xi(\partial^+)^{-2}\xi^2 &: (\delta x^-/\delta y^-)^{\frac{3}{2}}; \\ \xi^2(\partial^+)^{-2}\xi &: (\delta x^-/\delta y^-)^{\frac{3}{2}}. \end{aligned} \tag{5.21}$$

The above list splits into four types. (a) Products which contain no $\frac{\delta x^-}{\delta y^-}$ factors. They are all components of the color charge density, either the quark or the gluon component. These products can occur in any number of H_I's without reducing the divergence of the overall product. If these products are the only source of x-type operators, the overall divergence behaves as δy^-, that is, linearly. (b) Products which contain a factor of $(\delta x^-/\delta y^-)^{\frac{1}{2}}$. These products involve a single ξ. Since only an even number of ξ's can appear in the effective Hamiltonian, two such products are required from two separate H_I's, and the result is to generate a factor $(\delta x^-/\delta y^-)$, which implies a logarithmic divergence. If more than two such products occur, there is no longer any divergence. (c) Products which generate a factor $(\delta x^-/\delta y^-)$. If any such product occurs once, a linear divergence is converted to a logarithmic divergence, and if they occur more than once, there is no divergence. Finally, (d) products that scale as a higher than linear power of $(\delta x^-/\delta y^-)$. Such products cancel any divergence — even if present linearly.

As we have already explained, counterterms for linear divergences cannot have finite parts. Thus we are interested in logarithmic divergences. Even in this class, the power-counting analysis may be an overestimate since, for example, as seen in Sec. III B, a logarithmic divergence may disappear when a symmetric cutoff is used.

D. Examples

Now we provide examples of the determination of the divergence structure in perturbation theory using the qualitative phase space cell analysis described above. We consider the second-order shift in the energy of a gluon coming from a two-gluon intermediate state.

As candidates for H_I, we take

$$H_{I(1)} = g f^{abc} \int dz^- d^2 z_\perp \partial^i A_a^j A_b^i A_c^j, \tag{5.22}$$

$$H_{I(2)} = -g f^{abc} \int dz^- d^2 z_\perp \Big(\frac{1}{\partial^+}\partial^i A_a^i\Big) A_b^j \partial^+ A_c^j. \tag{5.23}$$

We separate the field operators into low-momentum parts which contain wavelets of width $\delta x_\perp, \delta x^-$ and high-momentum parts which contain wavelets of width $\delta y_\perp, \delta y^-$. In the discussion below we drop factors of g and color factors.

1. *Ultraviolet divergence*

To avoid confusion with infrared divergences, we set $\delta x^- = \delta y^-$. For a candidate H_I, we choose $H_{I(1)}$. Remember that to produce an ultraviolet divergence at least two operators have to belong to the high sector.

(a) Consider $H_{I(1)} \approx \int dz^- d^2 z_\perp (\partial^i A^j A^i)_{(y)} A^j_{(x)}$ and the energy shift $\Delta E \approx H_{I(1)} \frac{1}{D_E} H_{I(1)}$. Referring back to the scaling formula (5.14), $n = 2$. Hence the scaling behavior of the energy shift is $\frac{1}{(\delta y_\perp)^2} \times (\delta y_\perp)^2 \times \frac{1}{(\delta y_\perp)^2} \times (\frac{\delta x_\perp}{\delta y_\perp})^2 \times (\frac{\delta y_\perp}{\delta x_\perp})^2$, that is, $\Delta E \approx \frac{1}{(\delta y_\perp)^2}$, a quadratic ultraviolet divergence.

(b) Consider $H_{I(1)} \approx \int dz^- d^2 z_\perp \partial^i A^j_{(x)} (A^i A^j)_{(y)}$ and the energy shift $\Delta E \approx H_{I(1)} \frac{1}{D_E} H_{I(1)}$. In this case $n = 4$ and hence the scaling behavior of the energy shift is $\frac{1}{(\delta y_\perp)^2} \times (\delta y_\perp)^2 \times \frac{1}{(\delta y_\perp)^2} \times (\frac{\delta x_\perp}{\delta y_\perp})^2 \times (\frac{\delta y_\perp}{\delta x_\perp})^4$, that is, $\Delta E \approx \frac{1}{(\delta x_\perp)^2}$, a logarithmic ultraviolet divergence.

2. *Infrared divergence*

To avoid confusion we set $\delta x_\perp = \delta y_\perp$. Remember that to produce an infrared divergence at least two operators have to belong to the low sector. Thus, for example, we may take

$$H_{I(1)} \approx \int dz^- d^2 z_\perp \partial^i A^j_{(y)} (A^i A^j)_{(x)}, \tag{5.24}$$

$$H_{I(2)} \approx \int dz^- d^2 z_\perp \Big(\frac{1}{\partial^+}\partial^i A^i_{(y)}\Big) (A^j \partial^+ A^j)_{(x)}. \tag{5.25}$$

(a) Consider the energy shift $\Delta E \approx H_{I(2)} \frac{1}{D_E} H_{I(2)}$. According to our rules, $H_{I(2)}$ scales like δy^-. The energy denominator produces a factor $\frac{1}{\delta y^-}$. Another $H_{I(2)}$ produces a factor δy^-. Thus $\Delta E \approx \delta y^-$, which results in a linear infrared divergence.

(b) Consider the energy shift $\Delta E \approx H_{I(2)} \frac{1}{D_E} H_{I(1)}$. According to our rules, $H_{I(1)}$ scales like $\delta y^- \times (\frac{\delta x^-}{\delta y^-})$. The energy denominator produces a factor $\frac{1}{\delta y^-}$. $H_{I(2)}$ produces a factor δy^-. Thus $\Delta E \approx \delta x^-$, which results in a logarithmic infrared divergence.

To complete the analysis one must determine what

happens when $\delta y_\perp \ll \delta x_\perp$ and simultaneously $\delta y^- \gg \delta x^-$, as well as other double orderings involving drastically different transverse and longitudinal widths. We have not completed analyses for all such cases.

E. Structure of counterterms: summary

We have found that the power-counting rule for ultraviolet counterterms is the same (in $\delta x_\perp$) as for the canonical Hamiltonian, that there can be at most four operators scaling as $\frac{1}{\delta x_\perp}$. However, the counterterm has a complex nonlocality in the longitudinal coordinates. The reason for this is that the longitudinal distance scales for x-type and y-type wavelets overlap even when ultraviolet transverse divergences are produced. Thus the ultraviolet counterterms are built out of products up to fourth order in ξ, $\xi^\dagger$, $A_\perp$, and $\partial_\perp$ [see Eq. (3.16)] and have completely arbitrary longitudinal structure. As a result of the constraint from longitudinal boost invariance only vertex counterterms can involve *a priori* unknown functions of longitudinal variables.

The counterterms for infrared divergences, on the other hand, involve arbitrary numbers of quark and gluon operators. They have a complex nonlocality in the transverse variables. This is in contrast with the divergent counterterm for the canonical instantaneous four-fermion interaction which is local in the transverse direction. If we identify the counterterms arising from infrared gluons (small longitudinal momentum) as the source of transverse confinement, then the unknown nonlocal transverse behavior would have to include confining effects at large transverse separation.

From a physical point of view the appearance of long-range many-body interactions involving arbitrary numbers of quarks and gluons is inevitable if one allows a confining two-body interaction. It has long been appreciated in the CQM that if one uses confining two-body interactions, unphysical long-range van der Waals forces inevitably arise above 1+1 dimensions [41]. In the CQM various schemes allow the potential to distinguish between colored objects in different hadrons, but we have no such operators at our disposal in a field theory. Therefore the only way to cancel the residual long-range multipole interactions between color singlets is with long-range many-body interactions. It would be a failure of our approach if such operators were not allowed by the same arguments that lead to a confining two-body interaction. The possible impact such operators have on the predictive power of the theory is not known yet.

There is a question of whether the artificial potential will drastically alter the analysis of infrared divergences. We do not study this problem here.

As mentioned in Sec. II, one might worry that the appearance of functions of momenta in the counterterms could destroy the predictive power of the theory and lead to nonrenormalizability. However, these functions are needed to restore Lorentz covariance and gauge invariance as $g \to g_s$, and without such counterterms physical quantities will not even approach finite limits as cutoffs are removed for any coupling.

We do not expect any new parameters to appear in the properly renormalized theory; so all new counterterms must actually be determined by the finite set of canonical free parameters. This problem has been studied in Ref. [32], where a set of relationships called "coupling coherence" [42] were used to fix this relationship. Coupling coherence rests on the observation that only canonical variables should run independently with the cutoffs in renormalization group equations. To lowest orders in perturbation theory it has been explicitly demonstrated that coupling coherence fixes the bare Hamiltonian in scalar field theory, and that Lorentz covariance is restored by the resultant counterterms [19]. Whether coupling coherence helps solve the infrared problem has yet to be demonstrated, but it is at least able to deal with spontaneous symmetry breaking [32].

VI. CUTOFF SCHEME FOR THE HAMILTONIAN

In the previous sections we presented a qualitative analysis of divergences based on wavelets. Now we set up a precise momentum space framework for renormalization of the LFQCD Hamiltonian. We employ the "similarity renormalization scheme" [14,15], which allows one to avoid the difficulties often encountered in traditional perturbation renormalization schemes when using plane wave states to study the structures of divergences. Thus, although we use plane wave states to determine the form of the effective Hamiltonian, we may still set up the renormalization to follow the qualitative wavelet analysis of Sec. V. Of course, the assumption here is that the artificial Coulomb and linear potentials will not affect the structure of the divergences. As we have seen, the canonical Hamiltonian already leads to divergences at the tree level due to k^+ getting small. Beyond tree level, products of Hamiltonians also lead to divergences both due to k^+ getting small and $k_\perp$ getting large. We need to introduce a regulator before we can investigate these divergences and construct the corresponding counterterms. This is done here.

A. Cutoffs on constituents

Since the final step of the renormalization process involves the nonperturbative diagonalization of the Hamiltonian, we need to develop a cutoff procedure that is applicable to the Hamiltonian as a whole instead of just to perturbative calculations order by order. One way to accomplish this is to cut off the single particle momenta appearing in the field variables themselves. Cutoffs on the constituent momenta k^+ and $k_\perp$, which we call "constituent cutoffs," obviously violate the longitudinal and transverse boost symmetries of the light front. What does this violation mean? The direct effect of the cutoff is to eliminate states that would be present without the cutoff. For a given center of mass momentum, a key parameter is the lowest mass state that is not eliminated by the cutoff. This lowest mass depends on the center of

mass momentum chosen, and is degraded if $P_\perp$ increases or P^+ decreases.

If constituent cutoffs destroy light-front boost invariance except for a limited range of center of mass momenta, then, why do we want to use such cutoffs? One could instead employ, as has been suggested elsewhere (see, e.g., [19,35,43,44]), cutoffs which preserve both transverse and longitudinal boost invariance. We shall call such cutoffs "Jacobi cutoffs" for they act on the Jacobi or internal momenta of a constituent, which are defined relative to the center of mass momenta. Unfortunately, Jacobi cutoffs inevitably refer to extensive quantities of a state and thereby introduce nonlocalities in the Hamiltonian. If the cutoff on constituent i depends on the total momentum of the state, then a dependence on all spectators j will be introduced in any matrix element. Thus any counterterm may change when another spectator is included, which greatly complicates the renormalization process [19]. So there is a stiff price to pay for insisting on a regulator which preserves explicit boost symmetry.

We prefer to employ a constituent cutoff scheme because of the conceptual simplicity of its implementation. This is especially important for LFQCD, where the final diagonalization of the Hamiltonian will be done on a computer. In addition, we will be encountering nonlocal effective potentials which result from the similarity renormalization scheme, and it will be important to avoid nonlocalities from the regulator itself. Choosing constituent cutoffs ensures there is a limited possibility of confusing between different sources of nonlocalities. Moreover, as we show below, one can choose constituent cutoffs which would allow boost invariance to be maintained to a good approximation within a large domain of center of mass momenta. In the next section, we discuss the details of the cutoff scheme and map out the center of mass domain (the values of P^+ and $P^\perp$) in which when a cutoff constituent appears in a state, the internal mass of that state is guaranteed to be above an effective cutoff Λ^2.

B. Details of the cutoff scheme

We start with the formula for the total mass of an eigenstate of H_0 (where H_0 is the free part of the Hamiltonian) of n constituents with momenta $(k_i^+, k_{i\perp})$ and masses m_i:

$$M^2 = P^+ \sum_i \frac{m_i^2 + k_{i\perp}^2}{k_i^+} - P_\perp^2, \tag{6.1}$$

where $P^+ = \sum_i k_i^+$ and $P_\perp = \sum_i k_{i\perp}$. If we introduce the internal or Jacobi momenta $x_i = \frac{k_i^+}{P^+}$ and $q_{i\perp} = k_{i\perp} - x_i P_\perp$, then

$$M^2 = \sum_i \frac{m_i^2 + q_{i\perp}^2}{x_i}. \tag{6.2}$$

Thus the square of the total mass of the system is simply a sum of internal mass terms, which is a manifestation of the kinematical boost symmetries.

We need to prove that the partial sums of internal mass terms can always be lowered by replacing two constituents by a single constituent with the same total $q_\perp$ and x and the lower of the constituent masses, that is,

$$\frac{m_1^2 + q_{1\perp}^2}{x_1} + \frac{m_2^2 + q_{2\perp}^2}{x_2} \geq \frac{(m_1 + m_2)^2 + (q_{1\perp} + q_{2\perp})^2}{x_1 + x_2}. \tag{6.3}$$

Let $\xi_1 = \frac{x_1}{x_1 + x_2}$, $\xi_2 = \frac{x_2}{x_1 + x_2} = 1 - \xi_1$, $q_{1\perp} = r_\perp + \xi_1 q_\perp$, $q_{2\perp} = -r_\perp + \xi_2 q^\perp$, where $q_\perp = q_{1\perp} + q_{2\perp}$. Then

$$\begin{aligned} \frac{m_1^2 + q_{1\perp}^2}{x_1} + \frac{m_2^2 + q_{2\perp}^2}{x_2} &= \frac{1}{x_1 + x_2}\left[\frac{m_1^2 + r_\perp^2}{\xi_1} + \frac{m_2^2 + r_\perp^2}{\xi_2} + q_\perp^2\right] \\ &\geq \frac{1}{x_1 + x_2}\left[\frac{m_1^2\xi_2 + m_2^2\xi_1}{\xi_1\xi_2} + q_\perp^2\right]. \end{aligned} \tag{6.4}$$

But the minimum value of $\frac{m_1^2}{\xi_1} + \frac{m_2^2}{\xi_2}$ is $(m_1 + m_2)^2$. Hence

$$\frac{m_1^2 + q_{1\perp}^2}{x_1} + \frac{m_2^2 + q_{2\perp}^2}{x_2} \geq \frac{(m_1 + m_2)^2 + (q_{1\perp} + q_{2\perp})^2}{x_1 + x_2} \geq \frac{m^2 + (q_{1\perp} + q_{2\perp})^2}{x_1 + x_2}, \tag{6.5}$$

where m is the lower of the constituent masses. It follows then that any multiconstituent state with a given total x and $q_\perp$ must have an invariant mass which is greater than or equal to that of the state containing just two constituents of lowest mass m and having the same total $q^\perp$ and x.

We set constituent momentum cutoffs such that for states of center of mass momentum $(P_0^+, P_\perp = 0)$ the cutoff momenta first appear in states when the $(\text{mass})^2$ is $2\Lambda^2$ and then evaluate the range of center of mass momenta $(P^+, P_\perp)$ for which cutoff momentum constituents first appear at a $(\text{mass})^2$ of Λ^2 or higher. Thus all states with $(\text{mass})^2 < 2\Lambda^2$ and total momentum $(P_0^+, 0)$ are kept, and we must then restrict the range of $(P^+, P_\perp)$ so as to ensure that no state with this total momentum and $(\text{mass})^2 < \Lambda^2$ has a constituent beyond the cutoff boundary. This gives us a large domain to test whether covariance can be restored to good approximation with appropriate counterterms.

By our theorem, if a constituent of momentum $(k_1^+, k_{1\perp})$ and mass m_1 appears in a state of center of mass momentum $(P_0^+, 0)$, then the state of minimum total mass

containing this constituent contains a second constituent with momentum $(k_2^+, k_{2\perp})$, where $k_2^+ = P_0^+ - k_1^+$ and $k_{1\perp} = -k_{2\perp}$, and mass m, the minimum of the constituent masses. The mass of this state is

$$(\text{mass})^2 = \frac{m_1^2 + k_{1\perp}^2}{x_1} + \frac{m^2 + k_{1\perp}^2}{1 - x_1}, \tag{6.6}$$

with $x_1 = \frac{k_1^+}{P_0^+}$, $x_2 = \frac{k_2^+}{P_0^+}$. We therefore need to characterize the *boundary curve* in $x_1, k_{1\perp}$ space on which

$$\frac{m_1^2 + k_{1\perp}^2}{x_1} + \frac{m^2 + k_{1\perp}^2}{1 - x_1} = \frac{m_1^2}{x_1} + \frac{m^2}{1 - x_1} + \frac{k_{1\perp}^2}{x_1(1 - x_1)} = 2\Lambda^2. \tag{6.7}$$

Solving this equation for $k_{1\perp}^2$ we have

$$k_{1\perp}^2 = 2\Lambda^2 x_1(1 - x_1) - m_1^2(1 - x_1) - m^2 x_1. \tag{6.8}$$

For $\Lambda^2 \gg m_1^2$, we find $k_{1\perp}^2$ achieves its maximum value very close to $\frac{\Lambda^2}{2}$, when $x_1 = \frac{1}{2}$. To ensure no deterioration in the cutoff for momenta $P^+ > P_0^+$, we define the cutoff boundary curve to be

$$k_{1\perp}^2 = \frac{\Lambda^2}{2} - m^2 \qquad \text{for} \quad x_1 = \frac{k_1^+}{P_0^+} > \frac{1}{2} \quad \text{(including } x_1 > 1\text{)}, \tag{6.9}$$

while, for $x_1 < \frac{1}{2}$,

$$k_{1\perp}^2 = 2\Lambda^2 x_1(1 - x_1) - m^2, \tag{6.10}$$

which applies only in the domain $x_1 > \frac{m^2}{2\Lambda^2} + O(\frac{m^4}{\Lambda^4})$ for which $k_{1\perp}^2 \geq 0$. We will ignore corrections to the bound on x that are $O(\frac{m^4}{\Lambda^4})$, but a careful analysis must retain these. $x_1 < \frac{m^2}{2\Lambda^2}$ is not allowed. Note that x_1 is defined in terms of P_0^+, even for $P^+ \neq P_0^+$.

The reader may at first feel somewhat uneasy about the statement "including $x_1 > 1$." Consider for simplicity a two-body system of equal-mass particles. First consider the frame $P^+ = P_0^+$ and $P_\perp = 0$. The internal mass of the state is

$$M^2 = \left(\frac{m^2 + k_{1\perp}^2}{k_1^+} + \frac{m^2 + k_{2\perp}^2}{k_2^+} \right) P_0^+. \tag{6.11}$$

Define $x_1 = \frac{k_1^+}{P_0^+}$ and $x_2 = \frac{k_2^+}{P_0^+}$. Thus in the frame $P^+ = P_0^+$, $0 < x_1 < 1$, where we have dropped terms of order m^2/Λ^2. Next consider the frame $P^+ = \tilde{P}^+$. Let $c = \frac{\tilde{P}^+}{P_0^+}$. Thus in this frame $0 < x_1 < c$ and c is greater than 1 if $\tilde{P}^+ > P_0^+$. We also have $x_2 = c - x_1$ and $0 < x_2 < c$. If we did not extend the boundary as exhibited in (6.9), however, the x_i's would be limited as $0 < x_i < 1$, and one could not have a two constituent state with $\tilde{P}^+ > 2P_0^+$. Such a cutoff would likely be too restrictive.

We next determine the boundary curve in P^+ and $P_\perp$ space for which the cutoff mass is Λ^2; namely, constituents on the cutoff boundary occur only in states of $(\text{mass})^2 = \Lambda^2$ or higher. If the center of mass momentum of a state is $(P^+, P_\perp)$ and we consider one constituent $(k_1^+, k_{1\perp})$ on the cutoff boundary (6.9) and (6.10) with $x_1 = k_1^+/P_0^+$, then from our theorem above we know that the invariant mass of this state must be at least

$$M^2 = \frac{m^2 + (k_{1\perp} - \xi_1 P_\perp)^2}{\xi_1} + \frac{m^2 + (k_{2\perp} - \xi_2 P_\perp)^2}{\xi_2} = \frac{m^2 + (k_{1\perp} - \xi_1 P_\perp)^2}{\xi_1(1 - \xi_1)}, \tag{6.12}$$

where $\xi_1 = k_1^+/P^+$, $\xi_2 = k_2^+/P^+$, and the second equality follows from the relations $k_2^+ = P^+ - k_1^+$ and $k_{2\perp} = P_\perp - k_{1\perp}$. We ask, what must $(P^+, P_\perp)$ be to ensure that the minimum of this mass over all allowed values of k_1^+, with $k_{1\perp}^2$ on the boundary, is Λ^2?

First, note that M^2 is a minimum when $k_{1\perp}$ and $P_\perp$ are in the same direction. Let $\gamma = P^+/P_0^+$, so that $\xi_1 = x_1/\gamma$. Using (6.12) and the requirement that M^2 be greater than Λ^2, we find

$$x_1^2 P_\perp^2 - 2x_1\gamma \mid k_{1\perp} \mid \mid P_\perp \mid \geq \Lambda^2 x_1(\gamma - x_1) - \gamma^2(k_{1\perp}^2 + m^2). \tag{6.13}$$

Dropping the solution which excludes $P_\perp = 0$, we have

$$0 \leq \mid P_\perp \mid \leq \frac{1}{x_1} \left\{ \gamma \mid k_{1\perp} \mid - \left[\Lambda^2 x_1(\gamma - x_1) - \gamma^2 m^2 \right]^{1/2} \right\}. \tag{6.14}$$

Substituting for $k_{1\perp}$ from (6.9) and (6.10), dropping terms of order m^2/Λ^2, and minimizing the right-hand side with respect to x_1, we find

$$0 \leq \mid P_\perp \mid \leq \Lambda \left[(1 - \gamma)(2\gamma - 1) \right]^{1/2} \qquad \text{for} \quad 1/2 \leq \gamma \leq 3/4 \tag{6.15}$$

and

$$0 \leq \mid P_\perp \mid \leq \frac{\Lambda}{2\sqrt{2}} \qquad \text{for} \quad \gamma \geq 3/4. \tag{6.16}$$

Using the definition of γ, this implies that only states with $P^+ \geq P_0^+/2$ are allowed.

C. Cutoffs and field operators

To summarize the results of the previous section, the cutoff boundary on each constituent's momenta $(k_i^+, k_{i\perp})$ is specified by

$$k_{i\perp}^2 = 2\Lambda^2 \frac{k_i^+}{P_0^+}\left(1 - \frac{k_i^+}{P_0^+}\right) - m^2 \qquad \text{for} \quad \frac{m^2}{2\Lambda^2}P_0^+ < k_i^+ < \frac{P_0^+}{2} \tag{6.17}$$

and

$$k_{i\perp}^2 = \frac{\Lambda^2}{2} - m^2 \qquad \text{for} \quad \frac{P_0^+}{2} < k_i^+, \tag{6.18}$$

where m is the lowest of the constituent masses. Then, in a considerable range of center of mass domain ($P_\perp = 0, P^+ = \frac{P_0^+}{2}$ to $P_\perp = \frac{\Lambda}{2\sqrt{2}}, P^+ \geq \frac{3P_0^+}{4}$), when a cutoff constituent appears in a state, the internal mass of the state is guaranteed to be at least Λ^2. This domain for physics with cutoff $(\text{mass})^2 \geq \Lambda^2$ is shown in Fig. 4.

At all stages of the calculation we will also want to provide a buffer zone outside this constituent momentum cutoff boundary extending $k_{i\perp}^2$ roughly a factor of 2 and k_i^+ a factor of 1/2. We can accomplish this by setting the outside of the buffer zone at

$$k_{i\perp}^2 = 4\Lambda^2 \frac{k_i^+}{P_0^+}\left(1 - \frac{k_i^+}{P_0^+}\right) - m^2 \qquad \text{for} \quad \frac{m^2}{4\Lambda^2}P_0^+ < k_i^+ < \frac{P_0^+}{2} \tag{6.19}$$

and

$$k_{i\perp}^2 = \Lambda^2 - m^2 \qquad \text{for} \quad \frac{P_0^+}{2} < k_i^+. \tag{6.20}$$

The buffer zone allows the use of a smoothing cutoff in order to let interactions die gradually. In (6.17)–(6.20), the cutoff Λ eliminates both ultraviolet transverse and infrared longitudinal degrees of freedom. In order to define such a constituent cutoff which still limits the invariant mass of a state, however, we are forced to introduce a longitudinal momentum scale P_0^+. Dependence on this scale must also be eliminated as part of the renormalization process.

We now have the boundary on the degrees of freedom kept in $k_\perp$ and k^+. This is shown in Fig. 5. These cutoff boundaries are to be employed in the integrals over momenta in the momentum-space expansion of the field operators. The quark field operator is

$$\xi(x) = \sum_s \chi_s \int_c \frac{dk^+ d^2k_\perp}{16\pi^3}\left[b_s(k)e^{-ik\cdot x} + d_s^\dagger(k)e^{ik\cdot x}\right] \tag{6.21}$$

and the gluon field operator is

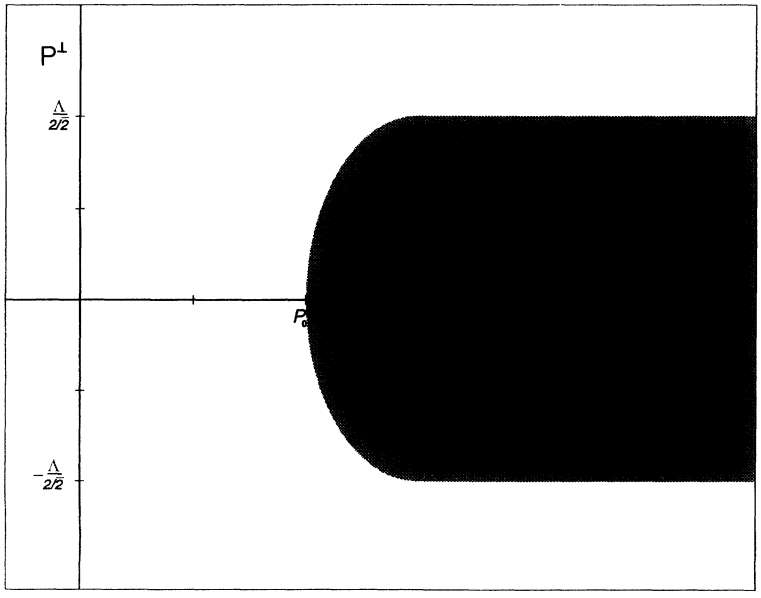

FIG. 4. Cutoff region of center of mass momenta.

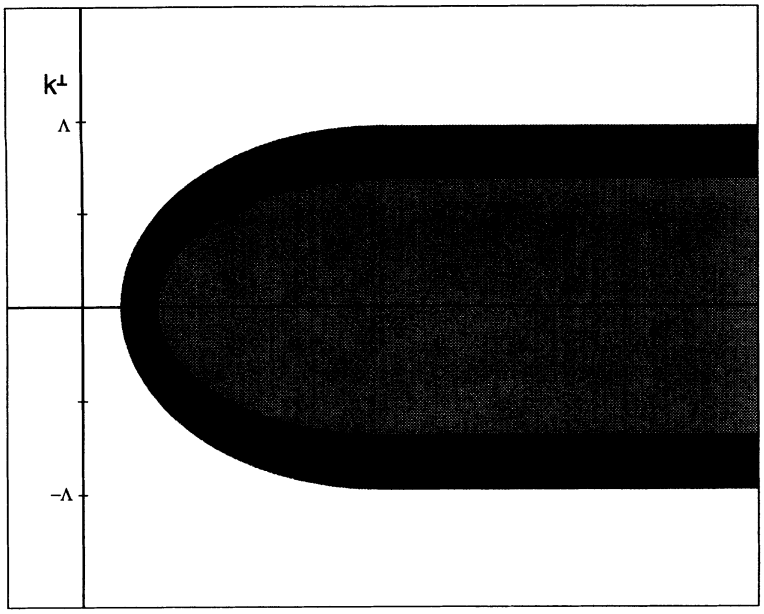

FIG. 5. Cutoff region of constituent momenta.

$$A^i(x) = \sum_\lambda \int_c \frac{dk^+ d^2k_\perp}{16\pi^3\sqrt{k^+}} [\epsilon^i_\lambda a_\lambda(k) e^{-ik\cdot x} + \epsilon^{i*}_\lambda a^\dagger_\lambda(k) e^{ik\cdot x}], \tag{6.22}$$

where color indices have been suppressed. If we choose sharp momentum cutoffs, the momentum integrals may be explicitly written as

$$\int_c dk^+ d^2k_\perp \equiv \int_{k^+_{\min}}^{P_0^+/2} dk^+ \int d^2k_\perp \theta(2\Lambda^2 x(1-x) - m^2 - k_\perp^2) + \int_{P_0^+/2}^{\infty} dk^+ \int d^2k_\perp \theta\Big(\frac{\Lambda^2}{2} - m^2 - k_\perp^2\Big), \tag{6.23}$$

where now $k^+_{\min} = \frac{m^2}{2\Lambda^2} P_0^+$.

With sharp momentum cutoffs it is possible to develop nonanalyticities in the structure of counterterms. We illustrate this with the following example.

Consider the type of transverse momentum integration that occurs in the gluon self-mass. In its simplest form this integral is

$$I = \int d^2k_{1\perp} d^2k_{2\perp}\, \delta^2(P_\perp - k_{1\perp} - k_{2\perp})\, \theta\big(\Lambda^2 - k_{1\perp}^2\big)\, \theta\big(\Lambda^2 - k_{2\perp}^2\big) \tag{6.24}$$

$$= \int d^2k_{1\perp}\, \theta\big(\Lambda^2 - k_{1\perp}^2\big)\, \theta(\Lambda^2 - (P_\perp - k_{1\perp})^2), \tag{6.25}$$

with Λ a very large parameter. Introducing the variable $\kappa_\perp$ by $k_{1\perp} = \kappa_\perp + \frac{1}{2}P_\perp$, $k_{2\perp} = -\kappa_\perp + \frac{1}{2}P_\perp$,

$$I = \frac{1}{2}\int_0^{2\pi} d\phi\, \kappa^2_{\max}, \tag{6.26}$$

with (for $P_\perp << \Lambda$)

$$\kappa_{\max} \simeq \mathrm{Min}\Big[\Lambda - \frac{1}{2} \mid P_\perp \mid \cos\phi, \Lambda + \frac{1}{2} \mid P_\perp \mid \cos\phi\Big]. \tag{6.27}$$

Then,

$$I_{\text{divergent}} = \pi\Lambda^2 - 2\Lambda \mid P_\perp \mid . \tag{6.28}$$

The sharp cutoff has given rise to a nonanalytic divergence. To avoid such nonanalyticities in the structure of counterterms, analytic cutoff functions are preferred. For example, the momentum integrals can be cutoff as

$$\int_c dk^+ d^2k_\perp \equiv \int_0^\infty dk^+ \int d^2k_\perp C\left(\frac{k_\perp^2 + m^2}{k_\perp^2 + m^2 + 4\Lambda^2 x/(1+4x)}\right), \tag{6.29}$$

where $x = k^+/P_0^+$. $\mathcal{C}(y)$ is a cutoff function which equals 1 for $y = 0$ and decreases analytically to 0 for $y = 1$. The integration over longitudinal momentum is thus cutoff at a minimum $k^+_{\rm min} = \frac{m^2}{2\Lambda^2}P_0^+$. As long as $\mathcal{C}$ is analytic the self-mass will have to be analytic in $P_\perp$; the $\mid P_\perp \mid$ divergence will disappear.

VII. SIMILARITY RENORMALIZATION SCHEME

The bare cutoff Hamiltonian will be solved in two stages. The first stage is a renormalization stage in which effects at relativistic momenta are computed using perturbation theory. These effects are computed to a specified order in g in perturbation theory. For the simplest computation the renormalization calculation is limited to second-order terms in g. To study the next level of complexity, the similarity renormalization program can be carried out to fourth order in g, but that is not attempted here.

The output of the renormalization stage is an effective Hamiltonian which is dominated in weak coupling by nonrelativistic relative momenta. The bound states of the effective Hamiltonian in weak coupling are pure $q\bar{q}$, pure qqq, or pure gg states, exactly as predicted in the CQM. All major effects of gluon emission and absorption, or more complex processes, are absorbed into the effective Hamiltonian for these states. Once the effective Hamiltonian is constructed, the computation of bound state energies involves readily executed numerical computations.

A new procedure for the renormalization of Hamiltonians has been developed by Głazek and Wilson to best meet the needs of light-front computations [14,15]. The new procedure is needed to simplify qualitative calculations leading to the effective Hamiltonian. Of especial importance is an ability to handle linear potentials correctly. The problem with a linear potential is that even if it has a small coefficient (even of order g^6), the linear potential becomes of order 1 or even larger simply by going to large enough distances. But once a linear potential has become large enough it can no longer be treated perturbatively and must instead be incorporated into an unperturbed Hamiltonian, for either qualitative or quantitative analysis. Since a crucial question is how linear potentials do or do not develop, a procedure which handles them sensibly is of critical importance.

Another requirement for the new renormalization procedure is that no small energy denominators should arise in any order of perturbation theory. That is, energy denominators of the form $1/(E - E')$ should never arise with $|E - E'|$ being far smaller that either E or E'. Normal perturbative treatments of field theoretic Hamiltonians lead constantly to such small energy denominators. But for exploring the complex phenomena of light-front renormalization, which will require crude and qualitative analyses, it is desirable to avoid encountering the possibly large effects resulting from such small denominators. Such large effects are very difficult to estimate using qualitative arguments. Large effects arise in particular when kinematic constraints force $E - E'$ to have a single sign yet allow it to be small. A typical example is collinear emission of gluons at large transverse momenta. In this case, the incoming and outgoing constituents all have large light-front energies due to their large momenta. Nevertheless, the final state energy is only slightly above the initial state energy, yet cannot ever be lower than the initial state energy.

The third requirement we place on the new renormalization procedure is that the effective Hamiltonian should have a Jacobi-type cutoff severely restricting internal momenta while the center of mass momenta are restricted only by the original bare cutoff. This will allow us to verify the restoration of longitudinal and transverse boost invariance in the effective Hamiltonian itself.

The first stage computation also identifies all cutoff dependences in the bare Hamiltonian, and therefore can be used to identify all needed counterterms to eliminate the cutoff dependence in perturbation theory, including dependences that violate as well as conserve boost invariance.

A. Similarity transformation of Hamiltonians

For now our discussion will be valid for any Hamiltonian with non-negative eigenvalues. Specialization to the light-front case occurs below in Sec. VII B. The basic idea of the "similarity renormalization scheme" is to develop a sequence of infinitesimal unitary transformations that transform the initial bare Hamiltonian H_B to an effective Hamiltonian H_σ, where σ is an arbitrarily chosen energy scale. When the transformations are multiplied together, one arrives at a transformation S_σ:

$$H_\sigma = S_\sigma H_B S_\sigma^\dagger. \tag{7.1}$$

The basic goal for the transformation S_σ is that H_σ should be in band-diagonal form relative to the scale σ. What this means, qualitatively, is that matrix elements of H_σ involving energy jumps much larger than σ (other than jumps between two large but nearby energies) will all be zero, while matrix elements involving smaller jumps or two nearby energies remain in H_σ.

We require that for $\sigma \to \infty$, $H_\sigma \to H_B$ and $S_\sigma \to 1$. The effective Hamiltonian we seek involves H_σ with σ of order the quark or gluon mass. The similarity operator S_σ may be expressed in terms of the anti-Hermitian generator of infinitesimal changes of scale T_σ as

$$S_\sigma = \mathcal{T}\exp\left(\int_\sigma^\infty d\sigma'\, T_{\sigma'}\right), \tag{7.2}$$

where $\mathcal{T}$ puts operators in order of increasing σ. Clearly, this satisfies the above limit condition. Using

$$T_\sigma = S_\sigma \frac{dS_\sigma^\dagger}{d\sigma} = -\frac{dS_\sigma}{d\sigma}S_\sigma^\dagger, \tag{7.3}$$

the differential form of (7.1) is

$$\frac{dH_\sigma}{d\sigma} = [H_\sigma, T_\sigma], \tag{7.4}$$

which is subject to the boundary condition $\lim_{\sigma\to\infty} H_\sigma = H_B$ from above. We shall never need to explicitly construct the similarity operator S_σ in what follows.

We need to specify the action of T_σ. We write $H_B = H_0 + H_I^B$, $H_\sigma = H_0 + H_{I\sigma}$, let E_i and E_j be eigenvalues of H_0, and denote any given matrix element of H_σ as $H_{\sigma ij}$. The differential equations of the similarity renormalization scheme [15] that determine both H_σ and T_σ are

$$\frac{dH_{\sigma ij}}{d\sigma} = f_{\sigma ij}[H_{I\sigma}, T_\sigma]_{ij} + \frac{d}{d\sigma}(\ln f_{\sigma ij}) H_{\sigma ij}, \tag{7.5}$$

$$T_{\sigma ij} = \frac{1}{E_j - E_i}\left\{(1 - f_{\sigma ij})[H_{I\sigma}, T_\sigma]_{ij} - \frac{d}{d\sigma}(\ln f_{\sigma ij}) H_{\sigma ij}\right\},$$

where $f_{\sigma ij} = f(x_{\sigma ij})$ with

$$x_{\sigma ij} = \frac{|E_i - E_j|}{E_i + E_j + \sigma}. \tag{7.6}$$

These equations are consistent with (7.4). The function $f(x)$ should be chosen as follows:

$$0 \le x \le \frac{1}{3}, f(x) = 1 \quad \text{(near diagonal region)};$$

$$\frac{1}{3} \le x \le \frac{2}{3}, f(x) \text{ drops from 1 to 0} \quad \text{(transition region)};$$

$$\frac{2}{3} \le x \le 1, f(x) = 0 \quad \text{(far off diagonal region)}. \tag{7.7}$$

$f(x)$ is to be infinitely differentiable throughout $0 \le x \le 1$, including the transition points 1/3 and 2/3.

It will be shown that with these definitions $H_{\sigma ij}$ is zero in the far off-diagonal region and $T_{\sigma ij}$ is zero in the near-diagonal region. The second claim is immediately obvious from the form of $T_{\sigma ij}$ in (7.5), for $1-f$ and $d_\sigma(\ln f)$ vanish when $0 \le x \le 1/3$. To see that $H_{\sigma ij}$ vanishes when $x \ge 2/3$, we first note that since H_0 is diagonal, $d_\sigma(\ln f) H_{0ij}$ vanishes identically (f is 1 and $d_\sigma f$ is 0 for $x = 0$), and from this result we can indeed declare that the unperturbed part H_0 of H_σ does not vary with σ, with T_σ being of order H_I or higher. Now we can rewrite Eqs. (7.5) as

$$\frac{d}{d\sigma}\left\{\frac{1}{f_{\sigma ij}} H_{I\sigma ij}\right\} = [H_{I\sigma}, T_\sigma]_{ij}, \tag{7.8}$$

$$T_{\sigma ij} = \frac{1}{E_j - E_i}\left\{(1 - f_{\sigma ij})[H_{I\sigma}, T_\sigma]_{ij} - \left(\frac{df_{\sigma ij}}{d\sigma}\right)\frac{1}{f_{\sigma ij}} H_{I\sigma ij}\right\}.$$

We will see below that H_I/f remains finite even when $f = 0$. Solving the first equation with the stated boundary condition at $\sigma \to \infty$ gives

$$H_{I\sigma ij} = f_{\sigma ij}\left\{H^B_{Iij} - \int_\sigma^\infty d\sigma' [H_{I\sigma'}, T_{\sigma'}]_{ij}\right\}. \tag{7.9}$$

Since $f(x)$ vanishes when $|x| \ge 2/3$, we find that $H_{\sigma ij}$ does indeed vanish in the far off-diagonal region.

That $T_{\sigma ij}$ is zero in the near-diagonal region means that a perturbative solution to $H_{\sigma ij}$ in terms of H^B_{Iij} will never involve vanishing energy denominators, which are a potential source of large errors in other perturbative renormalization schemes. That $H_{\sigma ij}$ is zero in the far off-diagonal region will help identify divergent terms and determine the form of counterterms necessary to remove these divergences. In LFQCD, we are considering cutoffs which severely break the symmetries of the canonical theory. The renormalization process is therefore sure to be quite complicated, and the advantage of the similarity renormalization procedure is that it allows a clean identification and separation of divergences.

Finally, we have to discuss renormalization conditions. The bare LFQCD Hamiltonian has a limited structure — canonical terms, an artificial potential, and renormalization terms. The renormalization counterterms are to be determined by fixing outputs: both physical masses and renormalized coupling constants defined in terms of measurable parameters, and a subset of the constraints of Lorentz covariance. These outputs are to be obtained perturbatively by solving the Hamiltonian bound state problem. But for now we mainly want the functional form of the counterterms, which has to precede determination of their strengths. The main requirement for counterterms in H_B is that they remove divergences in the integral over the commutator $[H_{I\sigma'}, T_{\sigma'}]$.

We can summarize the equations for $H_{I\sigma}$ and T_σ as

$$H_{I\sigma} = H^B_{I\sigma} + \underbrace{[H_{I\sigma'}, T_{\sigma'}]}_R, \tag{7.10}$$

where $H^B_{I\sigma ij} = f_{\sigma ij} H^B_{Iij}$ and the linear operation R is

$$\underbrace{X_{\sigma' ij}}_R = -f_{\sigma ij}\int_\sigma^\infty d\sigma' X_{\sigma' ij}. \tag{7.11}$$

Using the equation for $H_{I\sigma}$ allows us to write

$$T_\sigma = H^B_{I\sigma T} + \underbrace{[H_{I\sigma'}, T_{\sigma'}]}_T, \tag{7.12}$$

where

$$H^B_{I\sigma T ij} = -\frac{1}{E_j - E_i}\left(\frac{d}{d\sigma} f_{\sigma ij}\right) H^B_{Iij} \tag{7.13}$$

and

$$\underbrace{X_{\sigma' ij}}_T = -\frac{1}{E_j - E_i}\left(\frac{d}{d\sigma} f_{\sigma ij}\right) \times \int_\sigma^\infty d\sigma' X_{\sigma' ij} + \frac{1}{E_j - E_i}(1 - f_{\sigma ij}) X_{\sigma ij}. \tag{7.14}$$

This equation structure saves us from writing the solution for T_σ separately because it is obtained by substitution

from the equation for $H_{I\sigma}$; namely, $H^B_{I\sigma} \to H^B_{I\sigma T}$, and all higher-order terms have the substitution $\underbrace{\cdots}_{R\to T}$. So we can start writing the iterated solution for $H_{I\sigma}$:

$$H_{I\sigma} = H^B_{I\sigma} + \underbrace{[H^B_{I\sigma'}, H^B_{I\sigma' T}]}_{R} + \underbrace{[\underbrace{[H^B_{I\sigma''}, H^B_{I\sigma'' T}]}_{R'}, H^B_{I\sigma' T}]}_{R} + \underbrace{[H^B_{I\sigma'}, \underbrace{[H^B_{I\sigma''}, H^B_{I\sigma'' T}]}_{T'}]}_{R} + \cdots . \tag{7.15}$$

The counterterms in H^B_I must be chosen to cancel the divergences which occur in integrals over intermediate states at higher order in H^B_I, and such counterterms must also then be included in higher-order iterations. If a limit to this process exists, the Hamiltonian is said to be renormalizable.

B. Discussion of the scheme

Now we may discuss the similarity renormalization scheme in more detail. The ultimate aim of this scheme is to transform the Hamiltonian H_B into a manageable, band-diagonal form H_σ. H_B is the bare cutoff Hamiltonian, forced to be finite by the imposition of some cutoff Λ. The differential transformation framework produces a set of Hamiltonians $H_{\sigma'}$, where σ' ranges from $O(\Lambda)$ down to some scale σ and thereby dresses the Hamiltonian. One step in this process is the determination of the form of the counterterms which must be included in H_B so that each of the matrix elements of the transformed Hamiltonian $H_{\sigma ij}$ has no large dependence on Λ. This is the renormalization process: As we send $\Lambda \to \infty$, we get a renormalized, scale-dependent effective Hamiltonian H^R_σ. This does not finish the renormalization of the Hamiltonian, however, for the finite parts of the counterterms in H_B will produce in H^R_σ unknown constants and functions of momenta which must be adjusted to reproduce physical observables and to restore the symmetries which were broken by the cutoff Λ. These quantities are to be fixed, then, by solving H^R_σ, and one should be able to do this with a combination of few-body Hamiltonian methods and weak-coupling diagrams.

We show this renormalization scheme pictorially in Fig. 6. The grey area is the region where σ is large enough so that H_σ is equivalent to the bare Hamiltonian H_B. The necessary condition is that $|x_{\sigma ij}| \leq 1/3$ for all i and j, which is true for

$$\sigma \geq \frac{\Lambda}{2} - \frac{5\mu}{2}, \tag{7.16}$$

where Λ is the maximum and μ is the minimum energy of the free states of the cutoff Hamiltonian H_B. By lowering the scale σ below this region for a given Λ, we start transforming H_B — eventually producing a band-diagonal Hamiltonian at some sufficiently low scale. Thus we form a new "triangle of renormalization," as shown in Fig. 6. First, we eliminate degrees of freedom by fixing the cutoff at some value Λ_1, and we denote the corresponding bare Hamiltonian as H^1_B. Now we perform the unitary similarity transformation to bring the Hamiltonian to a band-diagonal form characterized by some scale σ_0, which we denote as H^1_0 in the figure. Next, we increase the cutoff to some value Λ_2 to get H^2_B and then transform via σ to get H^2_0, defined at the same similarity scale σ_0 as was H^1_0. As we increase Λ_N in this way, we end up with a sequence of band-diagonal Hamiltonians

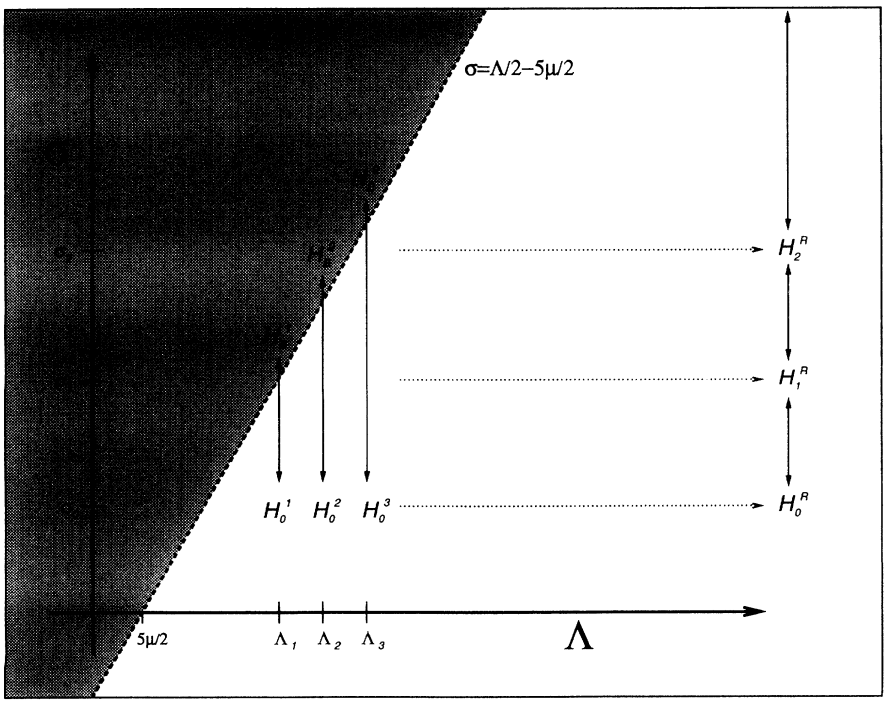

FIG. 6. Triangle of renormalization.

H_0^N. The renormalized Hamiltonian at scale σ_0 is the limit of this sequence, $H_0^R = \lim_{N\to\infty} H_0^N$.

Of course, we could use the similarity transformation to bring the effective Hamiltonian to any scale σ_n and obtain a set of sequences $\{H_n^N\}$. As we change σ, we change the characteristic scale, but the physics is invariant with respect to this change for large enough Λ_N. The utility of the similarity renormalization scheme is that the transformation is invertible, as indicated by the double-arrowed lines in Fig. 6. Thus, if we find a Hamiltonian that is finite and Λ independent for any one scale σ_n, the differential similarity framework guarantees that we can obtain a Hamiltonian that is finite and cutoff independent for all σ. Note that we require that each matrix element of H_σ be cutoff independent for external momenta which are small in comparison to the cutoff, which is more restrictive than just requiring this of the eigenvalues of H_σ.

We now discuss the choice of counterterms. We start with the bare cutoff Hamiltonian H_B, which consists of the canonical Hamiltonian with cutoff Λ plus a set of counterterms which have an explicit Λ dependence arranged so that physical observables obtained from H_B are Λ independent. These counterterms are at the outset undetermined. As we perform the similarity transformation, we get an effective Hamiltonian H_σ, where the scale σ replaces Λ. This is done through a precise differential framework. Qualitatively, we are separating high-energy degrees of freedom (of order Λ) from low-energy degrees of freedom (of order σ). In the language of the phase space cell analysis of Sec. V, we have $\Lambda \sim$ transverse (longitudinal) widths $(\delta y_\perp)^{-1}(\delta y^-)$, respectively, and $\sigma \sim$ transverse (longitudinal) widths $(\delta x_\perp)^{-1}(\delta x^-)$, respectively. Thus, by varying Λ, we determine which divergences have to be eliminated from H_σ. The counterterms which eliminate these divergences must be added to H_B, and so can have no dependence on σ. The structure of each counterterm $H_{Bij}^{\rm ct}$ is limited by the structure of the divergence it must cancel—namely, by the external legs associated with states i and j. Along with the diverging part of each counterterm, we may in principle associate an unknown finite piece, whose precise form is to be determined by fitting data and restoring symmetries. These terms must be restricted so that a piece which removes an ultraviolet divergence, for example, will have a precise behavior with respect to external transverse momenta, but may have a finite piece associated with it which contains an unknown function of the external longitudinal momenta—provided that function does not break boost invariance. A similar rule applies to counterterms for infrared divergences. However, remember that the individual constituents associated with external momenta do not correspond to physical states, and so we cannot include counterterms for apparent infrared divergences which would be eliminated upon integration with a test function.

Finally, we need to fill in some details in order to match the general presentation of the similarity scheme given here to the particular choices of light-front coordinates and the cutoffs on constituent momenta described in Sec. VI. The bare LFQCD Hamiltonian has a cutoff Λ which has the dimensions of transverse momentum. The cutoff Λ of Sec. VI is designed to simultaneously eliminate constituents with large light-front energies due to either large transverse or small longitudinal momenta. We want to define the light-front similarity scale to have the same dimensions as Λ and to be a true invariant-mass scale. The scale σ is defined through (7.6), which we now redefine for the light front as

$$x_{\sigma ij} = \frac{|P_j^- - P_i^-|}{P_i^- + P_j^- + P_\sigma^-}. \tag{7.17}$$

Here, P_i^- and P_j^- are the (off-mass-shell) light-front free energies of the states i and j (namely, sums over the states' constituents' light-front free energies), and

$$P_\sigma^- \equiv \frac{-2P_\perp^2 + \sigma^2}{P^+}. \tag{7.18}$$

Since $(P^+, P_\perp)$ is conserved in any process — that is, $H_{ij} \propto \delta(P_i^+ - P_j^+)\delta^2(P_{i\perp} - P_{j\perp})$ — we see that $x_{\sigma ij}$ as given in (7.18) is independent of the total longitudinal momentum P^+ and transverse momentum $P_\perp$. Defined in this way, the light-front similarity scale σ' interpolates from a mass scale $O(\Lambda)$ down to some final scale σ, which sets the mass scale of the bound states of the effective Hamiltonian. Moreover, from (6.1) and (6.2) we see that (7.17) reduces to

$$x_{\sigma ij} = \frac{|M_j^2 - M_i^2|}{M_i^2 + M_j^2 + \sigma^2}, \tag{7.19}$$

with M_i and M_j the total masses of the states i and j. So the similarity transformation replaces the cutoff Λ, which explicitly breaks boost invariance, with a boost invariant-mass scale σ.

VIII. EXAMPLE CALCULATION: SECOND-ORDER GLUON MASS CORRECTION

In this section we provide an example of the application of the new regulator scheme and the similarity transformation perturbation theory to second order in the coupling constant. We calculate the correction to the gluon mass coming from intermediate two-gluon states, which is depicted in Fig. 7. This correction contains severe divergences.

First, we need to find the explicit form for $H^{(2)}$ in (7.15). After substitution from the previous equations and use of the Hermiticity of H_I^B, we find

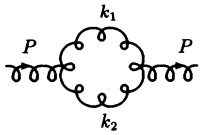

FIG. 7. Gluon mass correction from two-gluon intermediate states.

$$H^{(2)}_{I\sigma ij} = \underbrace{[H^B_{I\sigma'}, H^B_{I\sigma' T}]_{ij}}_{R} = \sum_k H^B_{Iik} H^B_{Ikj} \left\{ \frac{g_{\sigma jik}}{P^-_i - P^-_k} + \frac{g_{\sigma ijk}}{P^-_j - P^-_k} \right\}, \tag{8.1}$$

where the sum over intermediate states k includes an integration over momenta. The function g is

$$g_{\sigma ijk} = f_{\sigma ij} \int_\sigma^\infty d\sigma' f_{\sigma' ik} \frac{d}{d\sigma'} f_{\sigma' jk}, \tag{8.2}$$

and it serves to keep i and j in the near-diagonal and transition regions ($x_{\sigma ij} < 2/3$) and j and k in the transition and far off-diagonal regions ($x_{\sigma jk} > 1/3$). The identity $f_{\sigma ij} = f_{\sigma ji}$ and integration by parts give

$$g_{\sigma ijk} + g_{\sigma jik} = f_{\sigma ij}(1 - f_{\sigma ik} f_{\sigma jk}), \tag{8.3}$$

so that we can write

$$\frac{g_{\sigma jik}}{P^-_i - P^-_k} + \frac{g_{\sigma ijk}}{P^-_j - P^-_k} = \frac{1}{2} f_{\sigma ij}(1 - f_{\sigma ik} f_{\sigma jk}) \left\{ \frac{1}{P^-_i - P^-_k} + \frac{1}{P^-_j - P^-_k} \right\} - \frac{P^-_i - P^-_j}{2(P^-_i - P^-_k)(P^-_j - P^-_k)} (g_{\sigma ijk} - g_{\sigma jik}). \tag{8.4}$$

The first term is the same as that obtained in the Bloch renormalization scheme [19], but now modified so that the energy denominators never get small. The second term in (8.4) vanishes as $P^-_i \to P^-_j$. Divergences occur when P^-_k is much greater than P^-_i and P^-_j, in which case the first term in (8.4) will give the dominant contribution to (8.1).

For the gluon mass correction, the initial and final states have the same momenta, so that

$$H^{(2)}_{I\sigma ij} = \sum_k H^B_{Iik} H^B_{Ikj} \frac{1 - f^2_{\sigma ik}}{P^-_i - P^-_k}. \tag{8.5}$$

We denote the single gluon state as $|i\rangle = |P, a, \lambda\rangle$, where $P = (P^+, P_\perp)$, a, and λ are its momentum, color index, and helicity index. Using the diagrammatic rules for the canonical vertices [9], we have

$$\begin{aligned}
H^{(2)}_{I\sigma ij} &= \langle P, b, \lambda' | H^{(2)}_{I\sigma} | P, a, \lambda \rangle \\
&= -\frac{1}{2} \frac{1}{P^+} g^2 (f^{acd} f^{bdc}) \int_c \frac{dk^+_1 d^2k_{1\perp}}{16\pi^3} \frac{dk^+_2 d^2k_{2\perp}}{16\pi^3} \frac{\theta(k^+_1)}{k^+_1} \frac{\theta(k^+_2)}{k^+_2} \frac{16\pi^3 \delta^3(P - k_1 - k_2)}{P^-_i - P^-_k} \left[1 - f^2(x_{\sigma ik})\right] \\
&\quad \times \epsilon^{*i_4}_{\lambda'} \left\{ \delta_{i_3 i_2} \left[(k^{i_4}_2 - k^{i_4}_1) - \frac{P^{i_4}}{P^+}(k^+_2 - k^+_1) \right] + \delta_{i_2 i_4} \left[-(k^{i_3}_2 + P^{i_3}) + \frac{k^{i_3}_1}{k^+_1}(k^+_2 + P^+) \right] \right. \\
&\qquad \left. + \delta_{i_4 i_3} \left[(P^{i_2} + k^{i_2}_1) - \frac{k^{i_2}_2}{k^+_2}(P^+ + k^+_1) \right] \right\} \\
&\quad \times \left\{ \delta_{i_2 i_3} \left[(k^{i_1}_2 - k^{i_1}_1) - \frac{P^{i_1}}{P^+}(k^+_2 - k^+_1) \right] + \delta_{i_1 i_3} \left[(k^{i_2}_1 + P^{i_2}) - \frac{k^{i_2}_2}{k^+_2}(k^+_1 + P^+) \right] \right. \\
&\qquad \left. + \delta_{i_1 i_2} \left[-(P^{i_3} + k^{i_3}_2) + \frac{k^{i_3}_1}{k^+_1}(P^+ + k^+_2) \right] \right\} \epsilon^{i_1}_\lambda \\
&= \frac{g^2 C_A}{2P^+ 16\pi^3} \delta^{ab} \int_c dk^+_1 d^2k_{1\perp} dk^+_2 d^2k_{2\perp} \delta^3(P - k_1 - k_2) \mathcal{M}_{2\lambda\lambda'}(P, k_1, k_2)\big(1 - f^2_{\sigma ik}\big),
\end{aligned} \tag{8.6}$$

where the factor $\frac{1}{2}$ is the symmetry factor, $P^-_i = \frac{m^2_G + (P_\perp)^2}{P^+}$, $P^-_k = k^-_1 + k^-_2 = \frac{m^2_G + k^2_{1\perp}}{k^+_1} + \frac{m^2_G + k^2_{2\perp}}{k^+_2}$, $f_{\sigma ik} = f(x_{\sigma ik})$ with f given by (7.7) and $x_{\sigma ik}$ given by (7.17)–(7.19), $C_A \delta^{ab} = f^{acd} f^{bcd} = N\delta^{ab}$, and $\mathcal{M}_{2\lambda\lambda'}$ denotes the two vertices with the energy denominator.

To find the mass correction, we set $P_\perp = 0$ and define

$$H^{(2)}_{I\sigma ii}|_{P_\perp = 0} \equiv \frac{\delta m^2_G}{P^+} \delta_{\lambda\lambda'} \delta^{ab}, \tag{8.7}$$

where the mass shift is $\delta m^2_G = \delta m^2_{G\Lambda} + \delta m^2_{G\sigma}$.

Integration over k_2 and the cutoff scheme of Sec. VI lead to

$$\delta m^2_G \delta_{\lambda\lambda'} = -\frac{g^2 N}{16\pi^3} \int dk^+_1 d^2k_{1\perp} \theta^\Lambda_\epsilon(k_1) \theta^\Lambda_\epsilon(P - k_1) \mathcal{M}_{2\lambda\lambda'}(P, k_1, P - k_1)\big(1 - f^2_{\sigma ik}\big), \tag{8.8}$$

where

$$\mathcal{M}_{2\lambda\lambda'}(P,k_1,P-k_1)=\frac{1}{k_1^+}\frac{1}{P^+-k_1^+}\left[\frac{k_{1\perp}^2+m_G^2}{k_1^+}+\frac{k_{1\perp}^2+m_G^2}{P^+-k_1^+}-\frac{m_G^2}{P^+}\right]^{-1}$$
$$\times 4\left\{k_{1\perp}^2\left[\left(\frac{P^+}{k_1^+}\right)^2+\left(\frac{P^+}{P^+-k_1^+}\right)^2\right]\delta_{\lambda\lambda'}+2k_{1\perp}\cdot\epsilon_{\lambda'}^*k_{1\perp}\cdot\epsilon_\lambda\right\}, \tag{8.9}$$

and the cutoff function $\theta_\epsilon^\Lambda(k)$ is defined via (6.23) as

$$\theta_\epsilon^\Lambda(k)\equiv\theta(k^+-\epsilon)\left[\theta\left(\frac{P_0^+}{2}-k^+\right)\theta\left(2\Lambda^2\frac{k^+}{P_0^+}\left(1-\frac{k^+}{P_0^+}\right)-m^2-k_\perp^2\right)+\theta\left(k^+-\frac{P_0^+}{2}\right)\theta\left(\frac{\Lambda^2}{2}-m^2-k_\perp^2\right)\right], \tag{8.10}$$

with $\epsilon\simeq\frac{m^2P_0^+}{2\Lambda^2}$, Λ the bare cutoff, and m the smaller of m_G and m_F. We use sharp cutoffs here only for the purpose of illustration. We stress that smooth cutoffs are preferred so as to avoid nonanalyticities.

We write

$$\delta m_G^2\delta_{\lambda\lambda'}=-\frac{g^2N}{4\pi^3}I_{\lambda\lambda'}, \tag{8.11}$$

with

$$I_{\lambda\lambda'}=\int dxd^2k_{1\perp}\theta_\epsilon^\Lambda(xP^+,k_{1\perp})\theta_\epsilon^\Lambda((1-x)P^+,-k_{1\perp})$$
$$\times\left[2k_{1\perp}\cdot\epsilon_{\lambda'}^*k_{1\perp}\cdot\epsilon_\lambda+\left(\frac{1}{x^2}+\frac{1}{(1-x)^2}\right)k_{1\perp}^2\delta_{\lambda\lambda'}\right]$$
$$\times\frac{1}{k_{1\perp}^2+m_G^2[1-x+x^2]}\left[1-f^2(x_{\sigma ik})\right], \tag{8.12}$$

with

$$x=\frac{k_1^+}{P^+}\quad\text{and}\quad x_{\sigma ik}=\frac{k_{1\perp}^2+m_G^2(1-x+x^2)}{k_{1\perp}^2+m_G^2(1+x-x^2)+\sigma^2}. \tag{8.13}$$

So we see that the external (total) momentum P^+ enters only through the cutoffs. The term independent of $f_{\sigma ik}$ in (8.12) gives rise to divergent contributions as the cutoff Λ becomes large, as well as finite contributions, and the second term involving $f_{\sigma ik}^2$ is a finite, σ-dependent contribution ($f_{\sigma ik}$ cuts off the integration before it reaches the bare cutoff Λ).

Evaluating I for the case $P^+>P_0^+$, for example, the divergent part of the mass shift is

$$\delta m_{G\Lambda}^2=-N\frac{g^2}{4\pi^2}(F_1+F_2+F_3+F_4). \tag{8.14}$$

F_1 is the quadratic ultraviolet-divergent part:

$$F_1=\Lambda^2\left[\frac{1}{2}-\frac{P_0^+}{6P^+}-\frac{4P^+}{P_0^+}-\frac{4P^+}{P_0^+}\left(\frac{2P^+}{P_0^+}-1\right)\right.$$
$$\left.\times\ln\frac{2P^+-P_0^+}{2P^+}\right]. \tag{8.15}$$

F_2 is the logarithmic ultraviolet-divergent part:

$$F_2=-m_G^2\ln\Lambda^2\left[\frac{5}{6}-2\ln\frac{P^+}{P_0^+}\right]. \tag{8.16}$$

F_3 is the mixed ultraviolet- and infrared-divergent part:

$$F_3=4\Lambda^2\frac{P^+}{P_0^+}\ln\frac{P_0^+}{2\epsilon}-2m_G^2\left[\frac{P^+}{\epsilon}-\ln\frac{P_0^+}{\epsilon}\right]\ln\Lambda^2. \tag{8.17}$$

F_4 is the pure infrared-divergent part:

$$F_4=2m_G^2\frac{P^+}{\epsilon}\ln\frac{P_0^+}{\epsilon}-2\left(m^2+m_G^2+m_G^2\ln\frac{2}{m_G^2}\right)\frac{P^+}{\epsilon}$$
$$-m_G^2\ln^2\frac{P_0^+}{\epsilon}-2m_G^2\left(1-\frac{P^+}{P_0^+}-\ln\frac{2}{m_G^2}\right)\ln\frac{P_0^+}{\epsilon}. \tag{8.18}$$

Note that the mass shift is negative, as it must be in second-order perturbation theory.

The coefficients of the ultraviolet quadratic and logarithmic divergences are multiplied by functions of longitudinal momenta which are in accord with the power-counting rules but which are not boost invariant. We have to subtract them entirely, and the finite parts of these counterterms are just arbitrary constants since an arbitrary function of longitudinal momenta violates longitudinal boost invariance. The divergences arising from small longitudinal momenta also violate longitudinal boost invariance because of the cutoff scheme, and so these divergences are also to be subtracted away, leaving room for only an arbitrary constant.

The evaluation of the second term in (8.12) depends explicitly on the choice of the function f. For qualitative purposes, we may choose a step function, namely,

$$f(x)=\theta\left(\frac{1}{2}-x\right), \tag{8.19}$$

which results in the effective cutoffs for the Jacobi momenta:

$$\kappa_{\perp\max}^2=(\sigma^2+3m_G^2)x(1-x)-m_G^2,$$
$$\frac{m_G^2}{(\sigma^2+3m_G^2)}\le x\le 1-\frac{m_G^2}{\sigma^2+3m_G^2}. \tag{8.20}$$

These yield a result bounded by σ and finite as $\Lambda\to\infty$.

Thus, with the cutoff theory, even if we set the bare gluon mass to zero, the gluon mass correction δm_G^2 does not vanish. After subtracting the infinite mass correction, there remains a finite contribution which depends on the mass scale parameter σ. This dependence is altered by spectators because $x_{\sigma ij}$ changes when spectator energies change.

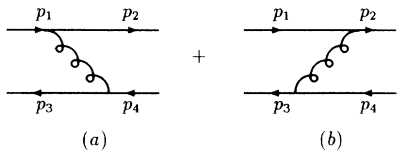

FIG. 8. Contribution to quark-antiquark scattering amplitude from gluon exchange.

IX. INFRARED COUNTERTERMS IN LOWEST-ORDER PERTURBATION THEORY

In Sec. IV we discussed the infrared counterterms in the canonical Hamiltonian itself. Products of the interaction Hamiltonian lead to light-front infrared (small k^+) divergences in addition to the ultraviolet (large $k_\perp$) divergences. Note that we do not have the conventional infrared divergence (small $k_\perp$) since gluons are massive. As we have pointed out there is a crucial difference between these infrared divergences and ultraviolet divergences.

In constructing counterterms for the infrared divergences in the products of the interaction Hamiltonian, we find strong cutoff dependence already in tree level amplitudes — for example, in the $O(g^2)$ quark-antiquark scattering amplitude. Here, what one has in fact are infrared *singularities*. When we diagonalize the Hamiltonian, these amplitudes are integrated with wave packet functions, and *nonintegrable* singularities in the amplitudes give rise to energy divergences. Thus to find the infrared counterterm it is not enough just to isolate the infrared singular amplitudes; we have to integrate the amplitude over the external leg with a wave packet function. For QED, in contrast, where the external legs correspond to physical particles, all tree level singularities have to cancel. No such cancellations will be assumed here.

In this section we outline the construction of infrared (small k^+) counterterms up to order g^2. The infrared divergences arise from either an exchanged infrared gluon or an exchanged infrared fermion in the intermediate state. The counterterms arising from infrared gluons are of interest when looking for the origin of confinement, and the counterterms arising from infrared fermions are of interest when looking for the origin of spontaneous chiral symmetry breaking.

A. Counterterms from infrared gluons

1. *Counterterms in the quark-antiquark sector*

The interaction Hamiltonian H_{qqg} gives rise to an effective Hamiltonian in second order whose matrix element for the $q\bar{q}$ states $|i\rangle = |p_1, s_1, \alpha_1; p_2, -s_2, \alpha_2\rangle$ and $|j\rangle = |p_3, s_3, \alpha_3; p_4, -s_4, \alpha_4\rangle$ (see Fig. 8) is given by

$$H^{(2)}_{I\sigma ij} = -g^2\, T^a_{\alpha_3\alpha_1} T^a_{\alpha_4\alpha_2} \mathcal{M}_{2ij}\, [\mathcal{F}_2\, f_{\sigma ij}\, (1 - f_{\sigma ik} f_{\sigma jk}) + O((P_k^-)^{-3})], \tag{9.1}$$

where p_n, s_n, α_n are the momentum, helicity, and color index of the nth quark,

$$\mathcal{M}_{2ij} = \chi^\dagger_{s_3}\left[2\frac{p_1^{i_1} - p_3^{i_1}}{p_1^+ - p_3^+} - im_F\left(\frac{1}{p_1^+} - \frac{1}{p_3^+}\right)\sigma^{i_1} - \left(\sigma^{i_1}\frac{\sigma_\perp \cdot p_{1\perp}}{p_1^+} + \frac{\sigma_\perp \cdot p_{3\perp}}{p_3^+}\sigma^{i_1}\right)\right]\chi_{s_1}$$
$$\times\chi^\dagger_{-s_2}\left[2\frac{p_4^{i_1} - p_2^{i_1}}{p_4^+ - p_2^+} - im_F\left(\frac{1}{p_4^+} - \frac{1}{p_2^+}\right)\sigma^{i_1} - \left(\sigma^{i_1}\frac{\sigma_\perp \cdot p_{4\perp}}{p_4^+} + \frac{\sigma_\perp \cdot p_{2\perp}}{p_2^+}\sigma^{i_1}\right)\right]\chi_{-s_4}, \tag{9.2}$$

$$\mathcal{F}_2 = \frac{\theta^\Lambda_\epsilon(p_1 - p_3)}{p_1^+ - p_3^+}\frac{1}{2}\left[\frac{1}{p_1^- - p_3^- - q^-} + \frac{1}{p_4^- - p_2^- - q^-}\right] + \frac{\theta^\Lambda_\epsilon(p_3 - p_1)}{p_3^+ - p_1^+}\frac{1}{2}\left[\frac{1}{p_2^- - p_4^- + q^-} + \frac{1}{p_3^- - p_1^- + q^-}\right], \tag{9.3}$$

and

$$f_{\sigma ij} = f(x_{\sigma ij}) \quad \text{with} \quad x_{\sigma ij} = \frac{|\, P^+P_j^- - P^+P_i^-\,|}{P^+P_j^- + P^+P_i^- - 2P_\perp^2 + \sigma^2}. \tag{9.4}$$

The function $\theta^\Lambda_\epsilon(k)$, which arises from the cutoffs on the intermediate gluon, is defined in Sec. VII:

$$\theta^\Lambda_\epsilon(k) \equiv \theta(k^+ - \epsilon)\left\{\theta\left(\frac{P_0^+}{2} - k^+\right)\theta\left[2\Lambda^2\frac{k^+}{P_0^+}\left(1 - \frac{k^+}{P_0^+}\right) - m^2 - k_\perp^2\right] + \theta\left(k^+ - \frac{P_0^+}{2}\right)\theta\left(\frac{\Lambda^2}{2} - m^2 - k_\perp^2\right)\right\}, \tag{9.5}$$

with $\epsilon = \frac{m^2 P_0^+}{2\Lambda^2}$, Λ the bare cutoff, and m the smaller of m_G and m_F. Here we have also defined

$$p^- = \frac{m_F^2 + p_\perp^2}{p^+}\ , \quad q^- = \frac{m_G^2 + (p_{1\perp} - p_{3\perp})^2}{p_1^+ - p_3^+}; \tag{9.6}$$

P_k^- denotes the intermediate state energy:

$$P_k^- = p_3^- + q^- + p_2^- \quad \text{for } p_1^+ > p_3^+ \quad \text{and} \quad P_k^- = p_1^- - q^- + p_4^- \quad \text{for } p_1^+ < p_3^+. \tag{9.7}$$

The expression for $\mathcal{F}_2$ can be further simplified:

$$\mathcal{F}_2 = \frac{\theta_\epsilon^\Lambda(p_1 - p_3) + \theta_\epsilon^\Lambda(p_3 - p_1)}{p_1^+ - p_3^+} \frac{1}{2}\left[\frac{1}{p_1^- - p_3^- - q^-} + \frac{1}{p_4^- - p_2^- - q^-}\right]. \tag{9.8}$$

To identify the infrared counterterms, we look for singular terms. We have, explicitly,

$$P_i^- = p_1^- + p_2^-,\ P_j^- = p_3^- + p_4^-. \tag{9.9}$$

The intermediate state energy is dominated by that of the infrared gluon: namely,

$$P_k^- \approx q^- \quad \text{for } p_1^+ > p_3^+, \quad P_k^- \approx -q^- \quad \text{for } p_3^+ > p_1^+. \tag{9.10}$$

As the gluon longitudinal momentum fraction reaches ϵ, both $x_{\sigma ik}$ and $x_{\sigma jk}$ become greater than $\frac{2}{3}$, and as a consequence $1 - f_{\sigma ik} f_{\sigma jk} \to 1$. The leading singular term is

$$4g^2 T^a_{\alpha_3\alpha_1} T^a_{\alpha_4\alpha_2} \delta_{s_1 s_3} \delta_{s_2 s_4} \left(1 - \frac{m_G^2}{(p_{1\perp} - p_{3\perp})^2 + m_G^2}\right) \frac{f_{\sigma ij}}{(p_1^+ - p_3^+)^2} [\theta_\epsilon^\Lambda(p_1 - p_3) + \theta_\epsilon^\Lambda(p_3 - p_1)]. \tag{9.11}$$

To find the infrared divergence we integrate over p_3 with a test function $\phi(p_3^+, p_{3\perp})$, which we may assume is nonzero only in the range where $f_{\sigma ij} = 1$. This evaluation is complicated by the cutoff function. Using the definition of θ_ϵ^Λ in (9.5), we find a divergent piece

$$I \equiv \int_\epsilon^{P_0^+/2} \frac{dk^+}{(k^+)^2} \int d^2k_\perp \phi(p+k) \theta\left(\frac{m^2}{\epsilon} k^+ \left(1 - \frac{k^+}{P_0^+}\right) - m^2 - k_\perp^2\right) \frac{k_\perp^2}{k_\perp^2 + m_G^2}, \tag{9.12}$$

where $k = p_3 - p_1$, and a similar piece for $p_1^+ - p_3^+ > \epsilon$, which is the same as (9.12) except that $\phi(p+k) \to \phi(p-k)$. To find the small-ϵ dependence in I, we write $k^+ = \epsilon x$, switch the order of integration, and expand in ϵ. The divergence has the form

$$\frac{2m^2}{\epsilon} \int d^2k_\perp \frac{k_\perp^2}{(k_\perp^2 + m^2)(k_\perp^2 + m_G^2)} \phi(p_1^+, p_{1\perp} + k\perp). \tag{9.13}$$

Hence we need to include a counterterm for this linear divergence in H_B:

$$4g^2 T^a_{\alpha_3\alpha_1} T^a_{\alpha_4\alpha_2} \delta_{s_1 s_3} \delta_{s_2 s_4} \frac{2m^2}{\epsilon} \frac{(p_{1\perp} - p_{3\perp})^2}{[(p_{1\perp} - p_{3\perp})^2 + m^2][(p_{1\perp} - p_{3\perp})^2 + m_G^2]} \delta(p_1^+ - p_3^+). \tag{9.14}$$

Without our cutoffs and for zero gluon mass we would find exactly the same counterterm but with the opposite sign as the counterterm for the instantaneous four-fermion interaction in the canonical Hamiltonian, and hence no $O(g^2)$ counterterm would be necessary for the linear infrared divergence. But our cutoff scheme, which is dependent on the choice of massive constituents and thereby eliminates zero modes, does not allow complete cancellation to occur.

There are also $\frac{1}{q^+}$ type singularities which lead to logarithmic infrared divergences. But these divergences are canceled from the two θ functions in (9.8). Thus there is no counterterm necessary to remove a logarithmic infrared divergence in $q\bar{q}$ scattering to second order [45]. However, as discussed in Sec. IV B for the canonical Hamiltonian counterterms, the use of a symmetric cutoff to ensure the cancellation of divergences from small positive and negative longitudinal momenta excludes any possibility of finite contributions from exact zero modes. To counter this elimination of zero modes, we can include a finite term analogous to (4.17). Here the transverse structure in $\mathcal{M}_2$, for example, the product of the first and last terms in (9.2), may keep such terms from vanishing, in contrast to terms corresponding to instantaneous zero-mode gluon exchange. The finite counterterms also involve a product of two fermion color charges as one needs to start building true confining potentials. True confining potentials confine only nonzero color charge states as opposed to the artificial potential which confines all states.

2. Counterterms in the quark-gluon sector

Now we consider the qg states. The effective Hamiltonian in second order (see Fig. 9) is given by

$$H^{(2)}_{I\sigma ij} = ig^2 f^{abc}\, T^b_{\alpha_2\alpha_1}\mathcal{M}_{2ij}\,[\mathcal{F}_2\, f_{\sigma ij}\,(1 - f_{\sigma ik}f_{\sigma jk}) + O((P^-_k)^{-3})], \tag{9.15}$$

for the states $|i\rangle = |k_1, \lambda_1, a; p_1, s_1, \alpha_1\rangle$ and $|j\rangle = |k_2, \lambda_2, c; p_2, s_2, \alpha_2\rangle$, where

$$\begin{aligned}\mathcal{M}_{2ij} = \epsilon^{*i_2}_{\lambda_2}\Big[&\delta^{i_1 i_3}\Big((k_1+q)^{i_2} - \frac{k_2^{i_2}}{k_2^+}(q^+ + k_1^+)\Big) + \delta^{i_2 i_3}\Big((k_2-q)^{i_1} - \frac{k_1^{i_1}}{k_1^+}(k_2^+ - q^+)\Big)\\ &+\delta^{i_1 i_2}\Big(-(k_1+k_2)^{i_3} + \frac{q^{i_3}}{q^+}(k_1^+ + k_2^+)\Big)\Big]\epsilon^{i_1}_{\lambda_1}\\ &\times\chi^\dagger_{s_2}\left[\frac{2q^{i_3}}{q^+} - im_F\left(\frac{1}{p_1^+} - \frac{1}{p_2^+}\right)\sigma^{i_3} - \left(\sigma^{i_3}\frac{\sigma_\perp\cdot p_{1\perp}}{p_1^+} + \frac{\sigma_\perp\cdot p_{2\perp}}{p_2^+}\sigma^{i_3}\right)\right]\chi_{s_1},\end{aligned} \tag{9.16}$$

$$\mathcal{F}_2 = \frac{\theta^\Lambda_\epsilon(p_1 - P_3) + \theta^\Lambda_\epsilon(p_3 - p_1)}{k_1^+ - k_2^+}\,\frac{1}{2}\left[\frac{1}{k_1^- - k_2^- - q^-} + \frac{1}{p_2^- - p_1^- - q^-}\right], \tag{9.17}$$

and

$$k_n^- = \frac{m_G^2 + k_{n\perp}^2}{k_n^+}\quad,\quad q^- = \frac{m_G^2 + (k_{1\perp} - k_{2\perp})^2}{k_1^+ - k_2^+}. \tag{9.18}$$

Again, to identify the infrared counterterms, we look for singular terms. As in the case of the quark–antiquark sector, the intermediate state energy is dominated by the infrared gluon and the factor $(1 - f_{\sigma ik}f_{\sigma jk})$ is replaced by 1. The most singular term (leaving out the factor $f_{\sigma ij}$) is

$$2ig^2 f^{abc}T^b_{\alpha_2\alpha_1}\delta^{i_1 i_2}\delta_{\lambda_1\lambda_2}\delta_{s_1 s_2}\frac{(k_1^+ + k_2^+)}{(k_1^+ - k_2^+)^2}\left(1 - \frac{m_G^2}{m_G^2 + (k_{1\perp} - k_{2\perp})^2}\right)[\theta^\Lambda_\epsilon(p_1 - p_3) + \theta^\Lambda_\epsilon(p_3 - p_1)]. \tag{9.19}$$

To find the divergence we must again integrate over k_2 with a test function, which again yields a linearly divergent term as above. Here also the cutoffs and nonzero gluon mass spoil any complete cancellation of this divergence with the counterterm for the two-quark–two-gluon instantaneous interaction.

After the subtraction of the linear divergence, a linearly singular term (proportional to m_G^2) survives, but as in the case of the $q\bar{q}$ scattering amplitude, there is no divergence after integrating the amplitude with a test function. There are also other $1/q^+$ terms in (9.18), but the logarithmic divergences they produce are canceled from the two θ^Λ_ϵ functions. However, as with the $q\bar{q}$ sector, even though the logarithmic divergence for small q^+ is canceled by that for small $-q^+$, we need to include a counterterm to account for the possibility of finite effects from exchange of gluons with exactly $q^+ = 0$.

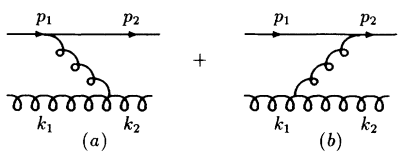

FIG. 9. Contribution to quark-gluon scattering amplitude from gluon exchange.

B. Counterterms from infrared fermions

In this subsection, we consider the contributions to the matrix elements of the effective Hamiltonian in the quark-gluon sector arising from quark exchange. First, we discuss the contribution from an intermediate one-quark–two-gluon state, as is shown in Fig. 10(a). The matrix element is given by

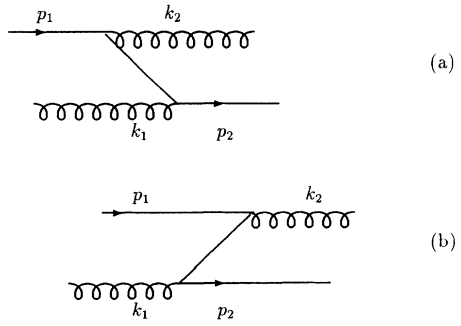

FIG. 10. Contribution to quark-gluon scattering amplitude from quark exchange.

$$H^{(2)}_{I\sigma ij} = g^2\ (T^a T^b)_{\alpha_2\alpha_1} \mathcal{M}_{2ij}\ [\mathcal{F}_2\ f_{\sigma ij}\ (1 - f_{\sigma ik} f_{\sigma jk}) + O((P_k^-)^{-3})], \tag{9.20}$$

where

$$\mathcal{M}_{2ij} = \chi^\dagger_{s_2} \epsilon^{*\perp}_{\lambda_2} \cdot \left[2\frac{k_{1\perp}}{k_1^+} + im_F \left(\frac{1}{p_2^+} - \frac{1}{p_3^+} \right) \sigma_\perp - \left(\sigma_\perp \frac{\sigma_\perp \cdot p_{3\perp}}{p_3^+} + \frac{\sigma_\perp \cdot p_{2\perp}}{p_2^+} \sigma_\perp \right) \right]$$
$$\times \left[2\frac{k_{2\perp}}{k_2^+} + im_F \left(\frac{1}{p_3^+} - \frac{1}{p_1^+} \right) \sigma_\perp - \left(\sigma_\perp \frac{\sigma_\perp \cdot p_{1\perp}}{p_1^+} + \frac{\sigma_\perp \cdot p_{3\perp}}{p_3^+} \sigma_\perp \right) \right] \cdot \epsilon^\perp_{\lambda_1} \chi_{s_1}, \tag{9.21}$$

$$\mathcal{F}_2 = \theta^\Lambda_\epsilon (p_1^+ - k_2^+) \frac{1}{2} \left[\frac{1}{p_1^- - p_3^- - k_2^-} + \frac{1}{p_2^- - p_3^- - k_1^-} \right], \tag{9.22}$$

with $p_3^+ = p_1^+ - k_2^+$, $p_{3\perp} = p_{1\perp} - k_{2\perp}$.

In the limit $p_3^+ \to 0$, we have

$$H^{(2)}_{I\sigma} \approx -g^2 T^a T^b \chi^\dagger (\sigma^\perp \cdot \epsilon^{*\perp})(\sigma^\perp \cdot \epsilon^\perp) \chi \frac{\theta^\Lambda_\epsilon (p_1^+ - k_2^+)}{p_1^+ - k_2^+}, \tag{9.23}$$

which leads to a logarithmic divergence when we integrate the effective Hamiltonian with wave packet functions which are functions of external momenta.

Next we consider the contributions to the matrix elements of the effective Hamiltonian in the quark-gluon sector arising from antiquark exchange, that is, from an intermediate two-quark–one-antiquark state, as is shown in Fig. 10(b). The matrix element is given by

$$H^{(2)}_{I\sigma ij} = -g^2\ (T^a T^b)_{\alpha_2\alpha_1} \mathcal{M}_{2ij}\ [\mathcal{F}_2\ f_{\sigma ij}\ (1 - f_{\sigma ik} f_{\sigma jk}) + O((P_k^-)^{-3})], \tag{9.24}$$

where

$$\mathcal{M}_{2ij} = \chi^\dagger_{s_2} \epsilon^{*\perp}_{\lambda_2} \cdot \left[2\frac{k_{1\perp}}{k_1^+} + im_F \left(\frac{1}{p_2^+} + \frac{1}{p_3^+} \right) \sigma_\perp - \left(\sigma_\perp \frac{\sigma_\perp \cdot p_{3\perp}}{p_3^+} + \frac{\sigma_\perp \cdot p_{2\perp}}{p_2^+} \sigma_\perp \right) \right]$$
$$\times \left[2\frac{k_{2\perp}}{k_2^+} - im_F \left(\frac{1}{p_3^+} + \frac{1}{p_1^+} \right) \sigma_\perp - \left(\sigma_\perp \frac{\sigma_\perp \cdot p_{1\perp}}{p_1^+} + \frac{\sigma_\perp \cdot p_{3\perp}}{p_3^+} \sigma_\perp \right) \right] \cdot \epsilon^\perp_{\lambda_1} \chi_{s_1}, \tag{9.25}$$

$$\mathcal{F}_2 = \theta^\Lambda_\epsilon (k_2^+ - p_1^+) \frac{1}{2} \left[\frac{1}{k_1^- - p_2^- - p_3^-} + \frac{1}{k_1^- - p_1^- - p_3^-} \right] \tag{9.26}$$

with $p_3^+ = k_2^+ - p_1^+$, $p_{3\perp} = k_{2\perp} - p_{1\perp}$.

In the limit $p_3^+ \to 0$, we have

$$H^{(2)}_{I\sigma ij} \approx g^2 T^a T^b \chi^\dagger (\sigma^\perp \cdot \epsilon^{*\perp})(\sigma^\perp \cdot \epsilon^\perp) \chi \frac{\theta^\Lambda_\epsilon (k_2^+ - p_1^+)}{k_2^+ - p_1^+}, \tag{9.27}$$

which leads to a logarithmic divergence when we integrate the effective Hamiltonian with wave packet functions which are functions of external momenta.

Note that if we keep both types of intermediate states, the singularity acquires a principal value prescription since the θ functions sum to 1, and thus no counterterm is needed. This is because the singularity occurs when the intermediate state energy is dominated by the exchanged quark or antiquark, in which case it does not matter if the other particles in the intermediate state are quarks or gluons. However, it is clear that the finite part of these diagrams will be affected differently, for the function $1 - f_{\sigma ik} f_{\sigma jk}$ in (9.23) will now cut off the two diagrams differently since the intermediate state energies are different when the exchanged quark and antiquark have finite energy. Thus we expect that at higher order there will be diagrams which contain quark or antiquark exchange of finite energy and have divergences associated with another process. Counterterms for these diagrams will have a different dependence for the intermediate qgg and $\bar{q}qq$ states and so a logarithmic divergence will not acquire a principal value prescription as here in second order. The counterterms necessary to remove such higher-order divergences will provide a possible source for explicit-chiral-symmetry breaking terms in the renormalized Hamiltonian.

Moreover, as with gluon exchange above, despite the cancellation of near-zero k^+ logarithmic divergences, we must include a finite term which might restore any physics lost by the elimination of exact zero modes. As discussed in Sec. IV B, there are finite noncanonical terms which have the structure of these logarithmic divergences and which satisfy the requirements of power

counting and boost invariance yet break chiral symmetry. Since such terms necessarily contain the effects normally associated with the vacuum, it is no surprise that they provide a source for chiral symmetry breaking (see the discussion of the sigma model in Appendix A).

Finally, a similar result applies for the matrix element describing quark-antiquark annihilation into two gluons, which involves the quark exchange shown in Fig. 11(a) and a similar diagram with an intermediate antiquark. We should here include a finite term so as to counter the removal of zero-mode fermion exchange, and this may include a piece which explicitly breaks chiral symmetry. It follows that the chiral-symmetry-violating term in the $q\bar{q}g$ coupling will have an arbitrary size due to renormalization from such a $q\bar{q}gg$ counterterm, as is depicted in Fig. 11(b). This term then need not vanish in the limit of only spontaneous chiral symmetry breaking.

C. Many-body infrared counterterms

While we provide no thorough discussion of higher-order counterterms, we need to clarify one qualitatively new feature that arises beyond second order. In Sec. IX A we showed that the matrix elements for gluon exchange include pieces that diverge like $1/(q^+)^2$, where q^+ is the longitudinal momentum exchange. This leads to divergences even at the tree level. These divergences require counterterms, and we have argued that the finite part of such counterterms may contain confining interactions unless boost invariance precludes this.

One example should adequately illustrate what happens at higher orders. In Fig. 12(a) we show a fourth-order tree diagram in which two gluons are exchanged between three quarks. To evaluate the matrix elements that arise in the effective Hamiltonian we must integrate over small q^+. Keeping only the most singular parts of the matrix elements, we encounter longitudinal integrals of the form

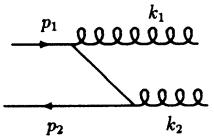

(a)

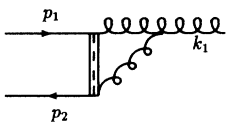

(b)

FIG. 11. Quark-antiquark annihilation and contribution to qqg vertex renormalization.

(a) (b)

FIG. 12. Higher-order multifermion processes requiring counterterms.

$$\int_\epsilon \frac{dq_1^+}{q_1^+}\int_\epsilon \frac{dq_2^+}{q_2^+}\left(\frac{1}{q_1^+}\right)^2\left(\frac{1}{q_2^+}\right)^2 q_1^+ q_2^+\left(\frac{M_1^2}{q_1^+}+\frac{M_2^2}{q_2^+}\right)^{-1}. \tag{9.28}$$

The entire product of matrix elements is relatively complicated, but this integral is easily analyzed. There is a $\ln^2(\epsilon M_1^2/M_2^2)$ divergence, and a $\ln^2(\epsilon M_2^2/M_1^2)$ divergence. There is actually a nested divergence in this diagram, which would be subtracted if one adds the appropriate third-order diagram; however, even after this subtraction one is left with $\ln^2(\epsilon)$ divergences.

Another simple example is shown in Fig. 12(b), in which there is a gluon exchanged between two quarks while one quark interacts through an instantaneous potential with a spectator. Regardless of the form of the instantaneous interaction, this diagram diverges logarithmically unless a symmetric cutoff on longitudinal momenta is used. As argued above, the presence of this potential logarithmic divergence indicates that the elimination of zero modes may produce an interaction with the operator structure in Fig. 11(b). This three-body interaction may be long range in the transverse direction, and it may be as strong as the two-body confining interactions. As we pointed out earlier, such long-range many-body interactions are required to cancel unphysical van der Waals forces if there is a confining two-body interaction [41].

X. LFQCD BOUND STATE COMPUTATIONS

Consider how bound states are handled in QED [46]. There one includes in the unperturbed Hamiltonian an instantaneous potential whose form is obtained from the general two-fermion four-point function. The precise choice of the potential to include in the unperturbed part is a matter of some art, since one must weigh the competing demands of making the unperturbed calculation as simple as possible while at the same time including a large part of the relevant physics and ensuring that perturbative corrections are small. Invariably, the bound state calculation reduces to the usual nonrelativistic Schrödinger equation in the appropriate limit, and the corresponding nonrelativistic states are used in the perturbative expansion. The precise details of any particular calculation will vary, and the most efficient methods can only be arrived at after some experience.

We want to take the same approach to bound states here, but we know from phenomenological constituent quark models that the confining potentials we need for

the bound state calculation are far different from the Coulomb-like potentials that arise at low order in the usual relativistic perturbation theory. We expect counterterms for the light-front infrared divergences to be the ultimate source of the needed potentials. For artificially small coupling, however, the artificial potential is the dominant confinement mechanism. The similarity renormalization scheme and massive constituents with cutoffs allow us to treat this confining potential in a weak coupling framework.

In this section, we outline the construction of the effective LFQCD Hamiltonian for low-energy hadrons and discuss the increasing levels of complexity in the LFQCD bound state computations in this formulation.

A. Effective LFQCD Hamiltonian and bound states

In the similarity renormalization scheme, the effective LFQCD Hamiltonian that will be used to compute the hadronic bound states is

$$H_{\sigma ij} = \lim_{\Lambda\to\infty} f_{\sigma ij}\left[H^B_{ij} + \sum_k \frac{1}{2} H^B_{Iik} H^B_{Ikj}\left(\frac{g_{\sigma ijk}}{P^-_j - P^-_k} + \frac{g_{\sigma jik}}{P^-_i - P^-_k}\right) + \cdots\right]. \tag{10.1}$$

H_σ causes transitions only between states staying "close to the diagonal" due to the factor $f_{\sigma ij}$, and the effects of transitions to and from intermediate states which are "far off diagonal" have explicitly appeared in the effective Hamiltonian H_σ as a perturbative expansion.

Recall that H^B_{ij} has the cutoff Λ which violates both longitudinal and transverse boost invariance. First we identify the counterterms that must be included in H^B so that the matrix elements of the effective Hamiltonian $H_{\sigma ij}$ have no divergent dependence on Λ. Then we send $\Lambda \to \infty$ so that cutoff dependence is removed from the effective Hamiltonian H_σ. As in standard perturbative renormalization theory, Λ dependence will be removed order by order in g_σ, where g_σ is the running coupling constant at the similarity scale in Hamiltonian matrix elements. This avoids having to solve the nonperturbative bound state problem to identify and remove Λ dependence.

There is a question whether $H_{\sigma ij}$ satisfies boost invariance after $\Lambda \to \infty$. There can be finite terms in H_σ which violate boost invariance, yet cannot justifiably be subtracted. Such terms might result, for example, as a by-product of divergent terms of the form $\ln \frac{\Lambda^2}{P_\perp^2}\, f(P^+)$, where $P_\perp$ and P^+ are external momenta. The $\ln \Lambda^2$ divergence must be subtracted. But the finite term $\ln P_\perp^2\, f(P^+)$ cannot be subtracted because no arguments exist that would justify such a nonanalytic $P_\perp$ dependence resulting from the effects of states above the cutoff. In this case violations of boost invariance can only disappear at special values of g where the coefficient of the boost-violating terms vanish. Clearly one such special value has to be $g = g_s$, as part of the restoration of covariance at g_s.

In the following it is assumed that the effective Hamiltonian H_σ has boost invariance simply as a result of taking the $\Lambda \to \infty$ limit. H_σ is generated as the first step in solving the bare cutoff Hamiltonian H_B. The second step is to construct bound states from H_σ. We may write the bound state equation as

$$\sum_j H_{\sigma ij}\psi_{N\sigma j} = \mathcal{E}_N \psi_{N\sigma i}, \tag{10.2}$$

where the sum over j includes a sum over Fock space sectors and integrals over momenta. The light-front energy of the Nth eigenstate is

$$\mathcal{E}_N = (M_N^2 + P_{N\perp}^2)/P_N^+, \tag{10.3}$$

where P_N^+ and $P_{N\perp}$ are the total longitudinal and transverse momenta of the eigenstate and M_N is its mass.

We will solve this field theoretic bound state problem in the standard fashion, using bound state perturbation theory. This requires us to identify a part of H_σ, $H_{\sigma 0}$, which is treated nonperturbatively to produce bound states. The essential simplification that makes further calculation possible is that $H_{\sigma 0}$ does not contain any interactions that change particle number, so that the methods of few-body quantum mechanics can be used to solve this initial nonperturbative problem. All field theoretic corrections that arise from particle creation and annihilation will then be treated perturbatively, as in QED. The potentials that appear in $H_{\sigma 0}$ must be chosen to make it possible for bound state perturbation theory to converge, and as stated above, this requires some art even in QED.

The bare cutoff Hamiltonian is divided as $H_B = H_0^B + H_I^B$. For the determination of the effective Hamiltonian H_σ, the unperturbed part of the bare Hamiltonian H_0^B is chosen to be that of free massive quarks and gluons with the standard relativistic dispersion relation in light-front kinematics. The interaction part H_I^B then contains the canonical interaction terms $H_{\rm int}$, renormalization counterterms $H_B^{\rm ct}$, and the artificial potential V_A. The artificial potential is itself separated as $V_A = V_0 + V_A^{\rm ct}$, with Coulomb and linear parts, $V_0 = V_C + V_L$, and counterterms $V_A^{\rm ct}$ which remove unphysical effects resulting from the choice of a massive gluon. For the bound state calculation, we want to choose the starting Hamiltonian to contain as much of the physics in as simple a form as possible. So we define

$$H_{\sigma 0ij} = f_{\sigma ij}\left(H^B_{0ij} + V_{0ij}\right) \tag{10.4}$$

and write the unperturbed bound state solutions as $\psi^{(0)}_{N\sigma j}$. These bound states will be pure $q\bar{q}$, pure qqq, or pure gg, as in the CQM.

The starting Hamiltonian is determined from the Fourier transforms of

$$H_0^B = \int dx^- d^2x_\perp \left\{ \frac{1}{2}(\partial^i A_a^j)^2 + m_G^2 A_a^{i2} + \xi^\dagger \left(\frac{-\partial_\perp^2 + m_F^2}{i\partial^+} \right) \xi \right\}, \tag{10.5}$$

$$V_0 = \int dx^- d^2x_\perp dy^- d^2y_\perp \left\{ -\frac{1}{4\pi} j^{+a}(x) \mathcal{V}_C(x,y) j^{+a}(y) + j^+(x) \mathcal{V}_L(x,y) j^+(y) \right\}, \tag{10.6}$$

where $\mathcal{V}_C$ and $\mathcal{V}_L$ are given by Eqs. (2.6) and (2.7), $j^{+a} = j_q^{+a} + j_g^{+a}$ is the color vector charge density, and $j^+ = j_q^+ + j_g^+$ is the color singlet charge density. This starting Hamiltonian determines the spectrum to order g_σ^4 and produces the zeroth-order bound states that are used to analyze radiative corrections starting at order g_σ^6.

The interaction part of the effective Hamiltonian can now be analyzed perturbatively, and it includes effective potentials that contain the effects of interactions involving far off-diagonal states as well as renormalization counterterms, which are determined order by order. Consider the effective Hamiltonian H_σ generated to second order in the renormalized coupling constant. The counterterms $H_B^{\rm ct}$ up to this order have been discussed in the Secs. IV B, VIII, and IX. They are the counterterms for the canonical instantaneous interactions, which can be combined as

$$H_{B2}^{\rm ct} = -\frac{g^2}{4\pi\epsilon} \int d^2x_\perp \left(\int dx^- j^{+a}(x^-, x_\perp) \right)^2, \tag{10.7}$$

and the counterterms from one-gluon exchange given in momentum space in (9.14) and (9.19), plus a similar term in the gluon-gluon sector. There are also quark and gluon mass counterterms, some of which we have given explicitly in Sec. VIII. The effect of these counterterms is to completely cancel the leading radiative corrections from instantaneous gluon exchange, all of which diverge or produce pathologies. In addition, as has been discussed in Secs. IV and IX, we need to include terms which counter the elimination of zero modes, such as (4.24):

$$H_{c3}^B = g^2 \int dx^- d^2x_\perp dy^- d^2y_\perp \xi^\dagger (\sigma_\perp \cdot A_\perp) \mathcal{O}_F(x,y) \times (\sigma_\perp \cdot A_\perp) \xi. \tag{10.8}$$

Such a counterterm can break chiral symmetry, for example, if $\mathcal{O}_F \sim m_F^{-1}(\sigma_\perp \cdot \partial_\perp)$. At this order, $\mathcal{O}_F$ must be determined phenomenologically; it remains to be seen whether coupling coherence and/or the restoration of Lorentz covariance will completely determine it at higher orders and as one lets $g \to g_s$. As discussed in Sec. IX, there may be many more such counterterms resulting from the elimination of zero modes. We have not written them down explicitly, but this must be done to compute order g_σ^6 shifts in the hadron spectrum.

What is the dependence of this effective Hamiltonian H_σ on the scale σ? Suppose we restrict the states to only a $q\bar{q}$ pair. Then only number-conserving (potential-like) terms in H_σ contribute. Now if we let the scale σ approach a very large number, only the original interactions in H_B survive since the factor $(1 - f_{\sigma ik} f_{\sigma jk}) \to 0$. Thus the canonical four-fermion interaction together with all counterterms survive, whereas the transversely smeared four-fermion interaction diminishes in strength. In the limit $\sigma \to \infty$ we are recovering H_B which is no surprise. In this limit the effects of higher Fock sectors (for example $q\bar{q}g$) can be recovered only by including them explicitly, and so it clearly becomes a poor approximation to include only the $q\bar{q}$ sector when σ becomes too large.

By lowering the similarity scale σ, we reduce the allowed range of gluon momenta which can contribute, for example, to the binding of a quark and antiquark in a meson. These effects must appear elsewhere, and we see that through the similarity transformation they are added directly to the Hamiltonian via the second- and higher-order terms in H_B in (10.1). Thus by lowering σ, we put the bare gluon exchange effects of H_B into a $q\bar{q}$ potential in the effective Hamiltonian H_σ perturbatively. This clearly changes the character of the bound state calculation. It changes from a field theoretic computation with arbitrary numbers of constituents to a computation dominated by an effective $q\bar{q}$ potential. If we choose the similarity scale σ to be just above the hadronic mass scale, the major effects come from the $q\bar{q}$ sector. The resulting nonrelativistic calculation will not see the scale σ in first approximation, since only states close to the diagonal, for which $f_{\sigma ij} = 1$ in (10.4), will contribute.

Consider Coulombic bound states with a Hamiltonian of the form $H = \frac{p^2}{m} - \frac{g^2}{r}$. $p \sim \frac{1}{r}$ and the energy of the bound state scales like g^4. Since r scales like $\frac{1}{g^2}$, if we add to the Hamiltonian a linear potential of the form αr and insist that the energy still scales like g^4 we infer that $\alpha \sim g^6$.

The bound state equation for the unperturbed effective Hamiltonian $H_{\sigma 0}$ can be written as

$$\left\{ \left[\frac{1}{p^+} p^2 + \frac{1}{p'^+} p'^2 \right] - \frac{g^2}{4\pi} \left[\frac{m_F}{p^+ r} + \frac{m_F}{p'^+ r'} \right] + \left(\frac{g^2}{4\pi} \right)^3 \beta \left[\frac{m_F^3 r}{p^+} + \frac{m_F^3 r'}{p'^+} \right] \right\} \Psi = \frac{4 m_F \mathcal{E}}{P^+} \Psi, \tag{10.9}$$

where P^+ is the center of mass longitudinal momentum. Using $p^+ \sim \frac{1}{2}P^+$ and $p'^+ \sim \frac{1}{2}P^+$, the fully nonrelativistic bound state energy is

$$\mathcal{E} = \left\langle \frac{p^2}{m_F} - \frac{g^2}{4\pi r} + \beta \left(\frac{g^2}{4\pi} \right)^3 m_F^2 r \right\rangle. \tag{10.10}$$

Now as expected, the uncertainty principle shows that $\mathcal{E}$ is minimized when r is of order $\frac{1}{g^2}$, and p is of order g^2 and hence $\mathcal{E}$ is of order g^4. Numerical computations can easily give precise results.

B. Potential instability problem

As we have argued in Sec. II E, we add an artificial potential to our effective Hamiltonian to ensure that the bound state structure is similar to that of the CQM. An additional benefit of including an artificial potential is that it allows the removal of a potential resulting from the choice of a massive gluon which might otherwise cause an instability in the bound state calculations.

We have shown in the previous sections that the introduction of a nonzero gluon mass leads to the incomplete cancellation of the linear interaction in the longitudinal direction between the canonical instantaneous interaction and the interaction arising from one-gluon exchange. The resulting interaction between the color charge densities is proportional to

$$g^2 T^a T^a \frac{m_G^2}{m_G^2 + (p_{1\perp} - p_{3\perp})^2} \frac{1}{(p_1^+ - p_3^+)^2}. \tag{10.11}$$

In the nonrelativistic limit, the transverse momentum difference in the denominator can be neglected in comparison to m_G^2, and this part of the effective Hamiltonian reduces to a pure linear interaction in the longitudinal direction. This linear interaction may cause an instability in the bound states when they are expanded to include higher Fock space sectors. Taking the expectation value of this term in a color singlet state consisting of a quark and an antiquark, namely, $|s_2\rangle = b^{i\dagger} d_i^\dagger |0\rangle$, we obtain the linear potential contribution to the energy. But the expectation value of the same interaction in a color singlet state consisting of a quark, an antiquark, and gluon, namely, $|s_3\rangle = [T^a]_i^j b^{i\dagger} d_j^\dagger a^{a\dagger}|0\rangle$, is the same as the previous case except that it is multiplied by the factor $-\frac{1}{2}C_A + C_F = -\frac{1}{6}$ for SU(3). This results in an linear potential which gives a *negative* contribution to the energy. This negative contribution leads to a possible instability for many-body bound states.

To remove the above instabilities in hadronic bound states, we need to subtract this linear interaction, as discussed in Sec. II E. We add this subtraction to the artificial potential with the form

$$\frac{g^2}{4}\left(1 - \frac{g^6}{g_s^6}\right) \int d^2x_\perp dx^- dy^-\ j^{+a}(x^-, x_\perp)|x^- - y^-|j^{+a}(y^-, x_\perp). \tag{10.12}$$

Here we multiply by a coefficient $(1 - g^6/g_s^6)$ rather than $(1 - g^2/g_s^2)$ to ensure that the order-g^6 linear artificial potential in (10.7) is always dominant for weak coupling. The introduction of an artificial linear potential in both the longitudinal and transverse directions then stabilizes the bound states for small running coupling constant g. It is not known yet whether this instability recurs for g near g_s and if so how to counter it.

C. Sources of complexity in the QCD computations

A basic goal of this paper is to structure a sequence of computations in LFQCD with growing levels of complexity. The major sources of the complexity will be reviewed here.

All computations envisioned here have two stages. The first stage is a computation of an effective Hamiltonian H_σ. We have defined σ to be a mass cutoff parameter, a mass above which states diminish in importance for further computations. The goal of the first stage is to compute H_σ with σ being just above the hadronic mass scale. In the simplest computation, H_σ consists of a truncated version of the canonical Hamiltonian (namely, $H_{I\sigma}^B$) combined with further corrections [from the commutator in (7.10)] computed only to order g^2, as in (10.1). From this, then, bound state energies are to be computed only to order g^4. This is a straightforward computation with the main concern to fix free parameters through a comparison with physical spectra after setting g^4 equal to g_s^4. The fit at this stage is extremely crude.

At this point the results are analogous to those for positronium with only a Coulomb interaction. There are additional terms in H_σ coming from one-gluon exchange that are order g^2, but because of their dependence on r they do not correct the energy until order g^6 or higher. They produce spin and orbital splittings, but before these splittings can be fully computed one must determine corrections to the kinetic energy of order g^2, corrections to the Coulomb interaction of order g^4, and one must allow corrections to the artificial linear potential of order g^8 in H_σ. Just as in QED, operators must be classified both on the basis of explicit powers of g multiplying them and on their implicit dependence on g arising from the fact that r scales like $1/g^2$ in the bound states. At each stage one must consistently retain all terms in H_σ that produce corrections of the same order in g after both explicit and implicit dependence on g is determined. This is standard bound state perturbation theory, with a linear potential added and forced to contribute at the same leading order as a Coulomb interaction, and with the underlying field theory producing additional interactions.

Actually there is an important subtlety here. One-gluon exchange falls exponentially fast at large r because of the gluon mass. To obtain an order g^6 spin splitting the gluon mass in the exchange interaction must be of order g^2 or 0, not of order 1. We allow the artificial potential to contain spin-dependent interactions at weak

coupling that vanish as $g \to g_s$, with a range governed by a mass that is order g^2. At no point do we allow the introduction of unphysically light constituents to obtain mass splittings, because there is no mechanism to prevent copious production of such light constituents in all hadrons as $g \to g_s$, and there is no evidence for the proliferation of light hadrons such constituents would necessitate even at weak coupling.

The calculation of all the terms in H_σ required to compute binding energies to order g^6 is complicated because of the large number of perturbative diagrams involved and the complexity of the cutoffs. However, there is a very interesting question that arises. The question is whether longitudinal boost invariance will be irretrievably violated by the fourth-order results. If the fourth-order results include logarithmic divergences due to the infrared cutoff, divergences which also have nontrivial dependences on transverse momentum, then there will be a boost invariance violation. The reason is that the logarithm will involve a ratio of an external longitudinal momentum divided by the cutoff momentum. While the cutoff dependence can legitimately be subtracted, the finite part of the logarithm cannot, and so results in a violation of longitudinal boost invariance. This violation would be similar to the violation of scale invariance of canonical equal-time QCD at zero mass. The scale invariance violation is never eliminated; it instead results in asymptotic freedom. A violation of boost invariance would likewise be irretrievable in weak coupling, and could only go away at a special value of g. Clearly, this special value would have to be g_s.

In addition, if the fourth-order computations turn up such logarithmic longitudinal divergences, then there would have to be finite subtractions accompanying the subtractions of the logarithmic cutoff-dependent divergences. These finite subtractions would involve arbitrary functions of transverse momentum—functions that could conceivably be the source of transverse linear potentials. Certainly, these finite subtractions would be direct reflections of vacuum effects, which means linear potentials would not be a surprise.

However, the most challenging problem to resolve is the computation of the effective Hamiltonian H_σ beyond fourth order. The major concern is the computation of higher-order corrections caused by removal of "wee parton" states. By "wee parton" states we mean states of high mass due to the presence of constituents in the infrared region and without large transverse momentum. The simplest example is a state with two equal-mass constituents but one having a far smaller longitudinal momentum (smaller x in Feynman's language) than the other. Their transverse momentum will be set to $p_\perp$ and $-p_\perp$, respectively. If one constituent has longitudinal momentum p^+, the other has momentum xp^+, with x small, then the states mass squared is about $\frac{m^2+p_\perp^2}{x}$, where m is the constituent mass. The problem is that when $p_\perp$ is small, masses count, which means there can be major corrections associated with actual values for bound state masses. This is a problem once the binding energies are themselves of order the constituent masses, namely, when g is near its relativistic value g_s.

This challenge will not be resolved easily. It is unlikely that it can even be seriously addressed until after the fourth-order computations are complete, and one can start estimating higher-order terms and determine the extent to which strong binding energies result in large higher-order terms in H_σ. This challenge is further enhanced by the problem of avoiding instabilities in H_σ itself for g near g_s.

XI. CONCLUSION

We have presented a framework for the computation of bound states in QCD that is based on Hamiltonian methods. The essential ingredients of our formulation are the use of light-front coordinates, nonzero quark and gluon masses, severe cutoffs on constituent momenta, and the similarity renormalization scheme. We have argued that this formulation of the theory removes all barriers to a treatment of hadrons in QCD which is analogous to that of bound states in QED. In particular, we have shown that in our formulation it is natural to choose a starting Hamiltonian which contains many characteristics of the constituent quark model, and therefore we expect that we may fashion this unperturbed Hamiltonian to model the basic physics well already at the outset. We take the view that the general principles of the CQM are true and propose to proceed from there. To achieve our perturbative starting point we must introduce artificial stabilizing and confining potentials to reproduce the necessary physics at small values of the coupling g, and we must extrapolate to the relativistic value of the renormalized coupling g_s. At g_s, the artificial potential must vanish, and the true dynamics will appear. The essential point to realize is that our formulation allows the possibility that this true dynamics may be discovered perturbatively.

Thus the price we pay for our new formulation—renormalization problems from severe light-front infrared divergences and the breaking of both gauge and Lorentz covariance—may eventually turn out to be relatively small in comparison to what we gain: Both confinement and chiral symmetry breaking may be studied with bound state perturbation theory. Moreover, the eventual restoration of Lorentz covariance, which requires the calculation of physical observables so as to complete the renormalization process, will be made easier by the expectation that bound states will be well approximated by nonrelativistic, few-body wave functions. The most daring aspect of this approach is the assignment of zero-mode contributions to counterterms for infrared divergences. There is no precedent for our analysis, and its worth can only be proven by obtaining satisfactory and relativistic results as $g \to g_s$.

The possibility of combining phenomenology and field theory at weak coupling opens a wide range of interesting computations. One feature essential for the feasibility of the entire enterprise is our contention that a massive gluon prevents the unlimited growth of the running coupling constant in the infrared domain. For this to happen all pure light-front infrared divergences (due to k^+ getting small) need to be canceled in the coupling constant

renormalization calculation. This needs to be demonstrated. Then there is the computation of bound states and hadronic observables. The use of an artificial potential and massive quarks and gluons makes this possible to leading order in a perturbative expansion, with more and more of the true physics being included as one moves to higher orders. As discussed in the context of lattice gauge theory by Lepage and Mackenzie [47], we must extrapolate to the relativistic value of the renormalized coupling in order to make the perturbative expansion legitimate. One can also readily conceive other instructive calculations which would not involve all the complications of low-energy QCD, such as the application of the framework developed here to the study of scalar field theory, QED, and especially heavy quark systems.

The possibility of constructing low-energy bound states in QCD through a combination of relativistic perturbation theory and many-body quantum mechanics defines a start-up phase with a wide range of new and tractable calculations. We have tried to emphasize those computations which are most immediately relevant and to define how these calculations can be carried out. The final demonstration of the feasibility of our approach awaits these computations.

ACKNOWLEDGMENTS

We acknowledge many helpful discussions over several years with D. Mustaki, S. Pinsky, and J. Shigemitsu. We would also like to acknowledge our useful interactions with S. Brodsky, M. Burkardt, D. H. Feng, R. Furnstahl, X. Ji, P. Lepage, and G.A. Miller. This research was supported in part by the National Science Foundation under Grants Nos. PHY-8858250, PHY-91029022, PHY-9203145, and PHY-9207889, by the Department of Energy under Grant No. DE-FG02-91ER40690, and by Komitet Badań Naukowych under Grant No. KBN 2 P302 031 05. Some of the figures in this paper were constructed using the package "FEYNMAN: A LaTeX Routine for Generating Feynman Diagrams," by Michael Levine, Cavendish-HEP 88/11.

APPENDIX A: σ MODEL WITH AND WITHOUT ZERO MODES

We will work only at the canonical or tree level here. The Lagrangian for the σ model is

$$\mathcal{L} = \frac{1}{2}(\partial_\mu \sigma)^2 + \frac{1}{2}(\partial_\mu \pi)^2 - V(\sigma^2 + \pi^2), \tag{A1}$$

where

$$V(\sigma^2 + \pi^2) = -\frac{1}{2}\mu^2(\sigma^2 + \pi^2) + \frac{\lambda}{4}(\sigma^2 + \pi^2)^2. \tag{A2}$$

This Lagrangian has a continuous symmetry corresponding to the transformation

$$\begin{aligned} \sigma \to \sigma' &= \sigma \cos\alpha + \pi \sin\alpha, \\ \pi \to \pi' &= -\sigma \sin\alpha + \pi \cos\alpha. \end{aligned} \tag{A3}$$

The extremum of the potential V is determined by

$$\begin{aligned} \frac{\delta V}{\delta \sigma} &= \sigma[-\mu^2 + \lambda(\sigma^2 + \pi^2)] = 0, \\ \frac{\delta V}{\delta \pi} &= \pi[-\mu^2 + \lambda(\sigma^2 + \pi^2)] = 0. \end{aligned} \tag{A4}$$

For $\mu^2 > 0$, the minimum of the potential is at $\sigma^2 + \pi^2 = \sigma_v^2 = \frac{\mu^2}{\lambda}$. There are an infinite number of degenerate vacuua. We can pick any one of them to be the true vacuum. For example, we can pick

$$\langle 0 \mid \sigma \mid 0 \rangle = \sigma_v \neq 0, \quad \langle 0 \mid \pi \mid 0 \rangle = 0. \tag{A5}$$

Then the symmetry is said to be spontaneously broken.

The conserved current associated with the symmetry of the Lagrangian is

$$J^\mu = \sigma \partial^\mu \pi - \pi \partial^\mu \sigma. \tag{A6}$$

The associated charge is

$$Q = \frac{1}{2}\int dx^- d^2x_\perp [\sigma \partial^+ \pi - \pi \partial^+ \sigma]. \tag{A7}$$

From the canonical commutation relations for σ and π fields, namely,

$$[\sigma(x), \sigma(y)] \mid_{x^+ = y^+} = -\frac{i}{4}\epsilon(x^- - y^-)\delta^2(x^\perp - y^\perp), \tag{A8}$$

$$[\pi(x), \pi(y)] \mid_{x^+ = y^+} = -\frac{i}{4}\epsilon(x^- - y^-)\delta^2(x^\perp - y^\perp), \tag{A9}$$

we have

$$\begin{aligned} [Q, \pi(0)] &= -i\sigma(0), \\ [Q, \sigma(0)] &= i\pi(0). \end{aligned} \tag{A10}$$

Thus we have

$$\langle 0 \mid [Q, \pi(0)] \mid 0 \rangle = -i\sigma_v \neq 0. \tag{A11}$$

Starting from $\partial^\mu J_\mu = 0$, we have

$$\frac{dQ}{dx^+} = 0. \tag{A12}$$

From (A11) it is also easy to verify Goldstone's theorem and assert the existence of a massless pion.

In the theory we have considered, zero modes are present, and as a result there is spontaneous symmetry breaking, the vacuum is nontrivial, $\langle 0 \mid \sigma(0) \mid 0 \rangle \neq 0$, and a massless pion is predicted.

Next we discuss the σ model with the zero modes removed. To construct the effective Hamiltonian we cannot use the symmetry (A3) as a guide but can rely on power counting and locality. The Hamiltonian is

$$P^- = \int dx^- d^2x_\perp [\tfrac{1}{2}(\partial_\perp \phi \cdot \partial_\perp \phi + \partial_\perp \pi \cdot \partial_\perp \pi) + V]. \tag{A13}$$

Since the symmetry is broken only in the σ sector, we insist that V is even in the π field so that the symmetry under $\pi \to -\pi$ remains. Thus, since no inverse powers of

mass are allowed, we can write

$$V = \frac{1}{2}m_\phi^2\phi^2 + \frac{1}{2}m_\pi^2\pi^2 + \lambda_1\phi^4 + \lambda_2\pi^4 + \lambda_3\phi^2\pi^2 + \lambda_4\phi^3 + \lambda_5\pi^2\phi. \tag{A14}$$

Since there are no zero modes, a term of the form $\lambda_6\phi$ vanishes upon integration in (A13) and so is not included.

The equations of motion are

$$\begin{aligned} -\partial^+\partial^-\pi + \partial_\perp^2\pi &= m_\pi^2\pi + 4\lambda_2\pi^3 + 2\lambda_3\phi^2\pi + 2\lambda_5\pi\phi, \\ -\partial^+\partial^-\phi + \partial_\perp^2\phi &= m_\phi^2\phi + 4\lambda_1\phi^3 + 2\lambda_3\pi^2\phi + 3\lambda_4\phi^2 + \lambda_5\pi^2. \end{aligned} \tag{A15}$$

Next we construct the covariant current operator J^μ. First we determine the canonical dimensions of the components J^+, J^- and $J^\perp$. Since the charge Q $(= \frac{1}{2}\int dx^- d^2x_\perp J^+)$ is dimensionless, the canonical dimension of J^+ is $J^+ \sim \frac{1}{x^-}\frac{1}{(x_\perp)^2}$. Since each term in $\partial^\mu J_\mu$ $[= \frac{1}{2}(\partial^- J^+ + \partial^+ J^-) - \partial^\perp \cdot J^\perp]$ should have the same dimensions, the canonical dimensions of the other components are

$$J^\perp \sim \frac{1}{(x_\perp)^3}, \quad J^- \sim \frac{x^-}{(x_\perp)^4}. \tag{A16}$$

The components of J^μ are to be constructed from the operators π, ϕ, ∂^+, ∂^-, and $\partial^\perp$ and constants. The constants are allowed to have dimensions of negative power of $x_\perp$ (as masses do) but no power of x^-. Since the operator $\frac{1}{\partial^+}$ does not appear in the canonical scalar field theory, we do not allow the operator $\frac{1}{\partial^+}$ to appear in the canonical current operator. We also implement the symmetry that J^μ has to change sign under $\pi \to -\pi$. Then the allowed structure of components of J^μ is

$$\begin{aligned} J^+ &= a_1\partial^+\pi + a_2(\partial^+\pi)\phi + a_3(\partial^+\phi)\pi, \\ J_\perp &= b_1\partial_\perp\pi + b_2(\partial_\perp\phi)\pi + b_3(\partial_\perp\pi)\phi, \\ J^- &= c_1\partial^-\pi + c_2(\partial^-\pi)\phi + c_3(\partial^-\phi)\pi. \end{aligned} \tag{A17}$$

Next we compute $\partial^\mu J_\mu$ and set the coefficients of terms involving derivatives which cannot be replaced by the equation of motion to be zero. Then we get

$$a_2 = -c_3, \quad a_3 = -c_2, \quad b_2 = -b_3. \tag{A18}$$

Further, from the structure of the equations of motion, we also have

$$b_1 = \frac{a_1 + c_1}{2}, \quad b_2 = -\frac{a_2 + c_2}{2}. \tag{A19}$$

Since the zero modes are dropped, we have the charge

$$Q = \frac{1}{2}\int dx^- d^2x_\perp [a_2\phi\partial^+\pi + a_3\pi\partial^+\phi]. \tag{A20}$$

Insisting that Q generates the correct transformation laws (A10), we arrive at

$$a_3 = -a_2. \tag{A21}$$

Without loss of generality we set $a_2 = 1$, and so

$$J^+ = a_1\partial^+\pi + \phi\partial^+\pi - \pi\partial^+\phi, \tag{A22}$$

$$J^- = c_1\partial^-\pi + \phi\partial^-\pi - \pi\partial^-\phi, \tag{A23}$$

$$J_\perp = \frac{1}{2}(a_1 + c_1)\partial_\perp\pi + \phi\partial_\perp\pi - \pi\partial_\perp\phi. \tag{A24}$$

Further, if J^+ and J^- are to transform as components of a covariant four-vector, we also have to set $c_1 = a_1$. Then

$$J^\mu = \phi\partial^\mu\pi - \pi\partial^\mu\phi + a_1\partial^\mu\pi. \tag{A25}$$

Since our effective Hamiltonian (even with explicit symmetry breaking) is supposed to give rise to the same physics as that of spontaneous symmetry breaking, we demand that the current is conserved. Using the equations of motion (A15),

$$\partial^\mu J_\mu = -(\phi + a_1)(m_\pi^2\pi + 4\lambda_2\pi^3 + 2\lambda_3\phi^2\pi + 2\lambda_5\pi\phi) + \pi(m_\phi^2\phi + 4\lambda_1\phi^3 + 2\lambda_3\pi^2\phi + 3\lambda_4\phi^2 + \lambda_5\pi^2) = 0. \tag{A26}$$

Setting the coefficients of the different combinations of field operators separately to zero, we have

$$m_\pi^2 a_1 = 0, \; m_\pi^2 - m_\phi^2 + 2\lambda_5 a_1 = 0, \; 4\lambda_2 - 2\lambda_3 = 0, \; 4\lambda_1 - 2\lambda_3 = 0,$$

$$2\lambda_5 - 3\lambda_4 + 2a_1\lambda_3 = 0, \; -\lambda_5 + 4\lambda_2 a_1 = 0. \tag{A27}$$

The solutions are

$$\lambda_1 = \lambda_2 = \frac{1}{2}\lambda_3 \equiv \frac{\lambda}{4}, \quad \lambda_5 = \lambda a_1, \quad \lambda_4 = \lambda a_1, \quad m_\phi^2 = m_\pi^2 + 2\lambda a_1^2, \tag{A28}$$

and

$$a_1 = 0 \quad \text{or} \quad m_\pi = 0. \tag{A29}$$

If we take $a_1 = 0$, then the potential is reduced to the canonical form (A2), and the current is also of the canonical form. This corresponds to the full canonical theory with a symmetry-preserving vacuum and a doublet in the spectrum. If we choose $m_\pi = 0$, we have

$$V = \frac{1}{2}m_\phi^2\phi^2 + \frac{\lambda}{4}(\phi^2+\pi^2)^2 + \sqrt{\frac{\lambda m_\phi^2}{2}}(\phi^2+\pi^2)\phi,$$

$$J^\mu = \phi\partial^\mu\pi - \pi\partial^\mu\phi + \sqrt{\frac{m_\phi^2}{2\lambda}}\,\partial^\mu\pi. \tag{A30}$$

Now the potential explicitly breaks the symmetry, and the current is different from the canonical one. The charge Q does not commute with the Hamiltonian, and

$$\frac{dQ}{dx^+} \neq 0. \tag{A31}$$

This corresponds to full canonical theory after a shift of σ to remove its vacuum expectation value. Thus we see that the power-counting rules allow us to reconstruct the theory without reference to the zero modes.

Thus in the theory with zero modes dropped and the zero pion mass, the Hamiltonian explicitly breaks the symmetry, the vacuum is trivial, and there is no longer the notion of spontaneous symmetry breaking. Current conservation is preserved and vastly reduces the number of free parameters present in the effective Hamiltonian constructed from power counting and forces the pion to remain massless.

Of course, we should emphasize that the σ model we have discussed is only at the tree level. For a complete understanding, we need to consider radiative corrections and the subsequent renormalization effects.

APPENDIX B: MORE ABOUT CHIRAL SYMMETRY ON THE LIGHT FRONT

In this appendix, we show that the normal chiral transformation on the quark field is inconsistent with the light-front constraint equation, where the latter is a result of the light-front equations of motion. We also show that chirality is the same as helicity on the light front. For further discussion, see Ref. [34].

Recall that in light-front coordinates, the quark field can be separated into the plus and minus components: $\psi = \psi_+ + \psi_-$, where $\psi_\pm = \frac{1}{2}\gamma^0\gamma^\pm\psi$, and only ψ_+ is a dynamical variable. The minus component ψ_- is determined by the light-front constraint

$$\psi_- = \frac{1}{i\partial^+}\left[\alpha_\perp\cdot(i\partial_\perp + gA_\perp) + \gamma^0 m_F\right]\psi_+. \tag{B1}$$

The normal chiral transformation is defined by

$$\psi \longrightarrow \psi + \delta\psi \quad \text{with} \quad \delta\psi = -i\theta\gamma_5\psi. \tag{B2}$$

However, in light-front coordinates, only ψ_+ is a dynamical variable, so that the chiral transformation acts only on ψ_+

$$\psi_+ \longrightarrow \psi_+ + \delta\psi_+ \ , \quad \delta\psi_+ = -i\theta\gamma_5\psi_+, \tag{B3}$$

and the transformation on ψ_- is given by the equation of constraint,

$$\begin{aligned}\delta\psi_- &= \frac{1}{i\partial^+}\left[\alpha_\perp\cdot(i\partial_\perp + gA_\perp) + \gamma^0 m_F\right]\delta\psi_+ \\ &= -i\theta\gamma_5\frac{1}{i\partial^+}\alpha_\perp\cdot\left(i\partial_\perp + gA_\perp\right)\psi_+ - i\theta m_F\gamma^0\gamma_5\frac{1}{i\partial^+}\psi_+.\end{aligned} \tag{B4}$$

Thus, the chiral transformation on ψ on the light front is

$$\begin{aligned}\delta\psi &= \delta\psi_+ + \delta\tilde{\psi}_- \\ &= -i\theta\gamma_5\psi_+ - i\theta\gamma_5\frac{1}{i\partial^+}\alpha_\perp\cdot\left(i\partial_\perp + gA_\perp\right)\psi_+ - i\theta m_F\gamma^0\gamma_5\frac{1}{i\partial^+}\psi_+.\end{aligned} \tag{B5}$$

If we naively use the form $\delta\psi = -i\theta\gamma_5\psi = -i\theta\gamma_5(\psi_+ + \psi_-)$,

$$\delta\psi = -i\theta\gamma_5\psi_+ - i\theta\gamma_5\frac{1}{i\partial^+}\alpha_\perp\cdot\left(i\partial_\perp + gA_\perp\right)\psi_+ - i\theta m_F\gamma_5\gamma^0\frac{1}{i\partial^+}\psi_+. \tag{B6}$$

This is obviously inconsistent with (B5), which is a consequence of the light-front equation of constraint.

For the massive quark theory,

$$\partial_\mu j_5^\mu = 2im_F\bar{\psi}\gamma_5\psi, \tag{B7}$$

where $j_5^\mu = \bar{\psi}\gamma^\mu\gamma_5\psi$ is the axial vector current. The axial vector charge on the light-front is then

$$Q_{\rm LF}^5 = \int dx^- d^2x_\perp j_5^+(x). \tag{B8}$$

Explicit calculation using the field expansions and normal ordering leads to

$$Q_{\rm LF}^5 = \int \frac{dk^+ d^2k_\perp}{2(2\pi)^3}\sum_\lambda \lambda\left[b_\lambda^\dagger(k)b_\lambda(k) + d_\lambda^\dagger(k)d_\lambda(k)\right]. \tag{B9}$$

Thus $Q_{\rm LF}^5$ measures the helicity.

In the canonical theory the chiral current is conserved for zero fermion mass. In the theory with the renormalized effective Hamiltonian we expect to observe the consequences of spontaneous symmetry breaking, signals of which are a conserved axial vector current and a zero mass pion. However, we do not expect to generate a massless pion unless the coupling g exactly matches its renormalized value g_s. Hence the issues of a massless pion

and a conserved axial vector current (which we expect to be noncanonical in form) can be addressed meaningfully only after we reach the relativistic limit of the theory.

APPENDIX C: NONRELATIVISTIC LIMIT OF MASSLESS GLUON EXCHANGE

In this appendix we discuss the nonrelativistic limit of one-gluon exchange; however, we insist on maintaining the separate dimensional assignments for longitudinal and transverse coordinates when taking this limit, and we arrive at results that differ substantially from other analyses which allow longitudinal and transverse dimensions to mix. Our entire program is based on separate power-counting analyses for these dimensions, and if they mix our power counting fails.

In second-order perturbation theory, the effective interaction Hamiltonian in the $q\bar{q}$ sector due to *massless* gluon exchange is

$$H^{(2)}_{I\sigma ij} = H^{(2)}_{I\sigma ij1} + H^{(2)}_{I\sigma ij2}, \tag{C1}$$

where

$$H^{(2)}_{I\sigma ij1} = -4g^2 T^a_{\alpha_3\alpha_1} T^a_{\alpha_4\alpha_2} \delta_{s_1 s_3} \delta_{s_2 s_4} \frac{1}{2} \frac{1}{(p_1^+ - p_3^+)^2} - g^2 T^a_{\alpha_3\alpha_1} T^a_{\alpha_4\alpha_2} \mathcal{M}_{2ij} \frac{1}{p_1^+ - p_3^+} \frac{1}{2} \left[\frac{1}{\frac{m_F^2 + p_{1\perp}^2}{p_1^+} - \frac{m_F^2 + p_{3\perp}^2}{p_3^+} - \frac{(p_{1\perp} - p_{3\perp})^2}{p_1^+ - p_3^+}} \right], \tag{C2}$$

$$H^{(2)}_{I\sigma ij2} = -4g^2 T^a_{\alpha_3\alpha_1} T^a_{\alpha_4\alpha_2} \delta_{s_1 s_3} \delta_{s_2 s_4} \frac{1}{2} \frac{1}{(p_1^+ - p_3^+)^2} - g^2 T^a_{\alpha_3\alpha_1} T^a_{\alpha_4\alpha_2} \mathcal{M}_{2ij} \frac{1}{p_1^+ - p_3^+} \frac{1}{2} \left[\frac{1}{\frac{m_F^2 + p_{4\perp}^2}{p_4^+} - \frac{m_F^2 + p_{2\perp}^2}{p_2^+} - \frac{(p_{1\perp} - p_{3\perp})^2}{p_1^+ - p_3^+}} \right], \tag{C3}$$

and

$$\mathcal{M}_{2ij} = \chi^\dagger_{s_3} \left[2\frac{p_1^{i_1} - p_3^{i_1}}{p_1^+ - p_3^+} - im_F \left(\frac{1}{p_1^+} - \frac{1}{p_3^+} \right) \sigma^{i_1} - \left(\sigma^{i_1} \frac{\sigma_\perp \cdot p_{1\perp}}{p_1^+} + \frac{\sigma_\perp \cdot p_{3\perp}}{p_3^+} \sigma^{i_1} \right) \right] \chi_{s_1} \times \chi^\dagger_{-s_2} \left[2\frac{p_1^{i_1} - p_3^{i_1}}{p_1^+ - p_3^+} - im_F \left(\frac{1}{p_4^+} - \frac{1}{p_2^+} \right) \sigma^{i_1} - \left(\sigma^{i_1} \frac{\sigma_\perp \cdot p_{4\perp}}{p_4^+} + \frac{\sigma_\perp \cdot p_{2\perp}}{p_2^+} \sigma^{i_1} \right) \right] \chi_{-s_4}. \tag{C4}$$

Let us denote the total momenta by $(P^+, P_\perp)$. For simplicity, we consider the case $P_\perp = 0$, that is, $p_{2\perp} = -p_{1\perp}$, $p_{4\perp} = -p_{3\perp}$. To get the form of the effective Hamiltonian in the nonrelativistic limit, as an example, we consider the matrix element for $s_1 = s_2 = s_3 = s_4 = \uparrow$. Then

$$\mathcal{M}_{2ij} = 4\frac{(p_{1\perp} - p_{3\perp})^2}{(p_1^+ - p_3^+)^2} - 2\frac{p_{1\perp}^2 (p_2^+ - p_1^+)}{p_1^+ p_2^+ (p_1^+ - p_3^+)} - 2\frac{p_{3\perp}^2 (p_3^+ - p_4^+)}{p_3^+ p_4^+ (p_1^+ - p_3^+)} - 2\frac{(P^+)^2}{p_1^+ p_2^+ p_3^+ p_4^+} p_1^L p_3^R, \tag{C5}$$

where $k^L = k^1 - ik^2$ and $k^R = k^1 + ik^2$. This gives, after simplification,

$$H^{(2)}_{I\sigma ij} = -g^2 T^a_{\alpha_3\alpha_1} T^a_{\alpha_4\alpha_2} \left[\frac{1}{2} \left(\frac{4m_F^2}{p_1^+ p_3^+} + 2\frac{(P^+)^2}{p_1^+ p_2^+ p_3^+ p_4^+} p_1^L p_3^R \right) \frac{1}{E_1} + \frac{1}{2} \left(\frac{4m_F^2}{p_2^+ p_4^+} + 2\frac{(P^+)^2}{p_1^+ p_2^+ p_3^+ p_4^+} p_1^L p_3^R \right) \frac{1}{E_2} - \frac{1}{E_1 E_2} (P^+)^2 \left(\frac{p_{1\perp}^2}{p_1^+ p_2^+} - \frac{p_{3\perp}^2}{p_3^+ p_4^+} \right)^2 \right], \tag{C6}$$

where

$$E_1 = (p_{1\perp} - p_{3\perp})^2 + \frac{m_F^2}{p_1^+ p_3^+} (p_1^+ - p_3^+)^2 - (p_1^+ - p_3^+) \left(\frac{p_{1\perp}^2}{p_1^+} - \frac{p_{3\perp}^2}{p_3^+} \right) \tag{C7}$$

and

$$E_2 = (p_{1\perp} - p_{3\perp})^2 + \frac{m_F^2}{p_2^+ p_4^+} (p_1^+ - p_3^+)^2 - (p_1^+ - p_3^+) \left(\frac{p_{3\perp}^2}{p_4^+} - \frac{p_{1\perp}^2}{p_2^+} \right). \tag{C8}$$

In the nonrelativistic limit, the term involving $p_1^L p_3^R$ is negligible compared to the mass term; in both E_1 and E_2 the third term is negligible compared to the first two terms; furthermore, $\frac{m_F^2}{p_1^+ p_3^+} \to (\frac{m_F}{p_1^+})^2$ and $\frac{m_F^2}{p_2^+ p_4^+} \to (\frac{m_F}{p_2^+})^2$. Thus

in the nonrelativistic limit, the effective interaction in the $q\bar{q}$ sector due to *massless* one-gluon exchange reduces to

$$\mathcal{H}^{\rm nr}_{2ij} = -4g^2 T^a T^a \frac{1}{2}\left[\left(\frac{m_F}{p_1^+}\right)^2 \frac{1}{(p_{1\perp}-p_{3\perp})^2 + (\frac{m_F}{p_1^+})^2 (p_1^+ - p_3^+)^2} + \left(\frac{m_F}{p_2^+}\right)^2 \frac{1}{(p_{2\perp}-p_{4\perp})^2 + (\frac{m_F}{p_2^+})^2 (p_2^+ - p_4^+)^2}\right]. \quad \text{(C9)}$$

The Coulomb interaction has the form $\frac{1}{p^2}$ in momentum space. If we further make the approximation for (C9) that $p_1^+ \approx m_F + p_1^z$ and $p_3^+ \approx m_F + p_3^z$, we arrive at the familiar Coulomb interaction in momentum space

$$\mathcal{H}_{cij} = -4g^2 T^a T^a \frac{1}{(\mathbf{p}_1 - \mathbf{p}_3)^2} \quad \text{(C10)}$$

with $(\mathbf{p}_1 - \mathbf{p}_3)^2 = (p_{1\perp} - p_{3\perp})^2 + (p_1^z - p_3^z)^2$. The Coulomb potential in position space is then obtained by the Fourier transformation

$$\frac{1}{(\mathbf{p}_1 - \mathbf{p}_3)^2} = \frac{1}{4\pi}\int d^3 r e^{i(\mathbf{p}_1 - \mathbf{p}_3)\cdot \mathbf{r}} \frac{1}{r}, \quad \text{(C11)}$$

with $r = |\mathbf{x} - \mathbf{x}'|$ the separation between the two fermions. Obviously, $H_c = -\int d^3x d^3x' j_q^a(\mathbf{x}) \frac{g^2}{4\pi r} j^a(\mathbf{x}')$ has lost boost invariance but has recovered rotational invariance.

We wish to represent the interaction $\mathcal{H}_2^{\rm nr}$ in a form where longitudinal boost invariance is kept. To do so, we use an interpolating Fourier transformation

$$\begin{aligned}
&\left(\frac{m_F}{p_1^+}\right)^2 \frac{1}{(p_{1\perp}-p_{3\perp})^2 + (\frac{m_F}{p_1^+})^2 (p_1^+ - p_3^+)^2} \\
&\quad \sim \frac{1}{4\pi}\int d\left(\frac{p_1^+}{m_F} y^-\right) d^2 y_\perp e^{i\left\{\left(\frac{m_F}{p_1^+}(p_1^+ - p_3^+)\right)\left(\frac{p_1^+}{m_F} y^-\right) - (p_{1\perp}-p_{3\perp})\cdot y_\perp\right\}} \left(\frac{m_F}{p_1^+}\right)^2 \frac{1}{\sqrt{y_\perp^2 + (\frac{p_1^+}{m_F} y^-)^2}} \\
&\quad = \frac{1}{4\pi}\int dy^- d^2 y_\perp \; e^{i\left\{(p_1^+ - p_3^+) y^- - (p_{1\perp}-p_{3\perp})\cdot y_\perp\right\}} \frac{m_F}{p_1^+} \frac{1}{\sqrt{y_\perp^2 + (\frac{p_1^+}{m_F})^2 (y^-)^2}},
\end{aligned} \quad \text{(C12)}$$

where $y_\perp = x_{1\perp} - x_{2\perp} \equiv \delta x_\perp$ is the transverse separation of the two constituents, but the longitudinal separation $y^- \equiv \delta x$ is more complicated since the above expression is not a complete Fourier transformation to light-front coordinate space. But for qualitative purposes we may define a light-front "radial" coordinate $r_1 = \sqrt{(\delta x_\perp)^2 + (\frac{p_1^+}{m_F})^2 (\delta x^-)^2}$, and we see from (C12) that $H_2^{\rm nr}$ has the form of the light-front Coulomb potential (2.6) which we have introduced in the artificial potential in Sec. II E. This light-front radial coordinate is invariant under longitudinal boosts. However, it is not invariant under transverse boosts. For more physical remarks, see Sec. II E.

Relativistically, the spinor matrix elements are different in different helicity sectors. In the nonrelativistic limit this helicity dependence vanishes, and we get the same interaction in all helicity sectors.

APPENDIX D: PHASE SPACE CELL DIVISION: EQUAL-TIME CASE

Let us try to motivate why a phase space cell analysis is useful for the study of Hamiltonians. Recall free field theory in equal-time coordinates. A free field is diagonalized in terms of momentum eigenstates. Thus it is customary to express free fields in terms of creation and annihilation operators for particles in plane wave states. The free Hamiltonian is

$$H_0 = \int d^3k \; \omega_k \; a_k^\dagger a_k, \quad \text{(D1)}$$

with $\omega_k = \sqrt{\mu^2 + k^2}$.

Next consider interactions. For illustrative purposes, we will choose a ϕ^3-type interaction,

$$H_{\rm int} = \int d^3x \int d^3k_1 \int d^3k_2 \int d^3k_3 a^\dagger(k_1) a(k_2) a(k_3) \, e^{-i(k_2 + k_3 - k_1)\cdot x}. \quad \text{(D2)}$$

Before trying to solve the Hamiltonian quantitatively, it is important to make qualitative estimates of various terms in the Hamiltonian. For this purpose, the creation and annihilation operators a_k and $a_k^\dagger$ are quite inappropriate. For example, the operator $a_k^\dagger$ creates a particle in a plane wave state and hence creates a state of infinite norm. Thus when we try to estimate the "order of magnitude" of $a_k^\dagger$ we get infinity. What can be done to avoid

this catastrophe?

It has been suggested [38] (also see [39]) some time ago that the creation and annihilation operators which depend on a continuous variable k be expanded in terms of a discrete, complete, orthonormal set of functions $u_i(k)$. Specifically,

$$a_k = \sum_i u_i(k) a_i \ , \tag{D3}$$

$$a_k^\dagger = \sum_i u_i^*(k) a_i^\dagger \ . \tag{D4}$$

The coefficients of this expansion are themselves creation and annihilation operators for particles in normalizable "wave packet" states. Now

$$H_0 = \sum_{i_1 i_2} C_{i_1 i_2} \, a_{i_1}^\dagger a_{i_2}, \tag{D5}$$

where

$$C_{i_1 i_2} = \int d^3k \, \omega_k \, u_{i_1}^*(k) u_{i_2}(k) \ . \tag{D6}$$

H_0 is now the Hamiltonian of an infinite number of oscillators coupled to each other (no longer diagonal). Now making H_0 diagonal means making self-interactions of the individual oscillators more important than interactions between different oscillators. Consider the matrix C. If the u_l's are orthogonal, C would be diagonal except for the factor ω_k. Even with the factor ω_k, one should be able to keep the off-diagonal elements small. If the u_i's are "properly chosen" (that is, as localized in momentum space as possible), then for distinct momentum shells i_1 and i_2, the functions u_{i_1} and u_{i_2} do not overlap very much. If u_{i_1} and u_{i_2} are in the same momentum shell but different spatial cells, this fact will be reflected in a rapid phase variation of $u_{i_1}^* u_{i_2}$ as a function of k, which again makes the integral small. Thus with a properly chosen set of u_i's, for order of magnitude estimates we need to consider only diagonal elements $C_{i_1 i_1}$ of C.

The interaction Hamiltonian in terms of wave packet states is

$$H_{\text{int}} = \sum_{i_1 i_2 i_3} a_{i_1}^\dagger a_{i_2} a_{i_3} D_{i_1 i_2 i_3}, \tag{D7}$$

with

$$\begin{aligned} D_{i_1 i_2 i_3} &= \int d^3x \int d^3k_1 \int d^3k_2 \int d^3k_3 u_{i_1}^*(k_1) u_{i_2}(k_2) u_{i_3}(k_3) \, e^{-i(k_2+k_3-k_1)\cdot x} \\ &= \int d^3x v_{i_1}^*(x) v_{i_2}(x) v_{i_3}(x). \end{aligned} \tag{D8}$$

If the u's are as localized as possible in momentum space, then the v's are as spread out as possible in coordinate space and hence the off-diagonal elements of D are as big as the diagonal elements of D. Thus if we want to approximate D by its diagonal elements for order of magnitude estimates, we need v's to be as localized in coordinate space as possible. Thus we clearly have to satisfy almost mutually exclusive requirements, which means that we have to settle for a compromise.

A qualitative implementation of the compromise is as follows. We choose $u_i(k)$ such that if Δk_i is the momentum width of the function $u_i(k)$ and Δx_i is the width of the Fourier transform $v_i(x)$ of $u_i(k)$, then the product $\Delta k_i \Delta x_i$ is near the lower limit set by the uncertainty principle, that is,

$$\Delta k_i \Delta x_i \approx \frac{1}{2} \ . \tag{D9}$$

The set of functions $\{u_i\}$ is chosen to be complete and orthonormal. What does this mean? Think of u_i as occupying a cell of unit volume in phase space. Completeness means that the total volume occupied by the u_i's must fill all space. Orthogonality means that the regions occupied by different u_i's do not overlap.

How are we going to divide the phase space into cells? Consider a one-dimensional example for visualization. Divide the momentum space into an infinite number of cells, the ith cell being

$$2^{-i} < k < 2^{-i+1} \ . \tag{D10}$$

For each momentum cell separately, divide the position space linearly into cells of the appropriate size. The position space coordinate is chosen to be $l \le 2^{-i} x \le l + 1$.

Let us give some examples. Consider $i = 0$. Then $1 < k < 2$, and the length of the momentum cell is $L_k = 1$. The position cell division is $l \le x \le l + 1$. Thus the position space coordinates are, for example,

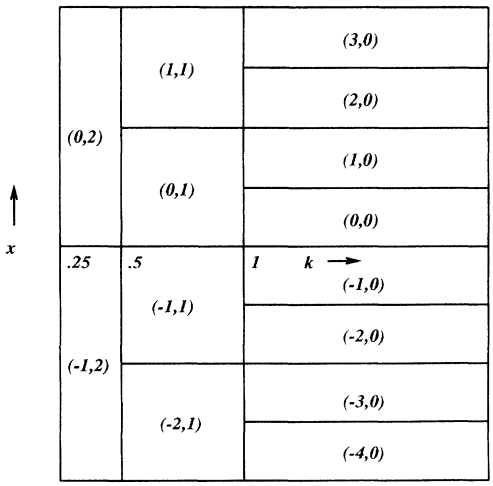

FIG. 13. Example of phase space cell division in one dimension.

$$\begin{aligned} l=-1 \quad & -1<x<0, \\ l=0 \quad & 0<x<1, \\ l=+1 \quad & 1<x<2, \end{aligned} \tag{D11}$$

and so on, so that each position space cell has length $L_x = 1$. Thus the " volume" of each phase space cell is $L_k L_x = 1$.

Consider $i = 1$. Then $\frac{1}{2} < k < 1$, and the length of the momentum cell is $L_k = \frac{1}{2}$. The position cell division is $l \leq \frac{1}{2}x \leq l+1$. Thus the position space coordinates are, for example,

$$\begin{aligned} l=-1 \quad & -2<x<0, \\ l=0 \quad & 0<x<2, \\ l=+1 \quad & 2<x<4, \end{aligned} \tag{D12}$$

and so on, so that each position space cell has length $L_x = 2$. Thus the "volume" of each phase space cell is again $L_k L_x = 1$.

One can label each phase space cell by (l, i). An illustration of the division of phase space into cells is given in Fig. 13.

Why have we chosen a logarithmic scale for momentum cells? One would like to have each momentum cell correspond to a distinct energy scale so that order of magnitude estimates become meaningful. A linear choice obviously fails for this purpose, while a logarithmic choice is the most obvious one that fulfills it. Note that there is nothing sacred about the factor of 2; for a specific example where the factor of 2 appears as the optimum choice, see Ref. [39].

[1] K. G. Wilson, "Initial Draft," report, 1989 (unpublished).

[2] K. G. Wilson, "Light-front QCD," OSU internal report, 1990 (unpublished).

[3] K. G. Wilson, "QCD: a weak coupling treatment on light fronts," report, 1993 (unpublished).

[4] K. G. Wilson, "Renormalization of QCD weak coupling model," report, 1993 (unpublished).

[5] R. J. Perry and K. G. Wilson, "Toward a Solution of QCD on the Light Front," report, 1991 (unpublished).

[6] T. S. Walhout, in *PANIC '93* (World Scientific, Singapore, in press).

[7] E. Tomboulis, Phys. Rev. D **8**, 2736 (1973); A. Casher, *ibid.* **14**, 452 (1976); W. A. Bardeen and R. B. Pearson, *ibid.* **13**, 547 (1976); C. B. Thorn, *ibid.* **19**, 639 (1979); **20**, 1934 (1979); W. A. Bardeen, R. B. Pearson, and E. Rabinovici, *ibid.* **21**, 1037 (1980); G. P. Lepage and S. J. Brodsky, *ibid.* **22**, 2157 (1980); V. A. Franke, Y. V. Novozhilov, and E. V. Prokhvatilov, Lett. Math. Phys. **5**, 239 (1981); **5**, 437 (1981); G. P. Lepage, S. J. Brodsky, T. Huang, and P. B. Mackenzie, in *Particles and Fields 2*, edited by A. Z. Capri and A. N. Kamal (Plenum, New York, 1983); St. D. Głazek, Phys. Rev. D **38**, 3277 (1988); S. J. Brodsky and G. P. Lepage, in *Perturbative Quantum Chromodynamics*, edited by A. H. Mueller (World Scientific, Singapore, 1989); E. V. Prokhvatilov and V. A. Franke, Yad. Fiz. **49**, 1109 (1989) [Sov. J. Nucl. Phys. **49**, 688 (1989)]; P. A. Griffin, Nucl. Phys. **B372**, 270 (1992).

[8] W. M. Zhang and A. Harindranath, Phys. Rev. D **48**, 4868 (1993).

[9] W. M. Zhang and A. Harindranath, Phys. Rev. D **48**, 4881 (1993).

[10] A. Harindranath and W. M. Zhang, Phys. Rev. D **48**, 4903 (1993).

[11] Casher [7] and Lepage and Brodsky [7].

[12] R. J. Perry, Phys. Lett. B **300**, 8 (1993).

[13] W. M. Zhang and A. Harindranath, Phys. Lett. B **314**, 223 (1993).

[14] St. D. Głazek and K. G. Wilson, Phys. Rev. D **48**, 5863 (1993).

[15] St. D. Głazek and K. G. Wilson, Phys. Rev. D **49**, 4214 (1994).

[16] R. J. Perry, A. Harindranath, and K. G. Wilson, Phys. Rev. Lett. **65**, 2959 (1990); A. Harindranath and R. J. Perry, Phys. Rev. D **43**, 492 (1991); R. J. Perry and A. Harindranath, *ibid.* **43**, 4051 (1991); St. D. Głazek and R. J. Perry, *ibid.* **45**, 3740 (1992); A. Harindranath, R. J. Perry, and J. Shigemitsu, *ibid.* **46**, 4580 (1992); S. Głazek, A. Harindranath, S. Pinsky, J. Shigemitsu, and K. G. Wilson, *ibid.* **47**, 1599 (1993); Y. Mo and R. J. Perry, J. Comput. Phys. **108**, 159 (1993); A. Harindranath, J. Shigemitsu, and W. M. Zhang, "Study of Utilizing Basis Functions to Solve Simple Light-Front Equations in 3+1 Dimensions," OSU report, 1992 (unpublished); M. Brisudová and St. D. Głazek, Phys. Rev. D (to be published).

[17] D. Mustaki, S. Pinsky, J. Shigemitsu, and K. Wilson, Phys. Rev. D **43**, 3411 (1991).

[18] St. D. Głazek and R. J. Perry, Phys. Rev. D **45**, 3734 (1992); B. van de Sande and S. S. Pinsky, *ibid.* **46**, 5479 (1992); St. D. Głazek and K. G. Wilson, *ibid.* **47**, 4657 (1993); St. D. Głazek, Acta Phys. Pol. B **24**, 1315 (1993); R. J. Perry and K. G. Wilson, Nucl. Phys. **B403**, 587 (1993); R. J. Perry, Ann. Phys. (N.Y.) (to be published).

[19] Perry [18].

[20] P. A. M. Dirac, Rev. Mod. Phys. **21**, 392 (1949).

[21] S. Weinberg, Phys. Rev. **150**, 1313 (1966).

[22] S. Fubini and G. Furlan, Physics **1**, 229 (1965); R. Dashen and M. Gell-Mann, Phys. Rev. Lett. **17**, 340 (1966). An initial light-front formulation of QCD inspired from the properties of light-front current algebra is H. Fritzsch and M. Gell-Mann, in *Proceedings of the XVI International Conference on High Energy Physics*, edited by J. D. Jackson and A. Roberts (Fermilab, Chicago, 1972), Vol. 2, p. 135. For more discussion on light-front current algebra, also see R. Jackiw, *Lectures on Current Algebra and its Applications*, Springer Tracts in Modern Physics Vol. 62 (Springer, New York, 1972); V. De Alfaro, S. Fubini, G. Furlan, and G. Rossetti, *Currents in Hadron Physics* (North-Holland, Amsterdam, 1973); E. Eichten, F. Feinberg, and J. F. Willemsen, Phys. Rev. D **8**, 1204 (1973); H. J. Melosh, *ibid.* **9**, 1095 (1974).

[23] R. P. Feynman, Phys. Rev. Lett. **23**, 1415 (1969); J. D. Bjorken and E. A. Paschos, Phys. Rev. **185**, 1975 (1969); R. P. Feynman, *Photon-Hadron Interactions* (Benjamin, Reading, MA, 1972); J. B. Kogut and L. Susskind, Phys. Rep. C **8**, 75 (1973). Early work on the field theoretic

realization of the parton model is S. D. Drell, D. J. Levy, and T. M. Yan, Phys. Rev. **181**, 2159 (1969); Phys. Rev. D **1**, 1035 (1970); **1**, 1617 (1970); and J. D. Bjorken, J. B. Kogut, and D. E. Soper, *ibid.* **3**, 1382 (1971).

[24] K. Bardakci and M. B. Halpern, Phys. Rev. **176**, 1686 (1968); L. Susskind, *ibid.* **165**, 1535 (1968); in *Lectures in Theoretical Physics*, edited by K. T. Mahanthappa and E. E. Brittin (Gordon and Breach, New York, 1969), Vol. XI-D, p. 135; S.-J. Chang and S.-K. Ma, Phys. Rev. **180**, 1506 (1969); J. B. Kogut and D. E. Soper, Phys. Rev. D **1**, 2901 (1970); H. Leutwyler, J. R. Klauder, and L. Streit, Nuovo Cimento A **66**, 536 (1970); F. Rohrlich, Acta Phys. Austriaca **32**, 87 (1970); R. A. Neville and F. Rohrlich, Nuovo Cimento A **1**, 625 (1971); S.-J. Chang, R. G. Root, and T.-M. Yan, Phys. Rev. D **7**, 1133 (1973); S.-J. Chang and T.-M. Yan, *ibid.* **7**, 1147 (1973); T.-M. Yan, *ibid.* **7**, 1760 (1973); **7**, 1780 (1973); S. J. Brodsky, R. Roskies, and R. Suaya, *ibid.* **8**, 4574 (1973); J. M. Namyslowski, in *Progress in Particle and Nuclear Physics*, edited by A. Faessler (Pergamon, New York, 1985), Vol. 14; A. Langnau and M. Burkardt, Phys. Rev. D **47**, 3452 (1993).

[25] G. 't Hooft, Nucl. Phys. **B75**, 461 (1974); H. Bergknoff, *ibid.* **B122**, 215 (1977); H. C. Pauli and S. J. Brodsky, Phys. Rev. D **32**, 1993 (1985); **32**, 2001 (1985); A. Harindranath and J. Vary, *ibid.* **36**, 1141 (1987); **37**, 1064 (1988); **37**, 3010 (1988); M. Sawicki and L. Mankiewicz, *ibid.* **37**, 421 (1988); **40**, 3415 (1990); T. Eller, H. C. Pauli, and S. J. Brodsky, *ibid.* **35**, 1493 (1987); M. Burkardt, Nucl. Phys. **A504**, 762 (1989); K. Hornbostel, S. J. Brodsky, and H. C. Pauli, Phys. Rev. D **41**, 3814 (1990); M. Burkardt, Nucl. Phys. **B373**, 613 (1992); S. Dalley and I. R. Klebanov, Phys. Rev. D **47**, 2517 (1993); and also see most of the references in [16].

[26] S. I. Nagornyi *et al.*, Yad. Fiz. **49**, 749 (1989) [Sov. J. Nucl. Phys. **49**, 465 (1989)]; A. C. Tang, S. J. Brodsky, and H. C. Pauli, Phys. Rev. D **44**, 1842 (1991); M. Burkardt, Nucl. Phys. **B373**, 371 (1992); M. Kaluza and H. C. Pauli, Phys. Rev. D **45**, 2968 (1992); M. Kaluza and H.-J. Pirner, *ibid.* **47**, 1620 (1993); M. Krautgartner, H. C. Pauli, and F. Wolz, *ibid.* **45**, 3755 (1992); Głazek and Perry [16]; Głazek, Harindranath, Pinsky, Shigemitsu, and Wilson [16]; P. M. Wort, Phys. Rev. D **47**, 608 (1993).

[27] T. Maskawa and K. Yamawaki, Prog. Theor. Phys. **56**, 1649 (1976); A. Harindranath and J. P. Vary, Phys. Rev. D **37**, 3010 (1988); G. McCartor, Z. Phys. C **41**, 271 (1988); Th. Heinzl, St. Krusche, and E. Werner, Z. Phys. A **334**, 443 (1989); Prokhvatilov and Franke [7]; G. McCartor, Z. Phys. C **52**, 611 (1991); F. Lenz, M. Thies, S. Levit, and K. Yazaki, Ann. Phys. (N.Y.) **208**, 1 (1991); P. P. Srivastava, presented at XIV Encontro Nacional de Particulas e Campos, Caxambu, 1993 (unpublished), and references therein; G. McCartor and D. G. Robertson, Z. Phys. C **53**, 679 (1992); D. G. Robertson, Phys. Rev. D **47**, 2549 (1993); M. Burkardt, *ibid.* **47**, 4628 (1993); C. M. Bender, S. Pinsky, and B. van de Sande, *ibid.* **48**, 816 (1993); S. Pinsky and B. van de Sande, *ibid.* **49**, 2001 (1994).

[28] For the development of the CQM, see M. Gell-Mann, Phys. Lett. **8**, 214 (1964); G. Zweig, CERN Reports Nos. Th. 401 and 412, 1964 (unpublished); in *Proceeding of the International School of Physics "Ettore Majorana,"* Erice, Italy, 1964, edited by A. Zichichi (Academic, New York, 1965), p. 192; H. J. Lipkin, Phys. Rep. C **8**, 173 (1973); O. W. Greenberg, Annu. Rev. Nucl. Sci. **28**, 327 (1978). For quark model reviews, see J. J. J. Kokkedee, *The Quark Model* (Benjamin, New York, 1969); F. E. Close, *Quarks and Partons* (Academic, London, 1979); A. Pickering, *Constructing Quarks* (University of Chicago Press, Chicago, 1984). This reference contains a carefully researched history of the quark hypothesis, and a complete bibliography. W. Lucha, F. F. Schöberl, and D. Gromes, Phys. Rep. **200**, 127 (1991).

[29] Susskind [24].

[30] Bardakci and Halpern [24].

[31] Bjorken, Kogut, and Soper [23].

[32] Perry and Wilson [18].

[33] Thorn [7].

[34] The details of chiral transformation in light-front coordinates for free fermion theory are discussed in D. Mustaki, "Chiral Symmetry and the Constituent Quark Model: A Null-Plane Point of View," Bowling Green State University report, 1994 (unpublished).

[35] Głazek and Perry [18].

[36] H. J. Lipkin and S. Meshkov, Phys. Rev. **143**, 1269 (1966). Also see Close [28].

[37] Bjorken, Kogut, and Soper [23]; also see Zhang and Harindranath [9].

[38] K. G. Wilson, Phys. Rev. **140**, B445 (1965).

[39] K. G. Wilson, Phys. Rev. B **4**, 3184 (1971).

[40] See, for example, I. Daubechies, *Ten Lectures on Wavelets*, CBMS/NSF Series in Applied Mathematics, No. 61 (SIAM, Philadelphia, 1992); *Wavelets and Their Applications*, edited by M. B. Ruskai *et al.* (Jones and Bartlett, Boston, 1992); C. K. Chui, *An Introduction to Wavelets* (Academic, Boston, 1992); *Wavelets, a Tutorial in Theory and Applications*, edited by C. K. Chui (Academic, Boston, 1992).

[41] R. S. Willey, Phys. Rev. D **18**, 270 (1978); G. McCartor, *ibid.* **18**, 3873 (1978); M. B. Gavela *et al.*, Phys. Lett. **82B**, 431 (1979); G. Feinberg and J. Sucher, Phys. Rev. D **20**, 1717 (1979); O. W. Greenberg and H. J. Lipkin, Nucl. Phys. **A370**, 349 (1981).

[42] R. Oehme and W. Zimmerman, Commun. Math. Phys. **97**, 569 (1985); R. Oheme, K. Sibold, and W. Zimmerman, Phys. Lett. **147B**, 115 (1984); W. Zimmerman, Commun. Math. Phys. **97**, 211 (1985).

[43] Lepage and Brodsky [7].

[44] Drell, Levy, and Yan [23].

[45] Głazek [18].

[46] See, for example, G. T. Bodwin and D. R. Yennie, Phys. Rep. C **43**, 267 (1978); G. T. Bodwin, D. R. Yennie, and M. A. Gregorio, Rev. Mod. Phys. **57**, 723 (1985); W. E. Caswell and G. P. Lepage, Phys. Rev. A **18**, 810 (1978); J. R. Sapirstein, E. A. Terray, and D. R. Yennie, Phys. Rev. D **29**, 2990 (1984).

[47] G. P. Lepage and P. B. Mackenzie, Phys. Rev. D **48**, 2250 (1993).

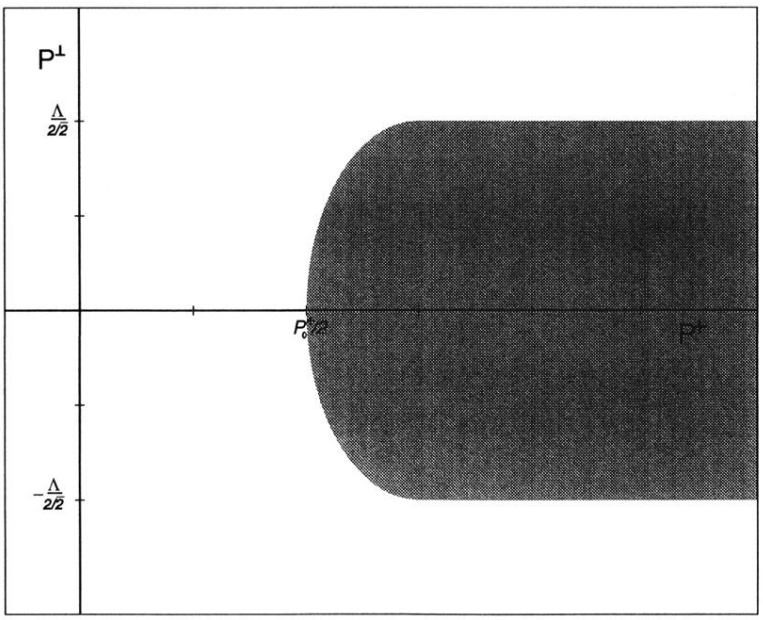

FIG. 4. Cutoff region of center of mass momenta.

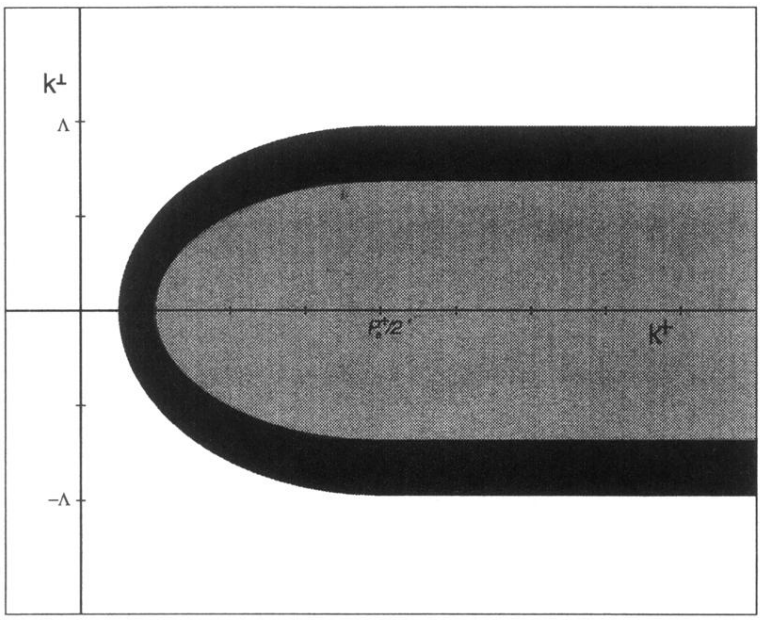

FIG. 5. Cutoff region of constituent momenta.

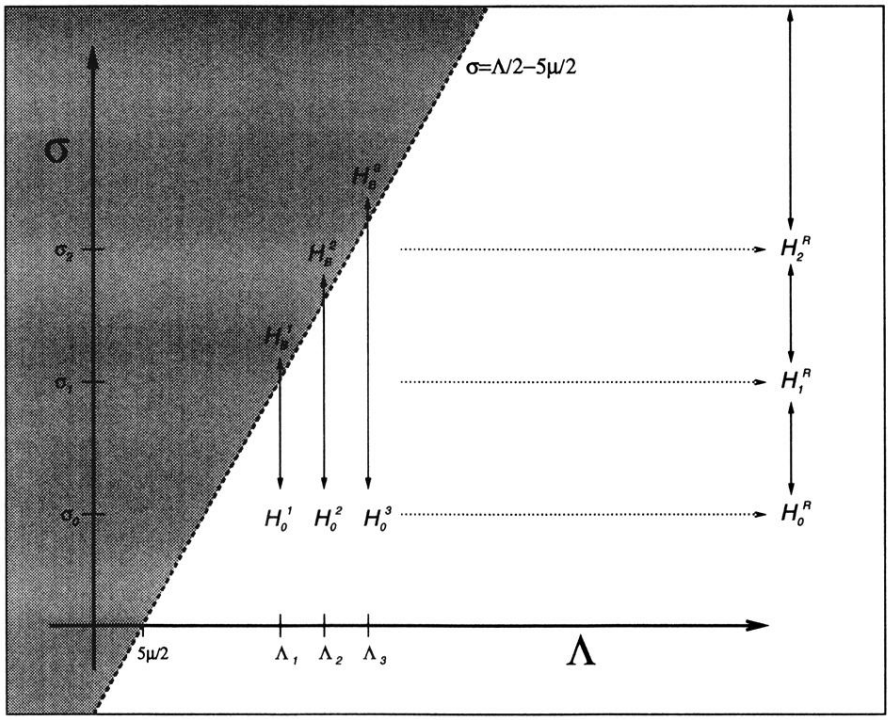

FIG. 6. Triangle of renormalization.